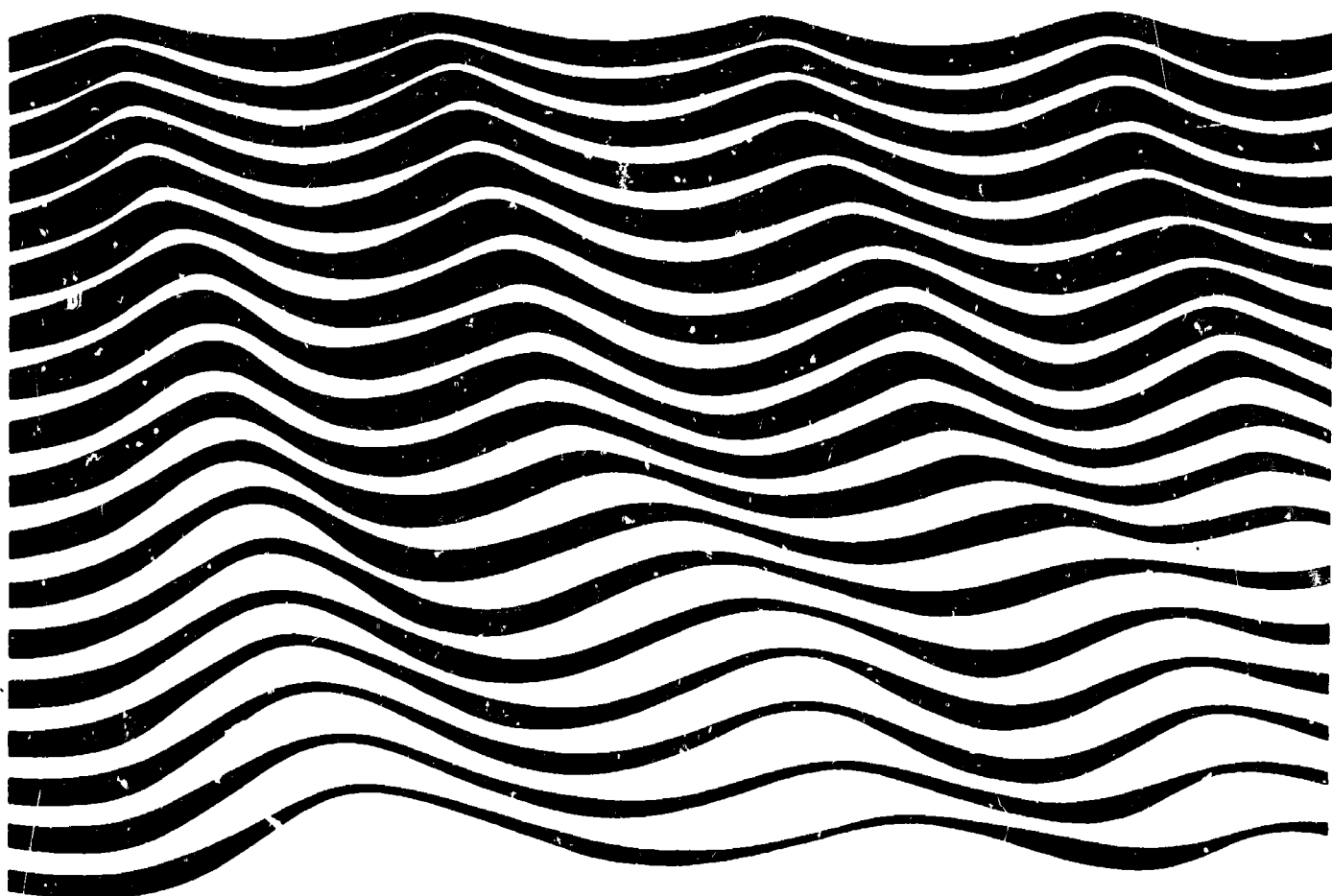


Unesco technical papers
in marine science 46

Opportunities and problems in satellite measurements of the sea

Report of
SCOR Working Group 70



Unesco 1986

UNESCO TECHNICAL PAPERS IN MARINE SCIENCE

Numbers 2, 3, 5, 6, 7, 9, 10, 11, 12, 13, 15, 16, 17, 18, 20, 21, 22 and 23, are out of stock.

For full titles see inside back cover.

Numbers 1, 4, 8 and 14 are incorporated in No. 27.

| No. | Year | SCOR WG | No. | Year | SCOR WG |
|--|------|------------|--|------|------------|
| 19 Marine Science Teaching at the University Level. Report of the Unesco Workshop on University Curricula-Available in French, Spanish and Arabic | 1974 | — | 36 The practical salinity scale 1978 and the international equation of state of seawater 1980. Tenth report of the Joint Panel on Oceanographic Tables and Standards, (JPOTS). Sidney, B.C., Canada, 1-5 September 1980. Sponsored by Unesco, ICES, SCOR, IAPSO. Available in Ar, Ch, F, R, S | 1981 | WG 10 |
| 24 Seventh report of the joint panel on oceanographic tables and standards, Grenoble, 2-5 September 1975; sponsored by Unesco, ICES, SCOR, IAPSO | 1976 | WG 10 | (Примечание: Этот доклад (текст идентичен) был первоначально издан только на английском языке под заголовком <i>Tenth report of the Joint Panel on Oceanographic Tables and Standards</i> (Десятый доклад Объединенной группы по океанографическим таблицам и стандартам)). Имеется на арабском, испанском, китайском, русском и французском языках. | | |
| 25 Marine science programme for the Red Sea: Recommendations of the workshop held in Bremerhaven, FRG, 22-23 October 1974; sponsored by the Deutsche Forschungsgemeinschaft and Unesco | 1976 | — | 37 Background papers and supporting data on the Practical Salinity Scale 1978. | 1981 | WG 10 |
| 26 Marine science in the Gulf area-Report of a consultative meeting, Paris, 11-14 November 1975 | 1976 | — | 38 Background papers and supporting data on the International Equation of State of Seawater 1980. | 1981 | WH 10 |
| 27 Collected reports of the joint panel on oceanographic tables and standards, 1964-1969 | 1976 | WG 10 | 39 International Oceanographic Tables, Vol. 3 | 1981 | WG 10 |
| 28 Eighth report of the joint panel on oceanographic tables and standards, Woods Hole, U.S.A., sponsored by Unesco, ICES, SCOR, IAPSO | 1978 | WG 10 | 40 International Oceanographic Tables, Vol. 4. (To be published) | 1982 | WG 10 |
| 29 Committee for the preparation of CLOFETA-Report of the first meeting, Paris, 16-18 January 1978 | 1979 | — | 41 Ocean-Atmosphere Materials exchange (OAMEX) Report of SCOR Working Group 44, Unesco, Paris, 14-16 November 1979 | 1982 | WG 44 |
| 30 Ninth report of the joint panel on oceanographic tables and standards, Unesco, Paris, 11-13 September 1978 | 1979 | — | 42 Carbon dioxide sub-group of the joint panel on oceanographic tables and standards. Report of a meeting Miami, Florida, 21-23 September 1981 sponsored by Unesco, ICES, SCOR, IAPSO | 1983 | — |
| 31 Coastal lagoon survey (1976-1978) | 1980 | — | 43 International Symposium on Coastal lagoons Bordeaux, France, 8-14 September 1981 Available in F and S | 1982 | — |
| 32 Coastal lagoon research, present and future, Report and guidelines of a seminar, Duke University Marine Laboratory, Beaufort, NC, U.S.A. August 1978. (Unesco, IABO). | 1981 | — | 44 Algorithms for computation of fundamental properties of seawater. Endorsed by Unesco/SCOR/ICES/IAPSO Joint Panel on Oceanographic Tables and Standards and SCOR Working Group 51. | 1983 | — |
| 33 Coastal lagoon research, present and future. Proceedings of a seminar, Duke University, August 1978, (Unesco, IABO). | 1981 | — | 45 The International System of Units (SI) in Oceanography Report of IAPSO Working Group on Symbols, Units and Nomenclature in Physical Oceanography. (SUN) | 1985 | — |
| 34 The carbon budget of the oceans. Report of a meeting, Paris, 12-13 November 1979 | 1980 | WG 62 | | | |
| 35 Determination of chlorophyll in seawater. Report of intercalibration tests sponsored by SCOR and carried out by C.J. Lorenzen and S.W. Jeffrey, CSIRO Cronulla, N.S.W., Australia, September-October 1978 | 1980 | — | | | |

**Unesco technical papers
in marine science 46**

Opportunities and problems in satellite measurements of the sea

**Report of
SCOR Working Group 70**

**Editor: J.F.R. Gower
Co-Editor: J.R. Apel**

Unesco 1986

ISSN 0503-4299

**Published in 1986
by the United Nations Educational,
Scientific and Cultural Organization,
Place de Fontenoy, 75700 Paris.**

Printed in Unesco's workshops.

**© Unesco 1986
*Printed in France***

**Reproduction authorized, providing that appropriate
mention is made of *Unesco Technical Papers in Marine
Science* and voucher copies are sent to the Division of
Marine Sciences.**

PREFACE

This series, the Unesco Technical Papers in Marine Science, is produced by the Unesco Division of Marine Sciences as a means of informing the scientific community of recent developments in oceanographic research and marine science affairs.

Many of the texts published within the series result from research activities of the Scientific Committee on Oceanic Research (SCOR) and are submitted to Unesco for printing following final approval by SCOR of the relevant working group report.

Unesco Technical Papers in Marine Science are distributed free of charge to various institutions and governmental authorities. Requests for copies of individual titles or additions to the mailing list should be addressed, on letterhead stationery if possible, to :

Division of Marine Sciences,
Unesco,
Place de Fontenoy,
75700 Paris,
France.

ABSTRACT

This report has been prepared for SCOR as a reasonably authoritative, yet concise publication of requirements, capabilities and present plans for acquiring and using ocean data from satellites. The various requirements for ocean data that can be addressed by satellites, and the capabilities of the different sensors, are considered in the first two sections. Examples of satellite data are shown in pictures and diagrams, and results are summarized, as far as possible, in tables.

The basic properties of satellites, their special advantages, as well as their draw-backs, are discussed. The importance of this new technology to developing countries is also considered, and the authors make a series of recommendations for improving the value of future missions by coordinating satellite programmes, improving data processing and distribution, and training personnel.

RESUME

Le présent rapport a été établi pour le SCOR en tant que récapitulation faisant raisonnablement autorité et cependant concise des besoins, possibilités et plans actuels concernant l'acquisition des données océaniques par satellite et leur utilisation. Les deux premiers chapitres traitent des divers besoins en données océaniques qui peuvent être satisfaits par satellite et des possibilités qu'offrent les différents capteurs. Des exemples de données recueillies par satellite sont fournis sous forme de photographies et de diagrammes, et les résultats sont résumés, dans la mesure du possible, dans des tableaux.

Les propriétés fondamentales des satellites sont exposées, en même temps que les avantages particuliers qu'ils présentent ainsi que leurs inconvénients. L'importance que revêt cette nouvelle technologie pour les pays en développement est aussi évoquée, et les auteurs font un certain nombre de recommandations visant à accroître l'intérêt des missions futures, notamment des recommandations relatives à la coordination des programmes de satellite, à l'amélioration du traitement et de la diffusion des données et à la formation du personnel.

RESUMEN

Este informe preparado para el SCOR es a pesar de su brevedad una presentación bastante completa de las necesidades, las capacidades y los planes en curso para la obtención y el uso de datos oceánicos obtenidos por satélites. En las dos primeras secciones se abordan las diferentes necesidades de datos oceánicos que se pueden obtener por satélite y las capacidades de los diferentes sensores. En gráficas y diagramas se presentan ejemplos de datos obtenidos por satélite y, en la medida de lo posible, los resultados se resumen en cuadros.

También se analizan las características fundamentales de los satélites, sus ventajas especiales y sus desventajas. Se considera asimismo la importancia de esta nueva tecnología para los países en desarrollo, y los autores recomiendan una serie de medidas para mejorar la utilidad de las futuras misiones, coordinando los programas por satélite, mejorando el procesamiento de datos y su distribución, y capacitando el personal.

РЕЗЮМЕ

Этот доклад подготовлен для СКОР и представляет собой довольно авторитетную хотя и краткую публикацию с изложением потребностей, возможностей и существующих планов в области получения и использования океанических данных, передаваемых с помощью спутников. В первых двух разделах рассматриваются различные потребности в океанических данных, которые могут передаваться через спутники, и возможности различных сенсорных устройств. Примеры спутниковых данных показаны на чертежах и диаграммах, а результаты, по мере возможности, обобщены в таблицах.

В докладе рассматриваются основные свойства спутников, их особые преимущества, а также недостатки. Излагается также значение этой новой технологии для развивающихся стран, авторы предлагают ряд рекомендаций в отношении повышения ценности будущих миссий путем координации спутниковых программ, совершенствования обработки и распространения данных, а также путем подготовки кадров.

خلاصة

أعدّ هذا التقرير من أجل سكور بوصفه مطبوعاً يعوّل عليه بصورة مناسبة مع أنه مختصر ، يتناول المتطلبات والامكانات والخطط الراهنة للحصول على البيانات الخاصة بالمحيطات عبر التوابع الصناعية والانتفاع بها . ويتضمن القسم الأول بحث مختلف الاحتياجات من البيانات الخاصة بالمحيطات التي يمكن نقلها عبر التوابع الصناعية وامكانات أجهزة الاستشعار المختلفة . وتعرض في صور ورسوم تخطيطية أمثلة للبيانات التي تنقل عبر التوابع الصناعية ويرد تلخيص للنتائج في جداول بقدر الامكان .

وتناقش الخصائص الأساسية للتوابع الصناعية ومزاياها الخاصة وأوجه قصورها . وتبحث أيضاً أهمية هذه التكنولوجيا الجديدة بالنسبة للبلدان النامية ، ويقدم المؤلفون مجموعة من التوصيات من أجل زيادة قيمة البعثات التي ستوفد في المستقبل عن طريق التنسيق بين البرامج الخاصة بالتوابع الصناعية وتحسين معالجة البيانات وتوزيعها وتدريب الموظفين .

内容概要

本报告是在使用卫星获取海洋资料和应用这些资料的条件、能力及现有规划方面为海洋研究科学委员会编写的一份具有一定权威性的简明出版物。报告头两部分论述了用卫星收集海洋资料的各种条件，以及各种探测器的能力；用图表说明了一些用卫星收集的资料的实例，并以表格形式对各种结果作了尽可能的归纳。

报告讨论了卫星的基本性能、其特殊优点及缺陷，还讨论了这种新技术对发展中国家所具有的重要性。对如何通过协调卫星计划、改进数据处理与分发和培训人员来提高今后工作的价值，作者也提出了一系列建议。

FOREWORD

Working Group 70 of SCOR was set up in 1982, at the Joint Oceanographic Assembly held in Halifax, N.S., Canada, to report on the problems involved in optimizing satellite ocean observations. Specific terms of reference are as follows:

1. To assess critically resolution and precision requirements for satellite instrumentation systems to ensure adequacy of remotely sensed data for various oceanographic tasks.
2. To review the present status of methodology and requirements for "ground truth" measurements of oceanic variables needed to assess and/or calibrate the results of measurements from satellites.
3. To consider the most effective means of making satellite data available in useable form to working scientists.
4. To make recommendations for coordination of traditional and satellite techniques required to optimize ocean observations.
5. To prepare a report with recommendations taking into account the outcome of the symposium on Oceanography from Space held at the JOA in 1982.

In fact the report takes into account the outcomes of many meetings and publications as well as the personal experience of working group members and other contributors.

The members of the working group are:

J. Gower, Institute of Ocean Sciences, Sidney, Canada (Chairman)
J. Apel, Johns Hopkins University/APL, Laurel, MD, U.S.A. (Vice Chairman)
T. Allan, Institute of Ocean Sciences, Wormley, U.K.
P. Gudmansen, Technical University of Denmark, Denmark
W. Hasselmann, Max Planck Institute, Hamburg, Germany
A. Morel, University of Paris 6, Villefranche sur Mer, France
B. Nalepo, Marine Hydrophysical Institute, Sevastopol, USSR
A. Shutko, Inst. of Radio Eng. and Electronics, Moscow, USSR
D. Spitzer, Netherlands Inst. for Sea Research, The Netherlands
A. Takeda, Nat. Centre for Disaster Prevention, Hiratsuka, Japan

(Full addresses are given in Appendix B.)

The first draft of the report was written by Allan, Apel, Gower, Hasselmann, Morel, Spitzer and Takeda at a working meeting held at the Maspalomas satellite receiving station of ESA in the Canary Islands in March 1983. Contributions to the final text were made by Gudmansen and Shutko of the working group. Gower and Apel have attempted to keep this final version up to date.

We are also grateful to the following for material and comments:

E. Njoku, NASA & JPL, U.S.A.
J. Creeden, NOSC, Newport, RI, U.S.A.
H. Edel, Department of Fisheries and Oceans, Ottawa, Canada
P.D. Bhavsar, SAC, Ahmedabad, India
K. Ya Kondratyev, Geophysical Observatory, Moscow, USSR
P.E. Dexter, Bureau of Meteorology, Victoria, Australia
V.V.R. Varadachari, NIO, Goa, India
F.P. Anderson, NRIO, Stellenbosch, South Africa
J.R. Lutjeharms, " " " "
P. Geerders, NCOG, De Belt, Netherlands
R. Charlan, Maspalomas Space Station, Canary Islands, Spain

Finally we thank Billie Mathias of IOS for typing the camera-ready text and tables of this report.

J.F.R. Cower
J.R. Apel

September 1985

EXECUTIVE SUMMARY

This report has been prepared for SCOR as a reasonably authoritative yet concise publication of requirements, capabilities and present plans for acquiring and using ocean data from satellites. The various requirements for ocean data that can be addressed by satellites are summarised in section 2 and the capabilities of different sensors are discussed in section 3. Various aspects of exploiting these capabilities to satisfy the requirements are discussed in section 4. This also includes general background information on satellites and their sensors. Section 5 highlights the problems faced by developing countries in acquiring and exploiting this data. Conclusions and recommendations are given in section 6.

Satellite sensors are limited by the capability of electromagnetic radiation to pass through the earth's atmosphere and return useful data to orbital altitudes. They cannot address many requirements for subsurface or chemical (such as salinity) ocean data. However, for properties that can be sensed remotely, particularly using microwaves to penetrate clouds and give results by night as well as by day, they give a new global coverage on repeated time scales, that allows large-scale experiments to be attempted for the first time.

The success of U.S. experiments to map ocean temperature, colour, roughness and elevation and to deduce such a variety of information from these is now inspiring other countries in Europe, and Japan. Canada, India and others, to launch their own systems, concentrating on their own problems. All polar orbiting satellites give near global coverage, so that a by-product of these national efforts can be a more or less coordinated satellite network.

It is fortunate, but no coincidence, that such capabilities are available at a time when awareness of global environmental and climate problems have become widespread.

These satellites will also make valuable measurements of ocean and coastal areas of more local interest to countries not directly participating in development of the technology. Such data can greatly benefit developing countries if arrangements can be made for training personnel and delivering the data to them.

General recommendations are made in this report for arranging to exploit the coming data by coordinating the satellite programs where possible, by using improved data processing and distribution and by training of personnel.

TABLE OF CONTENTS

| <u>Sections</u> | <u>Page</u> |
|---|--------------------|
| Abstract | 1 |
| Foreword | v |
| Executive Summary | vii |
| Table of Contents | ix |
| 1 Introduction | 1 |
| 2 Requirements for Satellite Ocean Observations | 3 |
| 2.1 Ocean Circulation | 3 |
| 2.1.1 Introduction | 3 |
| 2.1.2 Parameters Measurable from Space | 4 |
| 2.1.3 Measurement Accuracies | 4 |
| 2.2 Geoid/Gravity Field | 6 |
| 2.2.1 Introduction | 6 |
| 2.2.2 Requirements | 7 |
| 2.2.3 Other Geophysical Data | 9 |
| 2.3 Tides | 9 |
| 2.4 Surface Waves | 11 |
| 2.4.1 Operational Wave Data | 11 |
| 2.4.2 Wave Statistics | 12 |
| 2.5 Internal Waves and Other Quasi-Periodic Phenomena | 12 |
| 2.6 Air-Sea Interaction | 13 |
| 2.7 Marine Biology and Bio-Geochemical Processes | 15 |
| 2.7.1 Chlorophyllous Pigments Assessments and Primary Production Mapping | 15 |
| 2.7.2 Sediment Transport and Distribution, Seston Estimate | 16 |
| 2.7.3 Visualization of Dynamic Features | 17 |
| 2.7.4 Aerosol Distribution, Water Albedo, Climate Research | 17 |
| 2.8 Coastal Processes and Pollution | 18 |
| 2.8.1 Tidal Flats and Shallow Water | 18 |
| 2.8.2 Pollution and Anthropogenic Influences | 18 |
| 2.9 Sea Ice | 19 |
| 2.9.1 Effects on Transportation | 19 |
| 2.9.2 Effects on Weather and Climate | 20 |
| 3 Capabilities of Satellite Remote Sensors | 22 |
| 3.1 Radar Altimetry, Tracking and Orbit Determination | 22 |
| 3.1.1 Radar Altimeter | 22 |
| 3.1.2 Satellite Tracking and Orbit Determination | 24 |
| 3.2 Scatterometry | 26 |
| 3.3 Synthetic Aperture Radar (SAR) | 27 |
| 3.4 Microwave Radiometry | 29 |
| 3.4.1 Sea Surface Temperatures | 31 |
| 3.4.2 Surface Winds | 31 |
| 3.4.3 Atmospheric Water Vapour and Liquid Water | 31 |
| 3.5 Infrared Imagery | 31 |
| 3.5.1 Imagery of Surface Features | 32 |
| 3.5.2 Infrared Sea Surface Temperature Measurements | 33 |

| | | |
|---------|---|----|
| 3.6 | Visible Imagery | 34 |
| 3.6.1 | Imagery of Surface Features | 34 |
| 3.6.2 | Water Colour | 35 |
| 3.6.2.1 | Present Achievements for Case 1 Waters | 36 |
| 3.6.2.2 | Present Achievements for Case 2 Waters | 37 |
| 3.6.2.3 | Recommended Technical Developments for Future Water Colour Sensors | 37 |
| 3.6.2.4 | Recommended Studies | 38 |
| 3.7 | Lidar | 38 |
| 3.8 | Buoys | 39 |
| 4 | Use of Satellite Remote Sensing Data | 40 |
| 4.1 | Matching Satellite Capabilities to Oceanographic Requirements | 40 |
| 4.2 | Possible Types of Orbits | 41 |
| 4.3 | General Properties of Satellite Sensors | 43 |
| 4.3.1 | Field of View | 43 |
| 4.3.2 | Usable Wavelengths | 43 |
| 4.3.3 | Spatial Resolution | 44 |
| 4.3.4 | Data Bandwidth | 44 |
| 4.3.5 | Swath Width Covered | 44 |
| 4.3.6 | Environmental Limits to Coverage | 45 |
| 4.4 | Strategies for the Use of Satellite Data | 46 |
| 4.5 | Availability of Satellite Data | 49 |
| 4.5.1 | Data Processing and Distribution | 49 |
| 4.5.2 | Sources of Data | 51 |
| 5 | Applications in Developing Countries | 55 |
| 6 | Conclusions and Recommendations | 57 |
| 6.1 | Conclusions | 57 |
| 6.2 | Recommendations | 57 |
| 6.2.1 | General | 57 |
| 6.2.2 | Ocean Circulation, Tides and Geoid | 58 |
| 6.2.3 | Ice | 58 |
| 6.2.4 | Biology and Coastal Processes | 58 |
| 6.2.5 | Air Sea Interaction | 59 |
| 6.2.6 | Internal Waves and Other Surface Phenomena | 59 |
| 6.2.7 | Bottom Topography | 59 |
| 7 | Annotated Bibliography - General Reports | 61 |
| 8 | References | 66 |
| | Appendix A | |
| | Appendix B | |

FIGURES (in Sections as numbered)

| | Following Page |
|--|-------------------|
| 2.1.1 Frequency-Wavenumber Energy Content of Ocean Circulation . . . | 2 |
| 2.1.2(a) Pacific Average Surface Wind Stress Vectors (Ship & Islands) . | 2 |
| 2.1.2(b) Pacific Surface Wind Velocities (Satellite) | 4 |
| 2.1.3 Ocean Surface Currents (Historical Data) | 4 |
| 2.1.4(a) Global Sea Surface Temperature (Satellite) | 6 |
| 2.1.4(b) Sea Surface Temperature Anomalies in 1982/3 El Nino | 6 |
| 2.1.4(c) Global Sea Surface Temperature (Historical Data) | 6 |
| 2.1.5 CZCS Pigment Image of the Alaskan Stream | 6 |
| 2.1.6 Landsat MSS Image of Alaskan River Plumes | 6 |
| 2.2.1 Global Surface Gravity Anomaly (Satellite) | 8 |
| 2.2.2 Global Sea Surface Topography (Satellite) | 8 |
| 2.3.1 Global Ocean Tides (Satellite) | 10 |
| 2.4.1 Surface Waves and Fourier Transform (Satellite) | 10 |
| 2.5.1 Seasat SAR Image of Internal Wave Patterns | 12 |
| 2.7.1 CZCS Images of Gulf Stream and U.S. East Coast May 7 1979 . . | 16 |
| 2.7.2 CZCS Images of Gulf Stream and U.S. East Coast June 10, 1979 . | 18 |
| 3.1.1, Satellite Altimetry of Sea Surface Elevation and Slope | 22 |
| 3.1.2 Global Sea Surface Height Variability (Satellite) | 22 |
| 3.1.3 Global Significant Wave Height (Satellite) | 24 |
| 3.1.4 Global Average Wind Speeds (Satellite) | 24 |
| 4.4.1 Ocean Frequency/Wavenumbers Sampled by Satellites | 46 |
| 4.4.2 Global Coverage of Geosynchronous Satellites | 48 |
| 4.4.3 Global Coverage of (Landsat) Polar Orbiting Satellite Receivers | 48 |

TABLES (in Sections as numbered)

| | Following Page |
|-------|---|
| 2.6.1 | Satellite Observations Relevant to Air-Sea Interaction 14 |
| 2.7.1 | Optical Radiometry Applied to Marine Biology and Bio- Geochemical Studies 14 |
| 2.9.1 | Satellite Observations of Sea Ice 20 |
| 3.1.1 | Altimeter Missions 24 |
| 3.2.1 | Scatterometers 26 |
| 3.3.1 | Ocean Features Observed on SAR 28 |
| 3.3.2 | Synthetic Aperature Radars 28 |
| 3.4.1 | Passive Microwave Instruments 30 |
| 3.5.1 | Thermal Infrared Imaging Sensors 32 |
| 3.5.2 | Sea Surface Determinations 32 |
| 3.6.1 | Ocean Features Studied With Optical Imaging Sensors 34 |
| 3.6.2 | Classification of Water into Case 1 and Case 2 36 |
| 3.6.3 | Sensor Capabilities Needed for Water Colour Observations . . . 36 |
| 3.6.4 | Water Colour Scanners Launched or Planned 36 |
| 3.6.5 | Properties of the Coastal Zone Color Scanner (CZCS) 36 |
| 3.7.1 | Potential Ocean Lidar Capabilities 38 |
| 4.1.1 | Brief Guide to Satellite Remote Sensing of Oceans 40 |
| 4.2.1 | Expressions for Orbital Properties of Satellites 42 |
| 4.2.2 | Types of Orbit Useful in Remote Sensing Missions 44 |
| 4.5.1 | Satellite Sensor Ocean Data Now Being Collected 50 |
| A1 | Satellites of Importance to Oceanography |
| A2 | Microwave Band Names |

1. INTRODUCTION

This report has been prepared for SCOR as a document that brings together in one publication a reasonably authoritative yet concise compilation of requirements, capabilities and plans for data from ocean-looking satellites. The need for such a publication became apparent from repeated questions asked of satellite-oriented experts as to the "what, how, and where?" of ocean remote sensing. The audience to which it is addressed, therefore, is the working oceanographer, who needs no extended explanation of his science, but rather a properly specified objective statement of the remote measurement capability and perhaps its implications.

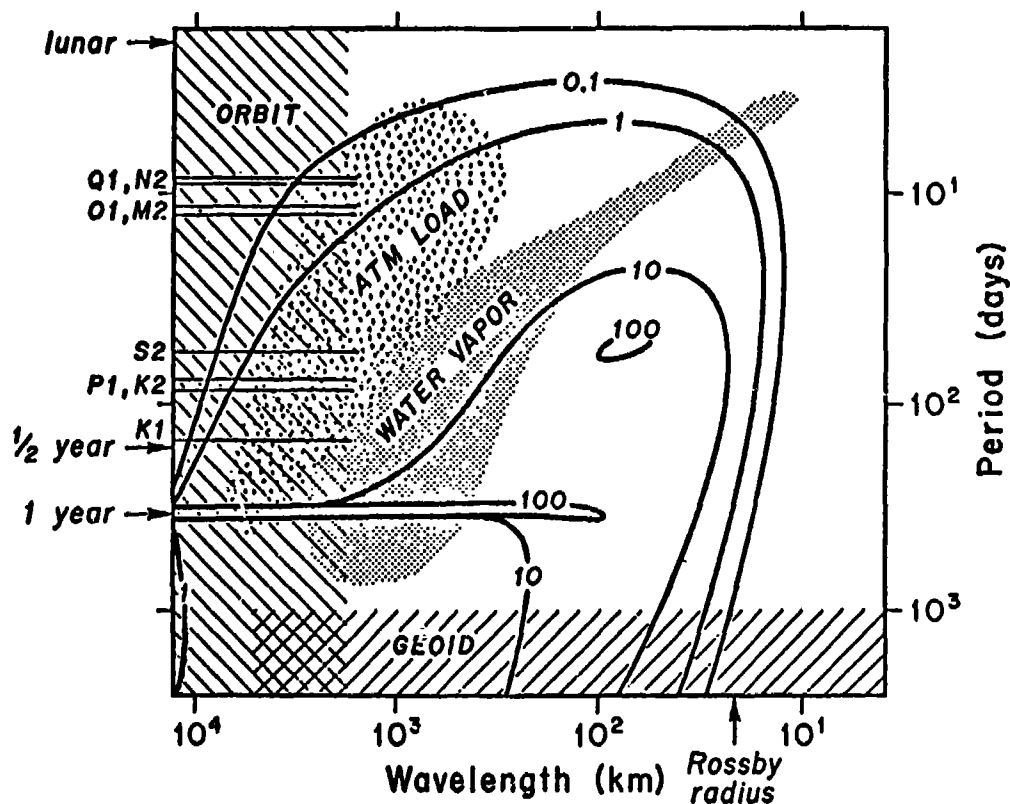
Satellite observations of the sea have progressed a very long distance from the first color photographs obtained from early manned spacecraft. The quality, type and sheer quantity of data have since increased manyfold, to the point where, for certain types of data sources, it becomes possible to speak of "remote measurement" rather than "remote sensing." In addition, the appreciation of the present and potential roles of remote sensing in the conduct of ocean science has been heightened considerably, and the limitations more fully understood. It is the authors' view that remote measurement is but one tool, albeit an increasingly important one, in the rapidly enlarging kit of tools available to the observer, and that for certain types of phenomena, it is becoming possible to make satellite measurements of the surface of the sea with a breadth, duration and accuracy greatly exceeding that of any other means. For example, a satellite-borne wind scatterometer is expected to deliver measurements of vector winds at the ocean surface equivalent to more than 20,000 ship observations per day, and to do so with an accuracy that meets or exceeds WMO specifications for wind measurements at sea. The impact of such a device in both marine science and weather forecasting is obvious.

One view of the practice of ocean remote measurement is that it is best carried out in conjunction with ship and buoy observations. The in-situ measurements may be used to check or correct the satellite data, to extend them below the surface, and to aid in the interpretation of the sometimes-odd signals appearing in the remotely sensed data. The satellite can then be used to interpolate between and extrapolate beyond the in-water measurements, perhaps both in space and time. For certain types of observations, this view is sensible; for others, such as altimetry, it may be that the power and trustworthiness of the satellite data allow them to be used independently or at least nonconcurrently with ship information.

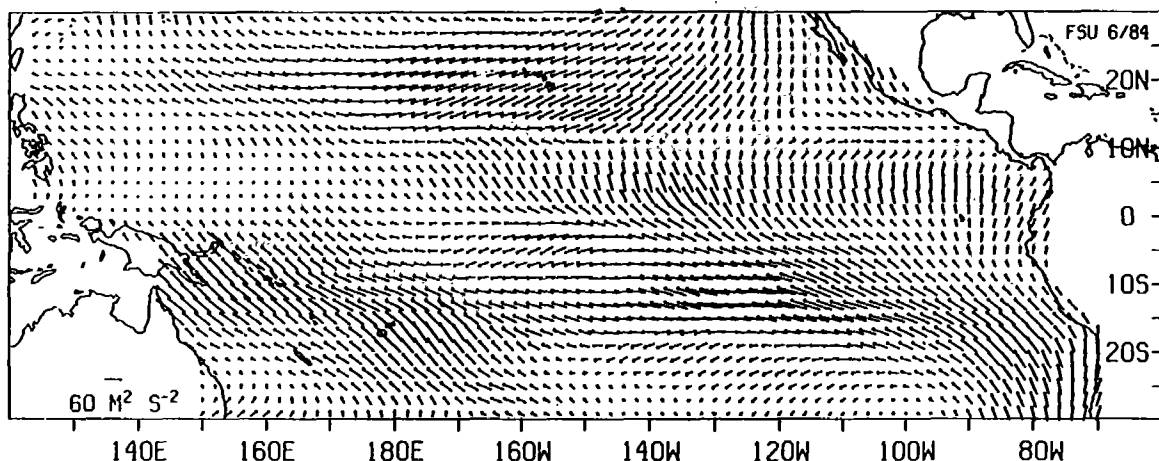
The organization of this report is reasonably clear from the Table of Contents, but some explanation may help. First, a discussion is held of requirements for the types of data that might be obtained from satellites; these requirements have been distilled from a number of documents referenced in the Annotated Bibliography, from discussions with oceanographers, and from the personal experience of the authors. They have been fitted into brief discourses of the oceanographic processes or problem of interest, e.g., the ocean's role in climate. Second, objective statements are made as to satellite sensor measurement capabilities and limitations, insofar as it has been possible to discern these boundaries. Third, discussions are given to establish further capabilities and bounds as regards the distribution of data in space and time. Fourth, an attempt is made to compare requirements with

capabilities, both present and promised, as much to indicate directions for future work in sensors and spacecraft as to provide ocean scientists with guidance on usage and trustworthiness. A short discourse on how data might be made more accessible and useful to the nonspecialist worker is included here. Another similar discussion follows on the use of remotely sensed information by developing countries. The main body of the report ends with a Conclusions and Recommendations section. Two final sections then list an annotated bibliography containing a brief description of the contents of recent relevant reports, and the list of references. Appendices contain a list of satellites and microwave band names, and the full addresses of working group members.

It is difficult to properly acknowledge the contributions from the large number of workers who helped to prepare the source material used here; many of their names can be found in the lists of committee members, editors, etc., of the references in the Bibliography; we must simply thank them collectively. Nor have we attempted to cite detailed sources for the requirements and capabilities listed, but rather have tried to assure authoritativeness by having two or more individuals review and concur with the numbers cited. Nevertheless, errors and differences of opinion may occur, and the authors take sole responsibility for the material herein.



2.1.1 A schematic diagram of the frequency-wave number energy content of ocean circulation. Contours are proportional to energy density. The shaded areas, give scales for atmospheric water vapor content and pressure loading (Munk & Wunsch, 1982).



2.1.2(a) Distribution of average surface wind stress vectors, in units of m^2/s^2 , for September 1978. Data are primarily from ships and island stations (Legler and O'Brien, 1984).

2. REQUIREMENTS FOR SATELLITE OCEAN OBSERVATIONS

This chapter lays forth a number of generalized requirements for satellite-derived information about the ocean, divided approximately according to the process or phenomenon of interest, e.g., ocean circulation, biology, etc. It does not attempt to be overly quantitative, but rather to present the rationale for a given measurement. The list is limited to those parameters that are currently known to be observable remotely.

2.1 Ocean Circulation

2.1.1 Introduction

The determination of the global circulation of the ocean is not only a classical problem of physical oceanography, but is also one of the main concerns of climate research because of the influence of the oceanic heat transport and storage on the global climate heat balance. The ocean circulation encompasses a wide range of interacting space and time scales, including basin-scale gyres, regionally driven flows such as the equatorial current systems and the Antarctic Circumpolar Current, intense western boundary currents, current and frontal instabilities with associated eddies and rings, and geographically limited but thermodynamically important upwelling processes. Although the ocean circulation is basically a three dimensional phenomenon strongly controlled by wind stress and by spatial temperature and salinity distributions, satellites can provide critical data on the surface fluxes driving the circulation and, through sea surface elevation measurements, on both the baroclinic and barotropic components of the flow field. In this respect satellites are valuable not only through their powerful sampling capabilities, but also in providing essential data which are very difficult to obtain by conventional means.

In the various oceanographic experiments being conceived for the World Climate Research Program (WCRP), such as the World Ocean Circulation Experiment (WOCE), Tropical Ocean-Global Atmosphere (TOGA) etc., satellites will play an essential role. However, they must be viewed always as one component within an integrated measurement strategy which includes research vessels, moored and drifting buoys, ships of opportunity and other measurement techniques. The optimal strategy depends on the time and space scales of the component of circulation of interest.

The wavenumber-frequency energy spectrum of the oceanic general circulation is sketched in Figure 2.1.1, which suggests that the most energetic regions of the spectrum are (a) the annual signal encompassing a wide range of wavelengths, and (b) mesoscale fluctuations with space and time scales near 100 km and 50 days, respectively. Also included in Fig. 2.1.1 are estimates of the spectrum of orbit errors; geoidal undulations, which have periods on geological time scales; the spectrum of atmospheric pressure loading on the ocean; and the contribution of water vapor to the error budget of satellite altimetry. The relevance of these latter estimates is discussed in the various portions of this report dealing with altimetry questions.

Equatorial dynamics are of special interest to climate studies as well as to oceanography. The vanishing of the horizontal component of Coriolis force at the equator results in a focused dynamical response of the ocean

within a very few degrees of the equator. This zone acts as a waveguide for trapped baroclinic Kelvin and Rossby waves, which propagate more rapidly than the midlatitude baroclinic Rossby waves and can therefore interact effectively in the climate system on the time scale of a few months. There is evidence that much of the large scale climate variability, as exemplified by the El Nino-Southern Oscillation (ENSO) phenomenon, is intimately related to equatorial ocean dynamics.

Western boundary currents, rings and eddies, while classified as mesoscale processes, must be regarded as an integral part of the large scale ocean circulation, since the western boundary currents are simply the concentrated return flow regions of the main basin scale circulation. It appears that most of the energetic eddies and rings observed in the ocean are shed from these currents through instabilities. The variability of time scales of these processes are comparable with the variability time scales of the large scale flow, but the spatial scales are as much as an order of magnitude smaller. For studies of climate dynamics, measurements of the fluctuations of the western boundary currents with associated nonstationary eddies, rings and the near recirculation region, could well provide a rewarding focus within the World Ocean Circulation Experiment. These regions make major contributions to oceanic heat transport and are also one of the most critical elements to be parameterized in general ocean circulation models.

Submesoscale circulation features such as upwellings, eddies and similar near-shore processes are smaller but important components of ocean circulation, and are often of interest in fisheries research and forecasting, and in determining the fate and effects of pollution.

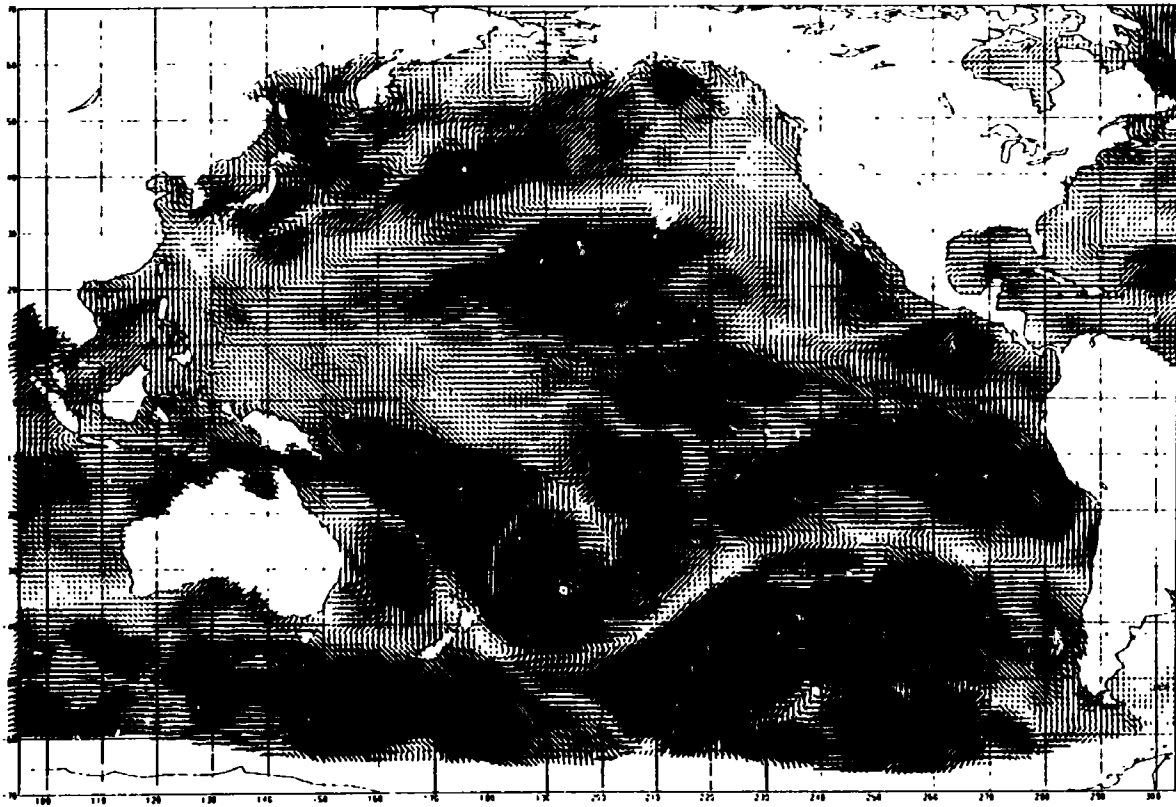
2.1.2 Parameters Measurable from Space

At least three oceanic surface fields of interest appear to be measurable from satellites on interesting time and space scales, although all three fields should be composited out of surface as well as space-derived data. They are: (a) the surface wind stress field and its curl, (b) the surface geostrophic pressure field, and (c) the surface temperature field. While not sufficient in themselves to determine the three-dimensional time-varying flow, these surface fields can be used as boundary conditions in dynamical models that take into account what is known about the vertical model structure for both velocity and density. The model output can then in principle yield the three-dimensional time-dependent flows. In addition satellite imagery of temperature and colour patterns, when gathered and analyzed properly, can make contributions to circulation studies by way of providing a technique for flow visualization.

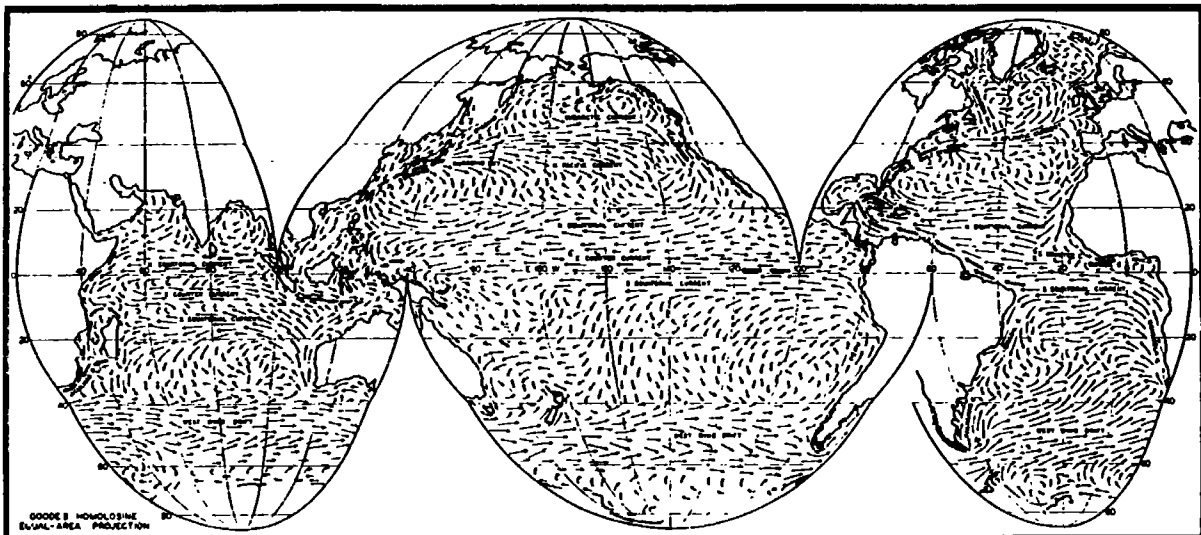
References in the annotated bibliography contain detailed discussions of the problems and methods of approach, as well as limited specifications of needed sensor and satellite characteristics. A short summary of these capabilities is presented here.

2.1.3. Measurement Accuracies

The large scale ocean circulation is driven by wind stress, the fluxes of heat and moisture across the air-sea interface, and density effects.



2.1.2(b) Surface wind velocities in the Pacific Ocean for 6 and 7 September 1978, as derived from the Seasat scatterometer. Large cyclonic motions are resolved by the 50-km footprint (Woiceshyn et al., 1984).



2.1.3 Composite of major ocean surface currents from historical data sources, for February-March (Sverdrup et al., 1962).

accuracy, although there remain unresolved problems in determining stress direction and in undersampling of the global wind field with respect to time. Additionally, cloud drifts obtained from geosynchronous satellites can be used to estimate wind speed and direction in the tropics and subtropics. It should be noted that the relevant driving force for the large scale ocean circulation is the curl of the wind stress, which is weighted towards shorter space scales than the stress itself. Figure 2.1.2(a) illustrates a surface wind stress field derived for the tropical Pacific from cloud drift data corrected using a planetary boundary layer model and ship observations. Figure 2.1.2(b) is a wind velocity field obtained from just two days of scatterometer data from Seasat. The resolution of midlatitude cyclones and basin-wide data on a much shorter time scale attest to the desirability of such data. The estimated accuracy of the wind speed and direction are ± 2 m/s and $\pm 20^\circ$, respectively. Even this two-day-averaged field is too long for weather forecasting purposes, however, with 12-hour updates being required for operation forecasts.

Since the maximum sea surface height differences associated with the large scale ocean circulation are of the order of 1 m, and many important features have signatures that are an order of magnitude less, the height accuracy requirement for the measurement of surface pressure gradients is of the order of a few cm. Altimeter measurements of the satellite height above sea level can be made to a precision of 2-3 cm, but to achieve the required accuracy for absolute sea level relative to an equipotential surface, both the geoid and the satellite orbit have to be known to the same accuracy. Figure 2.1.3 is a map of the general circulation of the ocean as derived from an analysis of a range of data sources, including ship drifts, the historical density data and a calculation of the baroclinic component of geostrophic flow. It is this field that one hopes to determine with satellites, chiefly via altimetry.

This historical surface current field gives no hint of the variability in the flow field in space and time known to exist in the ocean, nor of the annual and interannual fluctuation in circulation and heat transport that occur in concert with global changes in weather and short-term climate. A realization of the global circulation on intervals of 30-60 days with spatial resolutions of order 100-300 km is required for many maritime purposes. Speeds to within ± 20 cm/s and directions to $\pm 20^\circ$ are thought desirable, although for some purposes even higher accuracy is required.

Ocean viewing satellites can also contribute to the determination of upper ocean heat storage, and the sensible and latent heat and moisture fluxes across the air-sea interface by the combination of surface wind and surface temperature data. However, this information must be augmented by atmospheric temperature and humidity data from other sources in order to compute the fluxes using the standard bulk formulae. Present satellite SST data (Fig. 2.1.4.(a)) are probably sufficiently accurate (0.6 - 1.0°C) for estimating near surface heat storage, but in the heat flux calculation, the ocean temperature enters only in the air-sea temperature differences. Since the air temperature variations are normally considerably larger than the SST variations, and at present are not derivable from satellite observations, it is not yet possible to determine the fluxes satisfactorily. Additionally, this accuracy is only marginal for studying the thermodynamics of SST

anomalies themselves. It is hoped that instruments currently in development, with accuracies in the range of $0.3\text{--}0.5^{\circ}\text{C}$, will provide more useful surface temperature fields for these applications. Such fields need to be realized on 30-day, 200-km intervals at the coarsest, with finer divisions required for some purposes.

Figure 2.1.4(b)) illustrates the temperature anomaly in the eastern tropical Pacific for the extreme El Nino of 1982-83, as averaged over a one-month interval. A spatial resolution of 100-200 km and a temporal resolution of four weeks appear to be adequate for large scale temperature fields in climate-oriented studies.

Figure 2.1.4(c) shows an annual mean surface temperature obtained from surface data for 1978-81. Although the general morphology of this multiyear, multiseason average is quite similar to that in the one-month mean of Fig. 2.1.4(a), the variability in space and time associated with climate change (c.f. Fig. 2.1.4(b)) is of course not discernible in the long-term data set. The problems with temperature data are similar to those with circulation data. However, they appear to be closer to solution with current observations than many other geophysical quantities, except in regions of persistent cloud cover.

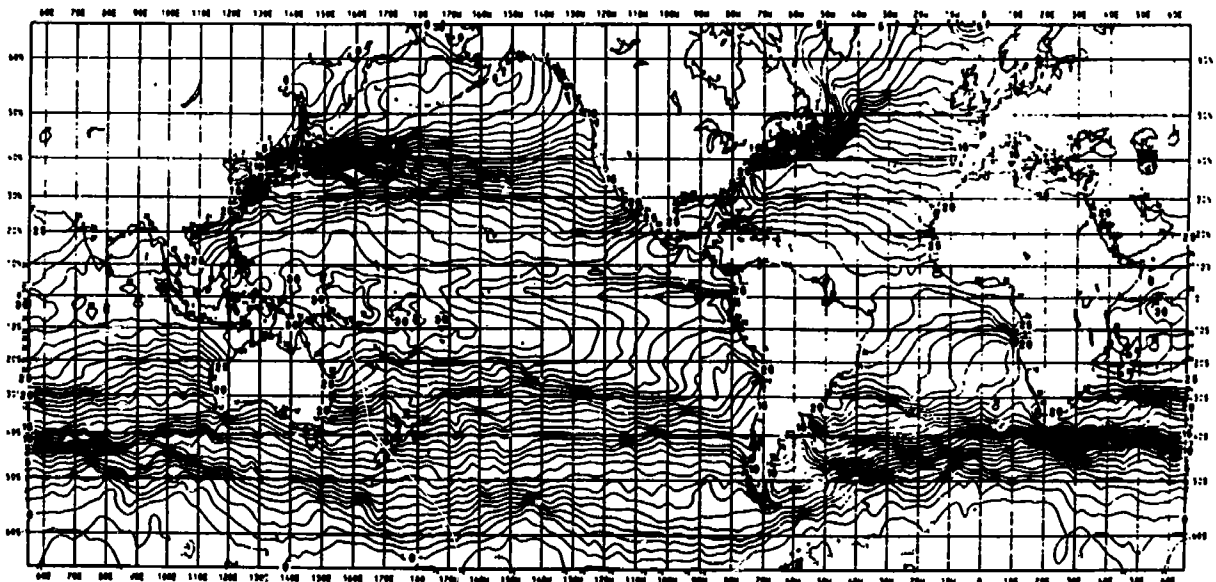
Satellite imagery that shows flow pattern can also be useful in circulation studies on a variety of scales. Fig. 2.1.5 shows an ocean colour image from the Coastal Zone Color Scanner in which the different chlorophyll pigment levels associated with water in and around the Alaskan Stream show the surface water flow patterns south of the Aleutian Islands. An example of a useful high-resolution visible image from the U.S. Landsat spacecraft is shown on Figure 2.1.6, which illustrates spatial variations in the coastal surface flow field in the Gulf of Alaska, as evidenced by the patterns of sediment-bearing waters. Ideally, studies require multiple images of the same locale repeated on a few-day time scale. This is rarely available for high resolution data, as discussed in section 4 of this report. Other examples of flow visualization in satellite visible imagery are illustrated in section 3.

2.2 Geoid/Gravity Field

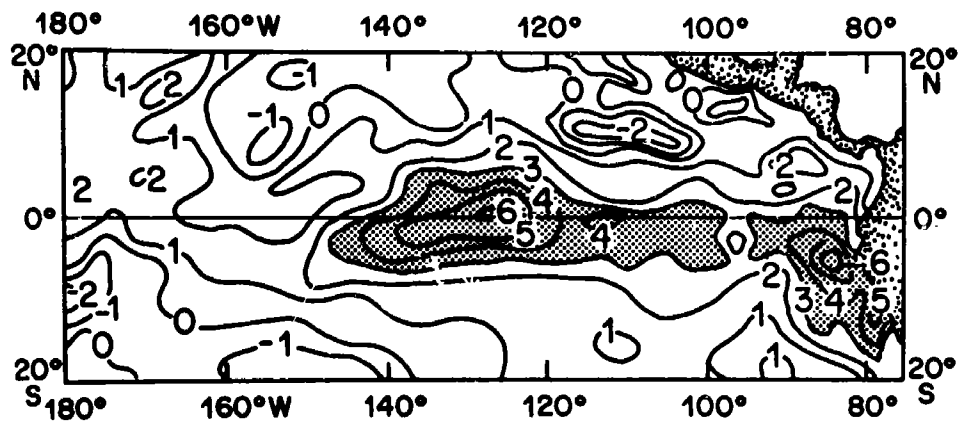
2.2.1 Introduction

The marine geoid and the surface gravity field are of importance to satellite oceanography because of the method of using a precision altimeter on an accurately tracked satellite to determine ocean surface currents; the means by which this is done are discussed in section 3.1.

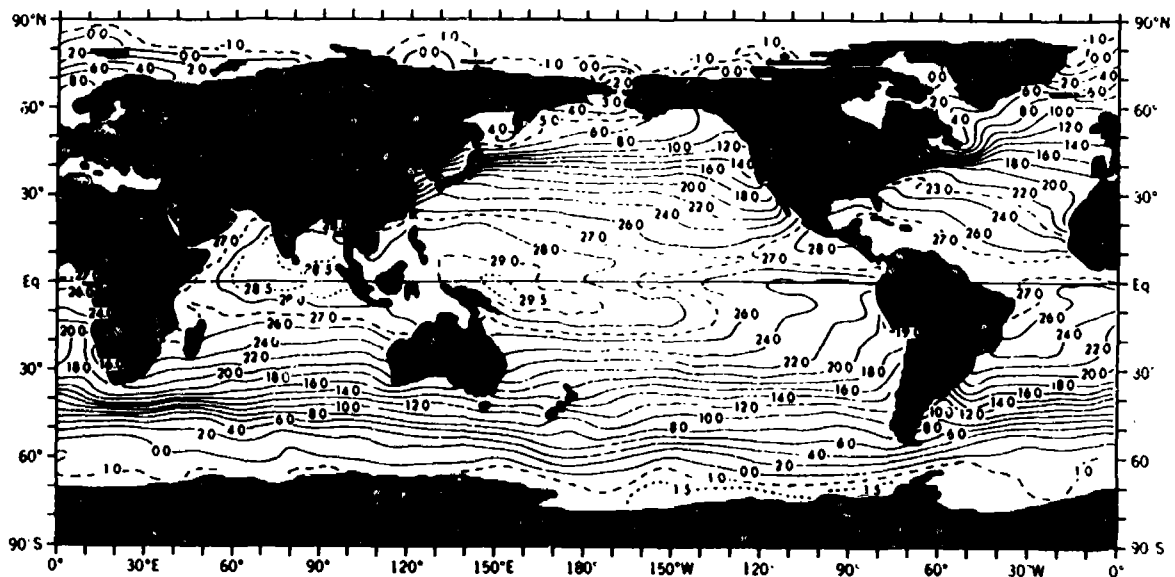
The greatest variation in the height of the sea surface measured by an earth-orbiting radar altimeter is caused by undulations in the shape of the geoid. The geoid is defined as the equipotential surface that would be assumed by a still, uniform ocean after removing the effects of external forces such as those due to tides, currents, storm surges, wind and atmospheric disturbances. Thus if the ocean and atmosphere were motionless the geoid would coincide with mean sea level.



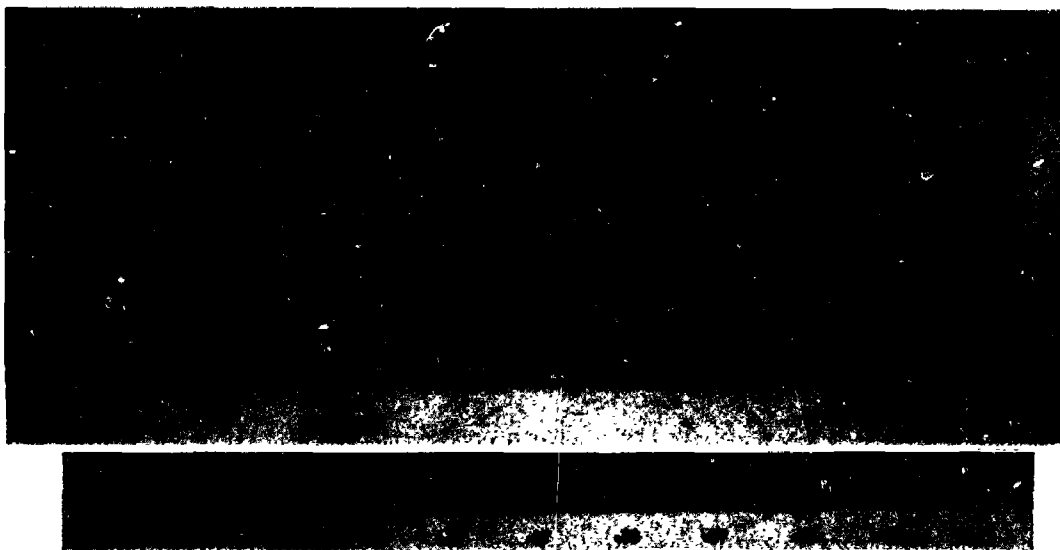
2.1.4(a) Isotherms of global sea surface temperature from the NOAA-7 AVHRR multi-channel infrared radiometer for December 1981 (NASA 1983d).



2.1.4(b) Isotherms of sea surface temperature anomalies in the eastern tropical Pacific at the maximum of 1982-83 El Niño event (Rasmussen et al., 1983).



2.1.4(c) Annual mean surface temperature isotherms as derived from historical data (Levitus, 1983).



2.1.5 Coastal Zone Color Scanner chlorophyll pigment image showing flow patterns associated with the Alaska Stream on July 10, 1979, in an area about 1100 km across, south of the Aleutian Islands. Cloud and land are masked to black. Cloud obscures the Bering Sea north of the Aleutian Islands, and appears in patches at the lower right. Unalaska Island is cloud-free at the centre left, as are the Shumagin Islands and Chirikof Island at the upper right. The Alaska Stream carries fresher water west, out of the Gulf of Alaska, in a narrow jet that follows the edge of the continental shelf and breaks into eddies south-west of Unalaska Island. (NASA image. NOAA 1977)



2.1.6 Landsat MSS visible image of a small section of the Alaska coast, showing near-shore flow patterns on sub mesoscales via suspended sediments. The area shown is 120 km across, and includes the mouth of the Copper River in a region where rivers carry a high load of glacial silt. Bad scan lines cross the upper half of the image. (NASA image. NOAA 1977)

The shape of the geoid, as measured as a departure from the reference ellipsoid of revolution, is irregular, because of gravity variations produced by an uneven distribution of mass within the earth's interior. Since by definition the force of gravity is everywhere perpendicular to the geoidal surface, a map of the geoid is integrally related to the gravity field. The precision of the Seasat altimeter was sufficient to delineate such geophysical features as the mid-Atlantic rift valley, seamount chains, and the Mendocino Fracture Zone in the Eastern Pacific, among many other features. Figure 2.2.1 is a pictorial representation of the gravity anomaly calculated from Seasat altimetry, and shows a high degree of correspondence between surface gravity and subsurface bathymetry. The range of anomaly shown is ± 25 mgal.

Variations in geoid surface elevation across the globe are substantially greater than the range of surface dynamic heights set up by ocean currents. Across the Atlantic for example the geoid drops from a height of + 64 m west of Ireland to - 50 m off Florida--an average gradient of about 2 m/100 km. By contrast a current of 15 cm/s at a latitude of 30° would produce a gradient of only 0.1 m/100 km. Geoidal slopes must therefore be known to better than 5% before the absolute value of current speeds can be determined.

Prior to 1958 little was known about the shape of the geoid and even maps published in 1963 show differences in height of 50 m from present day values. It was the observations of the perturbations of satellites' orbits caused by an uneven gravity field which allowed a progressively more detailed description of the shape of the geoid. The ellipsoidal oblateness of the earth is the major, large-scale feature of the earth's irregular shape. It causes the orbital plane of a satellite to precess about the earth's axis at a rate, depending on the altitude and inclination of the orbital plane, which can reach several degrees per day. A satellite orbit can be arranged so that this precession is exactly equal to one revolution per year (about 1° per day) and in such a direction that the plane of the orbit is stationary with respect to the sun. This gives the sun-synchronous orbit referred to elsewhere in this report.

Satellite orbits are also affected by smaller scale gravity variations, down to a limiting scale of a few hundred kilometers set by the satellite's altitude. The long wavelength component of precise gravity field of Goddard Earth Model (GEM) 10 for example was deduced from satellite orbit perturbations. It cuts off at a scale of about 1000 km, and represents the geoid to an accuracy of about 2m. Finer detail can be introduced either through lower-flying satellites or through satellite altimeter measurements of the precise shape of the sea surface. The latter, however, will have oceanographic signals as "noise" in it. GEM 10B used a combination of orbit perturbation, marine gravity measurements, and GEOS-3 altimeter data for this purpose and later models added the more precise but sparser Seasat data.

2.2.2 Requirements

The internal precision of the Seasat altimeter data set has been maximized by minimizing the rms height differences at orbit intersections. This method has been used to construct highly precise local sea surface topographies in the North-Eastern Pacific, the Caribbean and the Eastern seaboard of the USA, where rms topographic errors have been reduced to

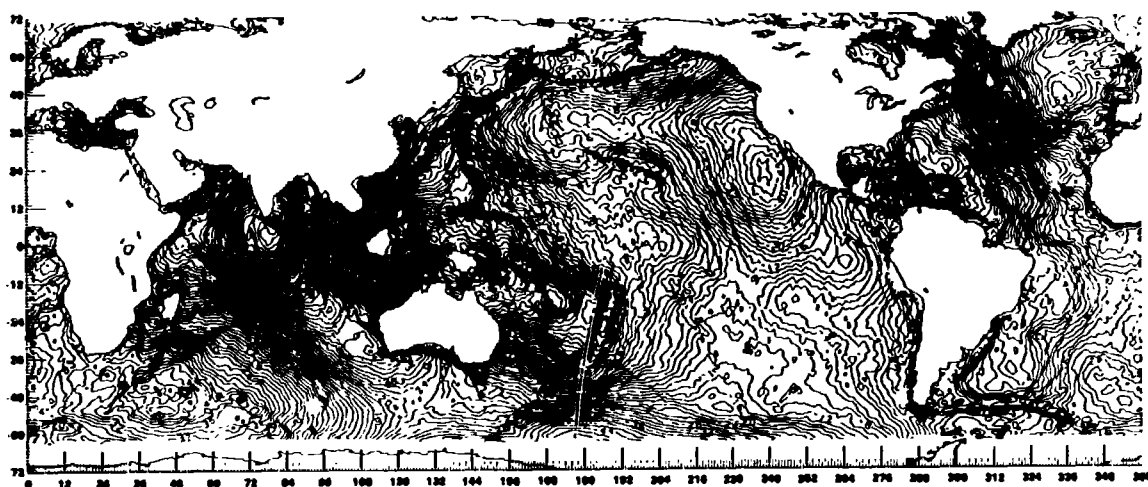
about 10-25 cm which is well into the level of oceanographic signals. This is encouraging, for although there remains the problem of integrating the altimetric geoid to the global model, the accuracies obtained over small areas begin to approach that required to measure both steady and time-varying ocean currents. A less accurate but global scale compilation of Seasat data resulted in the sea surface topographic map shown in Figure 2.2.2. This map, which represents departures from the reference ellipsoid, is internally accurate to rms crossover deviation of about 0.70 meters and shows the main ocean trenches and ridges. Satellite data gave a coverage along orbit tracks spaced about 100 km near the equator and extending to 70° north and south. Sea ice usually precludes measurements at higher latitudes. A future satellite carrying an altimeter with Seasat-like precision could cover a much finer grid if placed in a suitable orbit, i.e. one that covered many different tracks, in (say) six months, before repeating. The greater volume of data would also allow greater self consistency in the calculations, and hence greater accuracy in sea surface topography even in the presence of tracking errors of order 1-2 meters. This topography, however, still contains the oceanic signals and hence is not an accurate estimate of the actual geoid.

There remains the problem, then, of subtracting the actual precise geoid from the altimetric topography in order to obtain the residual oceanographic signals which may be considered to be composed of a temporal mean plus a fluctuating component (c.f. Figure 3.1.1 ahead). Measurement of these signals is presently a goal of satellite oceanography; meeting it requires some means of making an independent determination of the geoid. This could be done by integrating marine gravity obtained from ships, if they were uniformly available globally, but the existing data set misses the mark by a very large factor. The alternative scheme is to derive the global gravity field by flying a low satellite that is sensitive to short wavelength gravity perturbations. This is one purpose of the proposed NASA Geopotential Research Mission, GRM (formerly Gravsat), which will be made to operate as a drag-free satellite in a polar orbit at 160 km altitude sometime in the late 1980s. The GRM is expected to sense gravity features down to a wavelength of approximately 200 km, which corresponds to a scale of $1/k = 32$ km; this number is very close to the first-mode baroclinic Rossby radius of deformation in the ocean at mid-latitudes and it sets the transverse spatial scale of baroclinic flow. The gravity anomaly and the geoid from GRM are expected to have a precision of about 14 mgal and 18 cm, respectively, when averaged over 0.25° squares, or 2 mgal and 2 cm over 1.0° squares. The averaging size for the geoid should be varied to take into account the local variation in Rossby radius, which is smaller in regions of narrow, intense currents and broader in areas of weaker flow.

It appears to be an accident of nature that, where the horizontal scale of the current gradient is short and the attendant averaging square is small and hence the geoidal error large, the elevations due to the currents are also large. Where the currents are weaker, the horizontal scales are larger; but so are the geoidal averaging dimensions, with their concomitant decrease in geoid error. In both cases, the current-signal to geoid-noise ratio is approximately the same, with a value of order 5, i.e. 100 cm/18 cm and 10 cm/2 cm.



2.2.1 Map of surface gravity anomaly obtained from Seasat altimetry, showing crustal features such as deep ocean trenches, mid ocean ridges, seamount chains, and transform faults. There is a high correlation between small scale gravity anomalies and bathymetry. Anomaly range 25 mgal; accuracy 5-10 mgal; horizontal resolution 50-250 km (Haxby, 1984).



2.2.2 Map of sea surface topography relative to a reference ellipsoid, as obtained from 18 days of Seasat altimetric data used in orbit crossover analyses. Internal precision of order 0.7 m; contour intervals of 2 m (Marsh & Martin, 1982).

Hence, in this fashion, GRM would appear to meet the geoidal requirements for altimetric measurement of ocean currents in both the large set-up, narrow, western boundary currents and the small set-up, broad eastern currents and basin-wide gyres. These arguments weaken but are not invalidated near the equator.

In the absence of a mission such as GRM, it is nevertheless still possible to study the time variability of the ocean circulation by making a large number of repetitive altimetric measurements over the same track and subtracting out their average, a quantity that represents the mean sea level profile as the sum of the geoid and the mean ocean circulation. For climate applications, the variations of the ocean circulation are in fact as interesting as the mean circulation, and provide a more critical test of ocean circulation models. In this regard it is fortunate that the satellite altimeter can measure both the baroclinic and the barotropic geostrophic flow (except in the narrow equatorial band). The latter responds much more rapidly to changes in the wind field than the baroclinic flow associated with the ocean density distribution (weeks versus years). The space-time sampling ability of a satellite altimeter can in fact approach the natural space-time variability of the barotropic component of the ocean circulation of interest for climate studies. However, the repeating orbit characteristics are such that a trade-off is necessary between space and time scales, and a single altimetric satellite is marginally able to sample near the maximum of mesoscale energy identified on Figure 2.1.1. A repeat interval of 10-20 days and a repeat track spacing of 150-300 km are required, with the ground tracks overlying one another to within an error of less than 1-2 km. Under these conditions it is possible to obtain the temporal variability of sea surface heights and slopes along the subsatellite tracks, which can then be combined to form estimates of the oceanic eddy field. This is discussed later in Section 4.4 in somewhat more detail (c.f. Fig. 4.4.1).

2.2.3 Other Geophysical Data

Small scale geoid and gravity anomaly information are of interest to marine geodists and geophysicists in their own right. While it is beyond the scope of this report to consider the detailed research requirements in these disciplines, it should be observed that the oceanographic requirements for geoid heights appear to satisfy the current needs of geodists. The gravity anomalies from SEASAT altimetry are currently considered as the best available for a range of intermediate wavelengths, but need increased accuracy at longer and shorter wavelengths. GRM or similar missions can yield longer wavelength gravity readily, while precision altimetric satellites can in principle extend the short wavelength gravity observations down to scales near 15 km. With combined global anomaly and bathymetric data, for example, it appears possible to study such processes as crustal loading, isostatic adjustment and density anomalies.

2.3 Tides

Although various deep-sea tidal models have been proposed (Hendershott, 1973; Schwiderski, 1980) very few measurements have been made, largely due to the difficulty in deploying deep-sea pressure gauges over the reasonably long periods that are required. Tidal amplitudes contribute to variations in an ocean altimeter profile and since they can reach amplitudes > 1 m across an

ocean basin they should be capable of extraction from a precise altimeter's record provided other contributions to the signal can be estimated to sufficient accuracy.

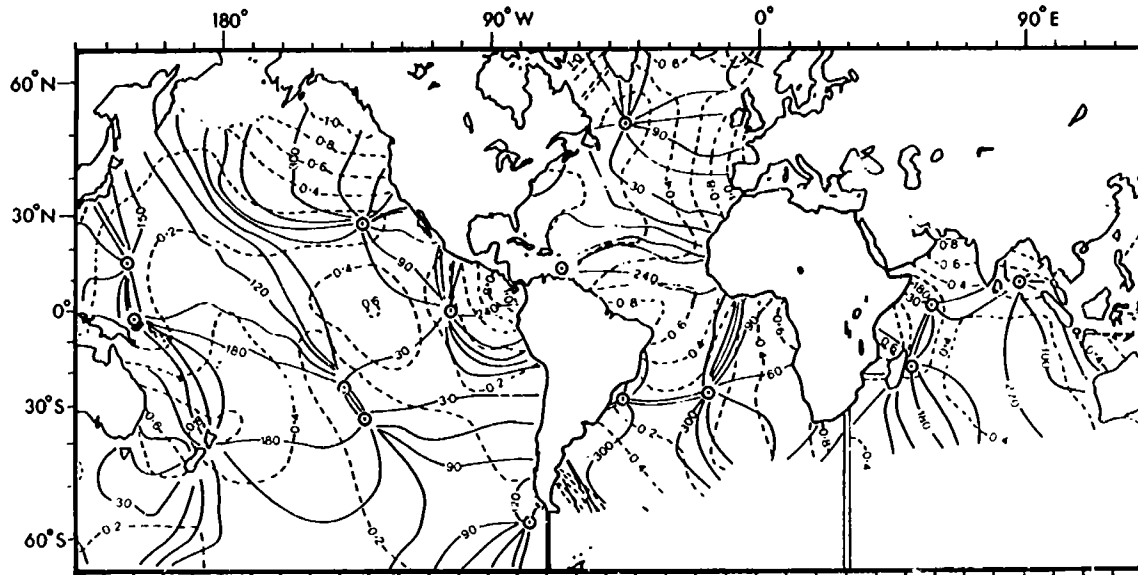
Analysis of Seasat's altimeter data has produced encouraging results. A method developed by Cartwright and Alcock (1981) is based on techniques applied originally over the North Sea where not only is an accurate tidal model available but where the gravity field is known through ship-borne surveys. Account was also taken of solid earth tides and surges caused by wind stress and atmospheric pressure, to minimize the altimeter's error budget. The method was then transposed to the less well-known Northeast Atlantic where oceanic loading effects as well as solid earth body tides had to be taken into account.

Analysis of the altimeter record showed repeatable data at short wavelengths, much of it correlated with bathymetric features, but with evident errors in the orbital corrections at long wavelengths, causing successive estimates of the surface height at any given point to vary within a range of 1-2 meters. The removal of linear trends (tilt and bias) reduced these discrepancies to the level of 0.1-0.2 m. A special technique of tidal analysis employing the discrepancies at track intersections was devised whereby all tidal elements in the area were expressed in terms of a two-parameter response operator on a representative tidal variation, together with a constant parameter to allow for the geoidal differences between each pair of crossing points. Forcing each of these parameters to sum to zero around every closed circuit of intercrossing point segments was a useful constraint on the overall solution.

Applying this procedure to the total available data set resulted in global tidal solution giving amplitude and phase of the open-ocean tides, as shown for the M2 component (Fig. 2.3.1). The array of M2 amplitudes and phases agreed reasonably well with the known tidal map of the area, within the limitations of the short satellite data set (3 months).

The Seasat orbit, being nearly sun-synchronous, aliased several components of the tidal frequency spectrum to very low, or zero, values. If tides are to be determined altimetrically, an orbit choice must be made such that reasonable record lengths of tidal excursions may be obtained. The subject is somewhat complicated, but has received ample consideration in the TOPEX report (NASA, 1981b), to which the reader is referred for additional information. Figure 2.1.1 also shows the periods of several of the tidal components superposed on the spectrum of the general circulation. The final selection of an altimetric orbit is a compromise between the needs for global coverage, precision in measuring sea surface topographic gradients, and the determination of tides. It should also be noted that among the several altimetric missions planned for the near future, only one precise determination is needed of the tidal signals that would be aliased in a sun-synchronous orbit.

Given a data record of proper characteristics, it is reasonably clear that considerable analysis is required to derive the tidal admittances. The latter could be described completely numerically or the data used to tune and verify existing models to higher precisions.



2.3.1 Amplitude and phase of global open ocean tides for the M_2 linear component, extracted from three months of Seasat altimetric data (IOS/NERC, 1985).



2.4.1 Shuttle Imaging Radar-B image, digitally processed, showing 200 m-long surface waves in the east Pacific hurricane Josephine, October 1984. Also shown is the two-dimensional Fourier transform of the scene, illustrating the narrow-bandedness of the waves, which have three distinct wave trains. Such a transform is related to the 2-D power spectral density of the wave field in a partially understood fashion, with current research suggesting it is the slope spectrum that the SAR yields (JHU/APL/Beal).

2.4 Surface Waves

Motivation in surface wave work has traditionally been based on two fields of application, which today may be regarded as of comparable economic importance: the forecasting of surface waves for offshore operations and ship routing, and the compilation of surface wave statistics for offshore and coastal engineering purposes. For both fields of application, simultaneous data on wind and wave fields are needed with demanding sampling requirements. For research studies surface waves cannot be treated as something separate from atmosphere-ocean fluxes; indeed, they form an essential part of air-sea interaction and have a strong effect on the fluxes. Satellites are ideally suited for gathering surface wave and wind data, particularly with regard to the wave fields. However, a single satellite in itself cannot meet all sampling conditions, although one satellite would already significantly upgrade the existing conventional data networks. Every effort should therefore be made to launch a two or three satellite system for wind and wave measurements in the late eighties, c.f. recommendations of the Chilton report (JSC/CCCO 1981).

2.4.1 Operational Wave Data

Wave prediction represents a two-scale problem which requires a corresponding measurement strategy. To determine the local two dimensional wavenumber spectrum of the wave field, continuous two dimensional sampling over an area of the order 5×5 km square is needed with a resolution of the order of 20 m. Figure 2.4.1 illustrates an 18×18 km² Shuttle Imaging Radar-B SAR image of the ocean surface in a hurricane, showing three intersecting trains of 200-m-long waves; also shown is the two-dimensional Fourier transform of the image, which demonstrates the narrow-band, unidirectional character of each of the waves trains. The Fourier transform of the SAR image is believed to be related to the two-dimensional slope spectrum of the waves, although the exact relationship is still a matter of active research.

For global or large scale wind and wave forecasts, the two dimensional wave spectrum and wind vectors are required on a grid of the order of 100-600 km spacing every 6-12 hours (with a finer grid in coastal areas). A SAR can satisfy both the local and large scale along-track sampling conditions through a burst sampling strategy.

The wind field and significant wave heights (H_s) can similarly be well sampled on the along-track direction by a scatterometer and altimeter, respectively. However, the wind and wave measurements from a single satellite are seriously sub-sampled in the cross-track (zonal) direction because of the relatively large, 25° longitude separation between consecutive orbits. The fact that the wind field can be measured over a swath of the water of 400 km does not significantly improve the zonal aliasing problem except at high latitudes. Similarly, the sampling in time is also marginal through the time separation between the ascending and descending orbits crossing over a given region of the ocean.

A system of two or three satellites would largely resolve the aliasing problem. Although this solution would clearly be highly desirable, it should be noted that the sampling question for satellites cannot be considered

independently of other measurement systems. Wave forecasts can be (and are) made from wind forecasts produced only from the conventional data base of the world weather observing system. A single satellite providing extensive wind and wave data over the data sparse regions of the world ocean would already significantly enhance sea surface wind and wave predictions.

Furthermore, an orbit optimised for sampling wind and wave fields is badly out of optimum for sampling ocean circulation variability, as is discussed ahead in Section 4.4.

2.4.2 Wave statistics

Time series of H_s and surface wind speed and direction are essential to the derivation of seasonal and extreme value estimates of wave and wind climate. Excellent statistics can also be derived from remotely sensed data. In order to allow for seasonal and inter-annual variations, records of several years' duration are required in each geographical area. For obvious reasons surface instrumental and visual ship's observations do not generate a data set of sufficient spatial and temporal continuity or resolution on a global scale, and data are particularly sparse in the polar seas, and away from main shipping routes. In fact, data with good time series are only available on the coasts of countries with developed offshore industries, and are generally thin on an oceanic scale. Remotely sensed data are therefore very important for the establishment of a global climatic data base of H_s . Apart from its scientific interest, such a data base is important in deriving design environmental statistics for offshore oil structures, insurance computations, safety, ship-routing, and operational planning of weather-sensitive activities such as pipe-laying, oil-rig installation, heavy lifts of oil-rig deck modules, etc. In the longer term directional and spectral data would be valuable, but a simple record of H_s would be a great advance on the present data base. Data banking of a global remote-sensed climatic data set of H_s is under discussion by the International Oceanographic Data Exchange Committee of IOC.

2.5 Internal Waves and Other Quasi-Periodic Phenomena

High-resolution imaging sensors, either optical or radar, have allowed the study of coherent internal waves by way of the surface signatures that these oscillations often present. The waves that have been observed appear to have been generated by tidal flows over bathymetric features, either the continental shelf slope or sills or other underwater ridges. The resultant internal waves have periods ranging from minutes to hours, but are modulated at tidal frequencies ranging from semi-daily to fortnightly, and therefore appear as packets that may propagate over large distances before being dissipated by shallow water or other processes. Often the waves are sufficiently nonlinear for them to take on characteristics of internal solitons. Fig. 2.5.1 shows a Seasat SAR image taken off Portugal exhibiting regularly spaced internal wave packets, with 310-m-long surface-wave swell, and 150-m breaking surf.

The solitons are rendered visible on the surface because the internal currents modulate the small-scale surface waves overlying the internal waves, leading to periodic variations of surface roughness (and hence optical or radar reflectivity) in a direction normal to the crests. Often the



2.5.1 Seasat SAR image taken off Portugal showing regularly spaced internal wave packets moving in from the Atlantic. The orderly spacing, assuming a tidal generation period of 12.4 hours, implies a velocity of 0.4 m/s slowing to 0.3 m/s nearer the coast. A surface wave swell of 310 m wavelength offshore moves in from the northwest, to shorten to about 150 m before breaking on the beach. North is to the left. (DFVLR image, IOS Canada/Gower).

signatures take the form of a linear region rougher than the surrounding sea, followed by another region of anomalous smoothness (a "slick") and then by normal sea state; this sequence repeats itself over each internal wave in the packet.

An understanding of the imaging mechanisms allows one to delineate the range of conditions under which internal waves may be studied via remote sensing. The waves must possess sufficient horizontal straining and coherence, and the wind must be sufficiently low for their signatures to be recognizable in the image. This may preclude the study, via remote sensing, of the usual deep-ocean, random-phase broad spectrum internal wave field described by the Garrett-Munk spectrum, for example. Second, the surface waves must not be so energetic as to show no modulation by the internal currents. This implies that even very coherent internal waves will not be visible under conditions of moderate-to-high wind speeds, say greater than 10-12 m/sec. For satellite observation with optical or near-IR sensors the region under study must be sufficiently cloud-free.

Coherent internal wave signatures have been observed in images or photographs taken from Landsat MSS, Seasat SAR and Shuttle SIR, Nimbus-7 CZCS, DMSP, and Apollo-Soyuz, and other manned missions. The sensors have been medium-to-high resolution devices--approximately 20 to 1000 m pixel size--and the requirement of 3 to 5 samples per wavelength for resolution then sets the lower wavelength limit of detectability, which is, for the above sensors, between 100 and 5000 m. This limit also depends on sensor viewing angle relative to the sun glitter pattern in the case of optical sensors, and sensor incidence angle in the case of SAR. In general, the observation of internal waves with optical sensors requires the area under investigation be viewed with some amount of sun glitter present in order to detect the variations in surface roughness. In the case of SAR, low incidence angles, of order 20°, are preferred to higher angles, say greater than 40°.

Beyond observations of coherent internal waves, other longer-wavelength, quasi-periodic phenomena sometimes appear in high-resolution imagery. The origins of these are not clear and little can be said of the requirements for their observation, therefore, other than of the need for repeated imagery and analysis and modelling of the phenomena.

2.6 Air-Sea Interaction

Air-sea interaction is important in various scales of atmospheric and oceanographic processes.

Global scale distribution of wind stress or of the curl of the wind stress are thought to be the most important components for maintaining the oceanic general circulation. A meridional change of heat flux across the ocean surface produces large effects on the earth's climate. Upwelling is a typical meso-scale phenomenon caused by wind stress.

Hurricanes and typhoons are generated by convergence of moisture-laden air involving much energy over the tropical ocean. The remarkable development of atmospheric disturbances frequently seen over seas off the east coasts of continents at mid-latitudes are the results of the dry and cold air mass

receiving large amounts of sensible and latent heat from the warm sea surface. These are typical meso-scale air-sea interaction processes that strongly affect daily weather.

Patches of cumulus over the ocean are the manifestation of small scale heat flux which involves the elements of energy transfer from ocean surfaces. Storm surges attacking coastal areas are essentially the wind set-ups of sea water caused by strong wind stress acting on the sea surface.

The fine structure of the upper layer of the ocean is considered to be critically controlled by the mixing due to wind stress and the stability of thermal stratification.

The various scales of air-sea interaction demonstrated above are essentially governed by the fluxes across the air-sea interface.

There are basically three methods to calculate these fluxes; the first is the direct method which computes a covariance between the turbulent component of vertical wind and the fluctuating component of the physical property whose flux is being considered. This method is not appropriate to satellite measurement. The second is the bulk method, computing a flux from mean wind speed, mean air-sea difference of a physical property and a transfer coefficient determined beforehand. The last is the budget method, obtaining the flux as a residual of the mass or energy budget of a certain column across the atmospheric and oceanic layer.

Observational components required for the air-sea flux determination are downwelling solar radiation, upwelling, back-radiation, wind speed and direction, moisture, temperature of the atmospheric surface layer and sea surface temperature, or air-sea temperature differences. Ocean current and vertical temperature profile of the ocean are also needed for a budget experiment of a mesoscale area. To the extent that satellite sensors can contribute to these measurements, they can assist in flux calculations, by both the bulk and the budget methods mentioned above.

Scatterometer wind is the most promising satellite-derived parameter contributing to the measurement of air-sea fluxes. The curl of wind stress, vector averaged over 2 degree squares and sampled at least once every two days is required to estimate the ocean Ekman transport which drives the general circulation system of the ocean. The accuracy of the Seasat type scatterometer meets the observational requirements.

At present, satellite measurements of the air temperature in the atmospheric surface layer and hence of the air-sea temperature difference are not feasible. For the capability of heat flux computation, strong efforts to develop suitable techniques of measuring air temperature and air-sea temperature difference are needed.

The sea surface temperature distribution of various scales over 1 km is detectable by a satellite thermal infrared scanner such as AVHRR. The atmospheric moisture distribution of horizontal scales larger than 100 km can be detected by the microwave radiometers similar to the SMMR.

Table 2.6.1 Satellite observations relevant to air-sea interaction.

| Required Observation | Parameters to be measured | Sensors required | Example |
|---|--|---|---|
| Energy & Water Budget Experiment over a whole ocean (like CAGE) | Incoming Radiation R_d or Cloud Amount Back Radiation R_u Surface Wind U Moisture e SST T_s Atmospheric Temp. T | Solar Radiation Sensors Visible and Infrared Radiometer Wind scatterometer Microwave Radiometer Infrared Radiometer Air temp. profiler | VISSR SASS SMMR VISSR/AVHRR VAS |
| Energy & Water Budget Experiment over a limited area | Incoming Radiation R_d (or Cloud Amount) Back Radiation R_u Surface Wind U Upper Layer Wind $U(Z)$ Ocean Current W or M (Mass Transport) Water Temperature $T_w(Z)$ Air Temperature $T_a(Z)$ | Solar Radiation Sensor Visible and Infrared Radiometer Wind Scatterometer Visible Infrared Camera on Geostationary Satellite Altimeter ? Air Temp. Profiler | VISSR SASS VISSR ALT ? VAS |
| Momentum Flux by Bulk Method | Surface Wind U | Wind Scatterometer | SASS |
| Sensible Heat Flux by Bulk Method | Surface Wind U SST T_s Surface Air Temp. T_a Air-Sea Temp. difference $T_a - T_s$ | Wind Scatterometer Radiometer ? ? | SASS AVHRR ? ? |
| Latent Heat Flux by Bulk Method | Surface Wind U SST T_s Moisture e | Wind Scatterometer Radiometer Multichannel Microwave Radiometer | SASS AVHRR SMMR |

Table 2.7.1 Optical radiometry applied to marine biology and bio-geochemical studies

| | Global scale processes | Mesoscale processes | Small scale processes |
|---------------------------|--|--|--|
| Problems addressed | Primary production Sediment transport Visualization of dynamic features Aerosol Content | Primary production variations Sediment transport (& pollution) Visualization of dynamic features Aerosol content Sea-ice delineation | Primary production (patchiness) Sediment transport especially near coasts Pollution Coastal Processes |
| Pixel size Swath width | 4 to 20 km Consistent with global requirements | 0.5 to 4 km 1500 to 2500 km | 0.01 to 0.1 km 50 to 500 km |
| Coverage | All oceans (in sight of geostationary positions will satisfy some requirements) | Global | Global. Adjustable pointing needed for faster repeat coverage of specific restricted zones of interest |
| Repetition rate | 1 or 2 per day | 3 to 6 days | 5 to 15 days |
| Methods | Optical: radiance measurements reduced at 3 channels (blue, green, near IR) IR: SST especially important | Multispectral radiance measurements including near IR Simultaneous SST determination needed Sun glint avoidance | Spectral radiance measurements including near IR SST determination needed |
| Conclusions | Large scale data coverage is needed. Geostationary option should be evaluated. Degraded spatial resolution option should be evaluated | CZCS type sensor can provide adequate data Degraded spatial resolution option should be evaluated | High resolution optical sensors required. Blue channel needed for primary production Pointable field of view needed for adequate repeat coverage |

Satellite sensors can contribute data for determining many of the values needed in these flux calculations (see Table 2.6.1). Required measurements for which no satellite technique is available are indicated by question marks. The repeated wide ocean coverage that satellites can give make them essential components of many planned (WOCE, TOGA) and proposed (CAGE) experiments.

2.7 Marine Biology and Bio-Geochemical Processes

Scientific objectives depend on the spatial scale considered. Some, clearly defined at global (world) scale, become less relevant on a smaller scale, whereas new ones appear. We emphasize here objectives which can be addressed by passive radiometry in the visible part of the spectrum, which is the main technique for bio-geochemical studies (see table 2.7.1).

2.7.1 Chlorophyllous Pigments Assessments & Primary Production Mapping

The colour change of the sea induced by the presence of primary producers (phytoplankton), or more precisely by the presence of photosynthetic pigments, is detectable from space (Fig. 2.7.1). This figure shows the variations of water colour mapped by the Coastal Zone Colour Scanner in an area about 1500 km by 1000 km over the Gulf Stream and associated shelf waters. These variations are interpreted in terms of the implied phytoplankton concentration (bottom), and the resulting attenuation of light (top) in the near surface water. The clearer, bluer water of the Gulf Stream (lower part of both frames) is represented by darker tones. Lighter tones show the turbulent patterns in the greener, more pigmented water to the north. Higher productivity is also indicated over Georges Bank, east of Cape Cod. Grey tones are quantified for both frames by the step wedge at the bottom.

With its repetitive mapping capabilities a satellite sensor can provide reliable information about the global evolution of the algal biomass in the near-surface layer. The knowledge of this evolution, combined with physical dynamics data and photosynthesis models, would allow primary productivity estimates to be greatly improved. At present, the annual amount of CO₂ fixed through photosynthesis is highly controversial and could be underestimated by a factor of 5 or 10. Methodology is likely at the origin of an under-evaluation in oligotrophic areas (approximately 80% of total productivity in 90% of the total ocean area). In coastal and more productive regions (20% of total productivity in 10% of the area), variability is higher and accuracy is limited by the duration, sampling rate and geographical extent of classical ship-bound programs. It is also believed that actual productivity is underestimated in all these regions, including upwelling areas.

The algal organic carbon provides energy for the whole food web, and the potential fish harvest depends upon it. It also represents a partial and temporary fixation of atmospheric CO₂, or even a carbon sink, through the deposit of biogenous detritus, mainly on the continental slopes.

A somewhat "rough" delineation of biomass could suffice provided that a continuing world coverage is ensured. This approximate delineation of the productive zones would document the question of the temporal response of biological processes to meteorological events or impulses, and would show start of blooms, zonal migration and extension of upwellings induced by trade winds and monsoons, etc.

A more accurate assessment of the pigment concentration is needed when studying the biological response to dynamic features at mesoscale (e.g. eddies, fronts, coastal upwellings) and when describing the biomass spatial distribution. Depending on the geometrical resolutions available, the distribution pattern could be usefully studied down to small scales < 0.1 km, to show details of phytoplankton patchiness.

The chlorophyllous concentration can presently be estimated from space within an accuracy of $\pm 35\%$ in "Case 1" waters (see Table 3.6.2 later) i.e. those not influenced by terrigenous influx (sediments and/or yellow substance). Most efforts have been concentrated on mesoscale observations. Pigment retrieval in "Case 2" waters needs further investigation and requires sensors with improved capabilities, particularly improved atmospheric corrections.

2.7.2 Sediment Transport and Distribution; Seston Estimate

In marine sedimentology and in general geochemical budget studies, the horizontal sediment fluxes (and the vertical fluxes deduced from them) and the bio-geochemical nature of the transported particulates are an essential input. The resuspension of sediments due to wave or tidal actions, the extension of river plumes related to river flows and the pattern of turbid patches related to wind stress and local currents, are also phenomena which can be studied by remote sensing (see figure 2.1.6 earlier). At a smaller scale the study of the land-water boundaries, (including wetlands and mangrove), and coastal management and protection could benefit from synoptic and repetitive data acquired from a satellite.

In the open ocean, far from the influence of land, the total suspended matter (seston) is correlated with the algal concentration. In this case the remote sensing of seston concentration reduces, at least to a first approximation, to the problem of pigment assessment discussed above. Most present day studies deal with these "Case 1" waters where seston and algal pigment form a single parameter.

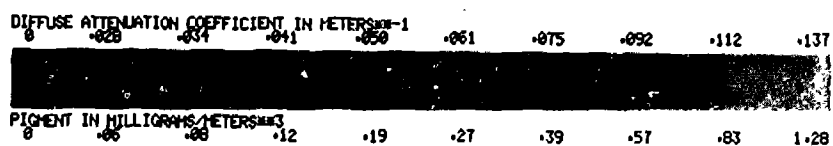
More problematic are the Case 2 waters where the nearly wavelength independent reflectance spectra of the non-chlorophyllous particulate material mask the signature of the phytoplankton, and where yellow substance, if present, also contributes to the colour change. Influence of all constituents must then be treated separately and more complex algorithms for retrieving their concentrations are needed. Sediment concentration values are not yet retrievable through the use of a single algorithm valid in all cases. However, the potential of remote sensing has been demonstrated in specific areas.



DIFFUSE ATTENUATION COEFFICIENT



PIGMENT



2.7.1 Processed Coastal Zone Color Scanner (CZCS) images showing the light attenuation (top), and phytoplankton pigment concentrations (bottom), in the near surface sea water off the U.S. East Coast on May 7, 1979. Land and clouds are masked to black. (NASA image. Gower, 1984)

2.7.3 Visualization of Dynamic Features

Apart from the problems of making quantitative estimates of pigment and/or seston, and to the extent that phytoplankton and other particulates (e.g. sediment), or optical properties in general can be considered as passive tracers of water movements, a visualization of dynamical features is possible through visible imagery. This ability is enhanced by the fact that a visible sensor "looks" into the sea and thus distinguishes between water masses which are hardly differentiated by their "skin" properties in the infrared or microwave regions of the spectrum. For large scale phenomenon, with strong surface temperature gradients, (e.g. western boundaries currents) no really new information is to be expected from colour imagery. However, studies of the associated, fluctuating mesoscale features (such as meanders, cores, eddies of different scales) can benefit from visible imagery. Lagrangian estimates of currents can be made from the trajectories of well identified patches. This imagery, in the near-future, will most likely provide a remarkable tool for the spatial and temporal description of structures at intermediate and small scales, even if this was not the initial aim.

Present visible imagery (CZCS) has revealed its potential in describing the oceanic structures from small to intermediate scales and appears to be not redundant with, and often richer than, thermal imagery. Figures 2.1.5, 2.1.6 and 2.7.1 provide examples of this. In figure 2.7.1, the more disordered motion in the right half of the scene indicates the effect of the chain of New England sea mounts, which crosses the centre of the image from north to south.

2.7.4 Aerosol Distribution, Water Albedo, Climate Research

Accurate corrections of the effect of the atmosphere are needed to recover the sea colour. Thus the distribution of aerosols--and perhaps an indication of their nature through their scattering properties--form a kind of by-product of dedicated water-colour instruments. The aerosol content allows geochemical studies of eolian transport to be made, and in addition is a parameter of prime interest in radiative transfer study and modelling.

This aerosol content is estimated from the observed radiance upwelling from the water surface at 670 nm, after correction for the computed Rayleigh scattering component. Water radiance at 670 nm is very low except when high seston is present and any observed radiance is therefore interpreted as being due to atmospheric haze. Fig. 2.7.2 shows an example of processed CZCS data in which the patterns of water radiance at 443 nm (bottom) which are influenced by phytoplankton and/or sediment content have been successfully separated from a strong radiance pattern due to a continental haze (top) near the coast of North America.

The present assessment of the aerosol content by passive techniques (e.g. CZCS) appears satisfactory above oceanic areas when Case 1 waters are encountered, (even if poor knowledge of the aerosol's optical properties prevents achieving an accurate atmospheric correction). For the sediment dominated Case 2 waters, there is an obvious interference between the aerosol

content and the in-water turbidity since both increase the reflectance in the red part of the spectrum, but in unknown proportions. Future sensors will extend spectral coverage into the near infra-red to help this separation.

The determination of the reflectance properties of a water body is in itself an important result since climate modelling implies the knowledge of the water albedo. Moreover the attenuation properties of the water, linked to the reflectance properties, provide information about the depth of penetration of visible radiation and thus about the thickness of layer where heat storage takes place. The upper panel of Fig. 2.7.1 shows an image whose grey levels are interpreted (bottom) in terms of the diffuse attenuation coefficients in m^{-1} .

All these derivative products (aerosol, albedo, heated layer), as well as the properties of the carbon cycle deduced from productivity studies, can contribute to improved climate modeling and research at regional and global scales.

2.8 Coastal Processes and Pollution

2.8.1 Tidal Flats and Shallow Water

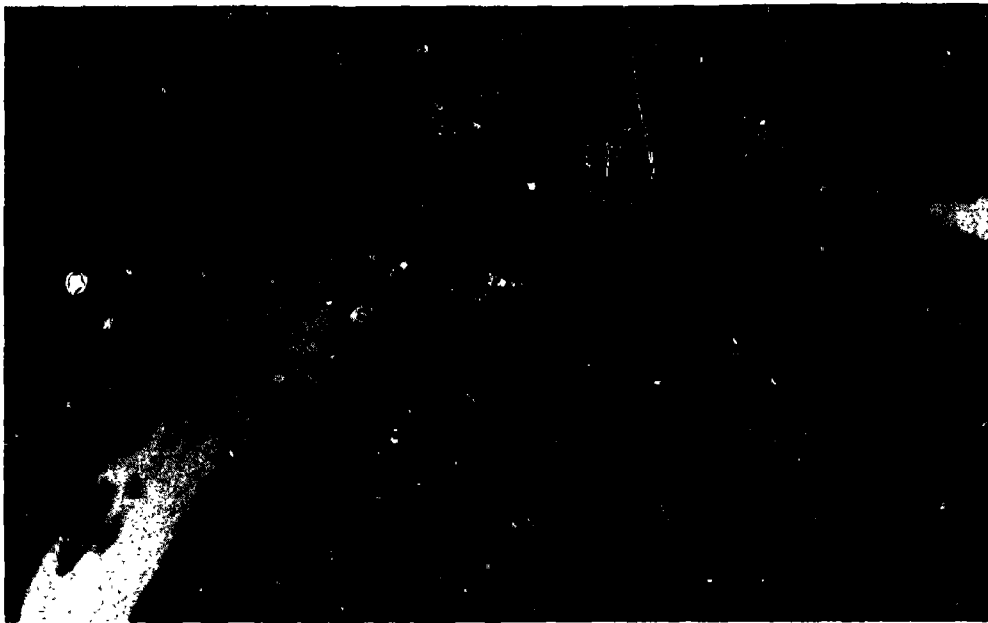
Interpretation of the reflectance (upwelling radiance) spectra of tidal flats and shallow water in coastal tidal regions requires a separate approach in making use of small scale observations. Besides sediment classification and coastal morphology surveys, synoptic pigment concentration measurements on the tidal flats would be helpful in the study of the various biological processes. For example, present estimates of the total primary production in the Wadden Sea, Holland, assign 50% to the production on the flats during low tides. Macrophytobenthos mapping and bathymetry, both as a function of space and time are other important objectives to be considered for remote (optical) sensing methods.

Also the heat balance investigations in the tidal areas, where the strong temperature gradients between the periodically drying tidal flats and the seawater (and their thermal interaction) substantially influence the aquatic ecological system, would benefit from remote satellite data on downwelling and upwelling solar fluxes (albedo) and on surface temperatures.

Most of the reported achievements deal with small scale analysis of Landsat imagery with respect to the sediment transport from estuaries to the open sea, mapping and classification of the tidal flat sediments, river runoff and erosion.

2.8.2 Pollution and Anthropogenic Influences

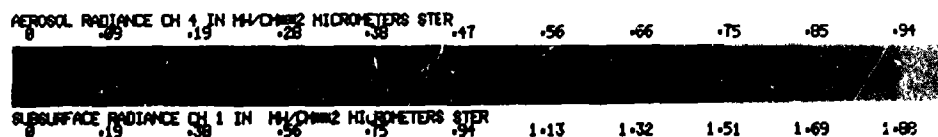
Pollution questions are relevant to the small or mesoscale, rather than the large scale. In coastal and estuarine areas pollution transport and dispersion is often related to sediment transport and distribution. The treatment of the pollution problem through remote sensing is thus bound with the monitoring of turbidity and in some cases, of eutrophication. At the present state of knowledge, there is apparently no specific method for remote monitoring of pollution by heavy metals, organic, organo-chlorines etc.



AEROSOL RADIANCE CH 4



SUBSURFACE RADIANCE CH 1



2.7.2 CZCS images for June 10, 1979, for the same area as Fig. 2.7.1 showing the computed atmospheric aerosol, or haze, signal (top), and the water leaving radiance in the blue band (bottom). The blue radiance is computed after removing the strong, along-shore haze pattern. Clouds, which obscure most of the U.S. and Canadian coastlines, and land, are masked to black. (NASA image. IOS/Canada, Cowar)

Of special interest, however, are the survey and monitoring of oil spills, involving their environmental consequences. A review of the present state of the art, (Ministere de l'Environnement, France, 1979), concluded that purely optical methods do not seem to be promising. Better results are obtained by thermal infrared and UV sensors. However UV imaging from satellites is problematic due to the large atmospheric effects. The presence of the oil film can increase or decrease the sea surface temperature and the surface reflectance depending on the type and thickness of the oil layer and on water quality, seastate, windspeed, etc.

Perhaps the best potential is offered by the passive and active microwave techniques (SMARR, SAR, scatterometer), since they can perform in all weather, day and night and in real time. Microwaves are backscattered by surface capillary waves, which are substantially influenced by the presence of oil slicks, at windspeeds between 1 to 20 m/s.

Several studies on industrial pollution, distribution and oil spills monitoring using Landsat imagery have been reported. Thermal pollution by the discharge of cooling water from power plants and other industry can also be observed in high resolution thermal infrared imagery.

A distinction must be made between the role of satellites in tracking the fate of known pollutants and in surveillance against excessive discharges of pollutants i.e. policing the seas. In the first case the use of satellites may be limited either by weather (for the optical and infrared sensors) or by the infrequent sampling imposed by the narrower swath microwave sensors. A synthetic aperture radar, for example, with a swath width of 100 km would be unable to provide useful tracking of a surface pollutant if deployed in a polar-orbiting satellite with a repeat period of several days.

However, if international agreement could be reached to discourage the excessive dumping of pollutants at sea then satellite surveillance might act as an effective deterrent, even if only relatively infrequent spot checks are possible.

2.9 Sea Ice

The maximum ice cover in the Arctic has been estimated at about 15.1 million km², while in the Antarctic the area covered is about 25.5 million km². There is a marked contrast between seasonal variations, fluctuations in the Arctic being about 20-25% while in the Antarctic they reach about 75% of the maximum. There is also a significant difference in the composition of the sea-ice cover, that of the Arctic having a multi-year component and a higher incidence of ridging and general deformation. In the Southern Ocean the annual northward drift of ice to warmer waters in the break-up season leads to the development of a high percentage of first-year ice in the following winter.

2.9.1 Effects on Transportation

The most immediate economic importance of sea ice is in its effect on shipping in the polar regions, especially in the Arctic where oil and gas developments are proceeding rapidly. Information on the large scale extent

and movement of ice is required for:

- . Support of offshore drilling and production operations.
- . Design of offshore structures in polar regions.
- . Improving the safety of navigation in the traditional shipping season.
- . Extending this season by providing data to improve ice cover forecasts.
- . Assisting in planning of ice breaking operations.
- . Support of fishing operations.

Satellites can provide optical, infrared or radar imagery from which accurate maps of ice cover can be compiled over large areas. Weather satellites provide full coverage, several times daily with 1 km resolution except when blocked by darkness and cloud in the case of visible imagery and by cloud in the case of infrared imagery. The Seasat SAR provided examples of precise ice mapping even though the low incidence angle caused a low and variable contrast between ice and water. In the future, routine ice mapping with satellite radar could operate in all weather, day or night, with the major limitation then being in the cost and power requirements of a radar capable of mapping a sufficiently wide swath to give acceptably frequent coverage. The Canadian Radarsat program proposes to use a radar, with a variable incidence angle, so that the area mapped can be steered to follow critical shipping routes in the Arctic. With future possible developments in power, microwave technology and preprocessing hardware, such satellite radars could provide the optimum sea ice mapping sensor. In the meantime airborne SAR is being used with considerable success.

2.9.2 Effects on Weather and Climate

Sea ice has several effects important to atmosphere-ice-ocean interaction which are highly relevant to world climate studies. In particular, it contributes to the thermodynamics by:

- . Increasing the surface albedo by up to a factor of 6.
- . Acting as a highly variable blanket insulating the relatively warm water from the cold atmosphere, and reducing the heat flow relative to open water by a factor of up to 100 in multi-year ice.
- . Substantially modifying the latent heat changes, both in its own formation and melting, and in preventing evaporation of the surface waters, thus modifying the seasonal temperature cycle.
- . Modifying the heat flow through the upper layers of the sea ice by increasing convection down to approximately 25 m. Since the ice holds only about 10% of the salt in the water, the water just below the ice is more saline and convection is enhanced.

Table 2.9.1

Satellite observations of sea ice

| Information needed | Sensor | Typical Resolution | Comments |
|------------------------------------|--------------------|--------------------|--|
| Ice cover maps | visible scanner | 0.1 to 1 km | High visible reflectance difference leads to easy ice/sea discrimination at adequate resolution; limited by cloud and darkness. |
| | thermal IR scanner | 1 km | Low ice/sea temperature difference causes problems. Useful in Arctic night, limited by cloud; resolution adequate. |
| | SAR | 0.20 to 1 km | Variable ice/sea contrast (of either sign) causes problems at steep incidence angles. Resolution adequate. Narrow swath coverage only, with present systems. All weather, day/night. |
| | SMMR | 30 km | Spatial resolution > 30 km, is insufficient for some studies. Multiband observations give fractional cover in each pixel. All weather, day/night data. |
| Ice edge location | ALT | 1 km along track | All weather day/night. |
| Surface roughness | ALT | 1 km along track | All weather day/night. |
| | SCAT | 30 km | All weather day/night. |
| First year/multi year ice fraction | SMMR | 30 km | All weather day/night. |
| Ice surface temperature | thermal IR scanner | 1 km | Blocked by cloud. |
| | SMMR | 30 km | Penetrates cloud. |

Additionally, snow cover has a very high albedo for shortwave radiation (low emissivity) and a very low albedo for longwave (infrared) radiation. Because of the above effects, climate studies require detailed information on the extent and variability of sea ice cover. Ice absorbs much of the incident energy from ocean waves by scattering, bending, ridging and fracture, leading to the opening and closing of leads which either stay open for a substantial time or re-freeze with only a thin layer of ice cover, substantially affecting heat exchange. Apart from the leads, there are within the ice-pack substantial open water areas entirely surrounded by ice polynyas) which also have a considerable effect on the net heat transfer.

Particular parameters of importance that can be examined by satellite sensors (see table 2.9.1) are:

- . Position of the ice-edge (atmospheric jet streams and depression tracks in the North Atlantic tend to be displaced parallel to the ice limit)
- . Ice concentration
- . Ice type - first year or multi year
- . Location and size of ice-free areas within the pack (leads, polynyas)
- . Surface roughness (as a measure of wind-ice coupling and its effect on ice movement and ice fracture).

International interest in the ocean cryosphere is revealing itself in, for example, the Marginal Ice Zone Experiment (MIZEX), which involves the USA, Canada, UK, France, Iceland, Norway, Denmark, Sweden, Germany, France, Ireland and Finland.

3. CAPABILITIES OF SATELLITE REMOTE SENSORS

This chapter gives short summaries of the capabilities of satellite-borne remote sensors and other instruments, to provide data of relevance to the ocean community. The discussions are purposefully light on the technical side and instead speak to the issues of providing information. The chapter confines itself to instrument capability, leaving to Chapter 4 the means by which these relate to requirements, since the questions of coverage, repeatability and the like, depend profoundly on the satellite and orbit on which the sensor finds itself.

3.1 Radar Altimetry, Tracking and Orbit Determination

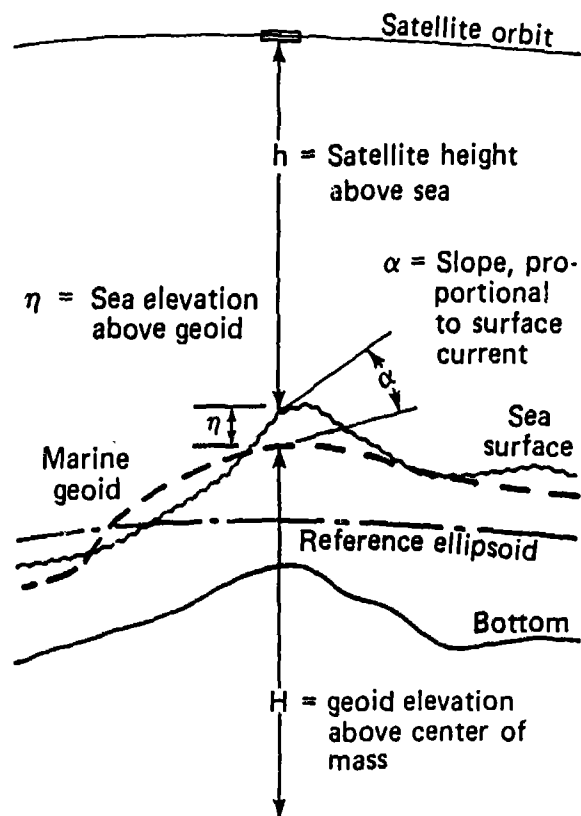
3.1.1 Radar Altimeter

The radar altimeter is an electronically sophisticated but conceptually simple device which, in Seasat, measured the height of the spacecraft above the sea surface (about 800 km), to a precision of about 10 cm and in TOPEX plans to improve this to 2 cm. This satellite sensor offers much promise to many different earth sciences (Born, 1984, AGU 1983). In principle, it is able, when combined with other data and with physical models, to provide information on the marine geoid, gravity anomalies, surface current speeds, tidal elevations, wave heights, wind speeds, ice cover and roughness, ice cap elevations, and indeed, any other process that changes the mean elevation or roughness of the sea surface on a large scale.

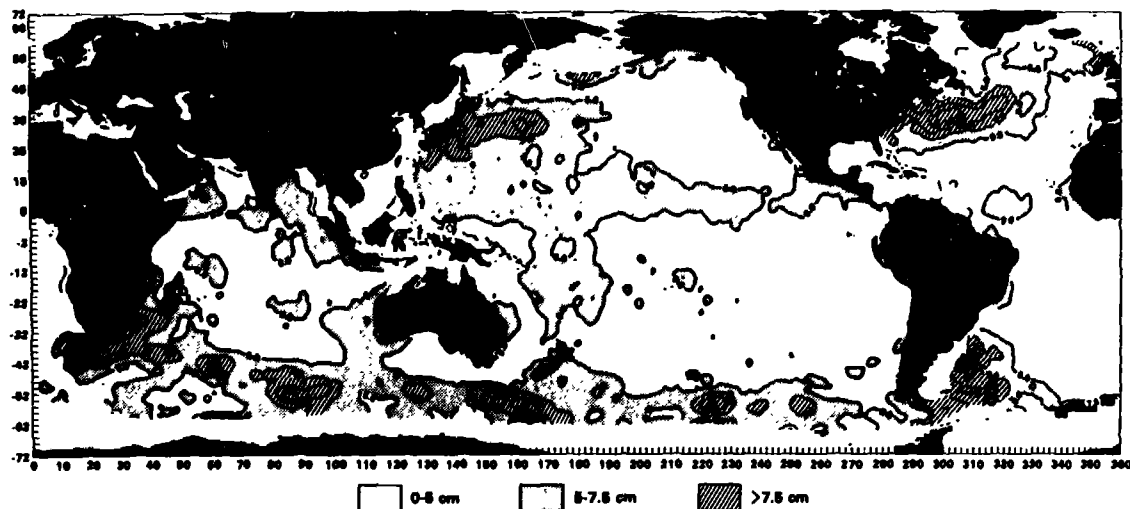
The most subtle and difficult of these measurements is the current determination, the principle of which is illustrated in Figure 3.1.1. This figure shows the various surfaces of relevance to the problem—the ellipsoidal earth, departures of the marine geoid (an equipotential) from that ellipsoid, and the further departures of the actual ocean surface from the geoid. It is the latter that one attempts to determine via altimetry, since the slope of the ocean surface relative to the geoid is proportional to the current speed at right angles to the satellite path. Thus slopes give information on kinetic energy of flow, while elevations give analogous information on the potential energy. To make these topographic measurements requires highly precise determinations of orbit, geoid, and altitude above the sea; there are several corrections required for ionospheric density, atmospheric pressure and water vapor, sea state, tides, and other secondary effects.

Global measurements of surface winds and waves offer obvious economic benefits to a variety of marine activities -- forecasting, offshore exploration, ship routing, etc. — as well as contributing to the study of large-scale air/sea interaction processes. The long-term monitoring of ocean topography, together with measurements on the variation of the polar ice cap which can also be made with the altimeter, yields information of value to the world climate research programmes.

Recent analyses of the Seasat altimeter data set has revealed a remarkably detailed surface topography which closely resembles the underlying sea-floor topography. Future altimeter missions should therefore produce charts which are of just as great geophysical interest as oceanographic.



3.1.1 Measurement of sea surface elevation and sea surface slope from satellite altimeters. A precise knowledge of orbit and marine geoid are required. Slope is proportional to the component of geostrophic surface current at right angles to the sub-satellite track (NASA, 1983c)



3.1.2 RMS surface height variability in sea surface heights as derived during the 27-day repeat period of Seasat. The high-variance areas are found in the meander regions of the major ocean systems (Cheney and Marsh, 1981)

The altimeter makes basic measurements of three types as a function of distance along the satellite sub-orbital path:

(a) The time delay between the transmission and return reception of the compressed radar pulse, along with precision orbit determinations, can be used to construct the topography of the sea surface.

(b) The broadening of the leading edge of the returned pulse can be used to derive significant wave height, H_g , and the exact pulse shape can be used to glean information on higher-order moments of the probability distribution function for sea surface heights.

(c) The amplitude of the returned pulse determines the normalized radar cross-section per unit area of the sea surface, σ_0 , from which one can calculate surface wind stress and speed, u^* and U , under certain assumptions.

The Seasat Data Utilization Project at the Jet Propulsion Laboratory (NASA 1981a) gave the following rms precisions for various quantities derived from that satellite.

(a) Satellite-to-surface height precision: $\pm 5-8$ cm for $H_g < 5$ m; ± 10 cm for $H_g < 10$ m; ± 15 cm for $H_g < 15$ m.

(b) Significant wave height H_g (defined as 4 times the standard deviation of a Gaussian sea): the lesser of $\pm 0.1H_g$ or 0.3 m, for $H_g < 8$ m.

(c) Radar backscatter cross-section, σ_0 : ± 1 dB for $2 < U < 25$ ms^{-1} ; implying a wind speed accuracy of about ± 2 ms^{-1} .

(d) Radial component of orbit determination ± 70 cm globally, with ± 50 cm ultimately determinable.

(e) Corrections to data: height bias, 11 cm; electromagnetic mean sea level bias $-0.05H_g$; error in correction for propagation through the ionosphere, ± 3 cm; error in correction for propagation through the wet troposphere, ± 3 cm.

The altimeter measures these quantities along a narrow swath approximately 2-5 km wide directly under the satellite. From spatial and temporal amalgamations of these data come global fields of considerable interest to the ocean community. Examples from Seasat provide useful guides for future spacecraft carrying altimeters. Figure 3.1.2 illustrates the variability in sea surface heights as determined during 27 days of the repeat-orbit period of Seasat. The largest standard deviation, of order 20 cm, is found in the regions of western boundary currents and the Antarctic Circumpolar Current. The observation period is less than one characteristic period for mesoscale motion. More extended data sets will allow much better estimates of variance to be made.

Figure 3.1.3 is a compilation of global significant wave heights, H_g , for the entire three months of Seasat's life. The time interval encompassed the Austral winter, and the figure therefore reflects the higher winter wave conditions in the Southern Hemisphere.

Figure 3.1.4 similarly displays isotachs of surface wind speed for the same period as Fig. 3.1.3. The asymmetry between southern and northern hemispheres is again apparent, with some regions showing three-month-average wind speeds in excess of 10 m/s.

It is clear that such data sets are potentially of great value to scientists and marine interests. Their application to particular problems must be tempered by a detailed understanding of the basic measurements, and the reader is referred to the literature for more information (e.g. references at the start of this section).

Table 3.1.1 summarizes characteristics of past and future altimeter missions, insofar as the latter are known.

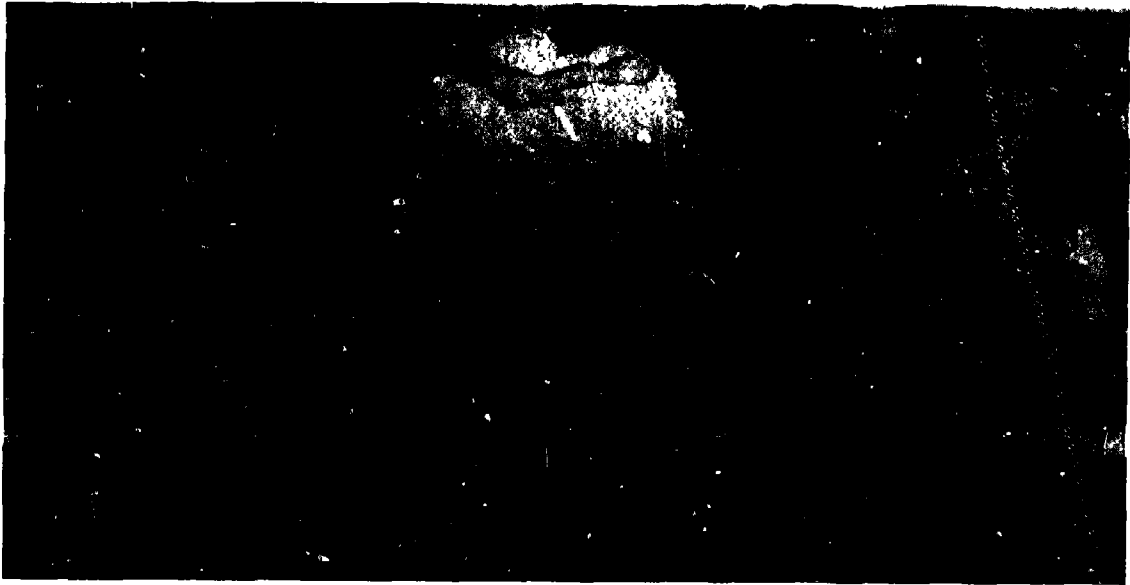
3.1.2 Satellite Tracking and Orbit Determination

Adequate tracking of a satellite's position forms an integral part of all earth surveillance programmes. For most sensors the requirement is to reduce errors in locating data points or objects seen in images to acceptable levels, or to levels comparable to errors from other sources, e.g. attitude uncertainties or instrument resolution. However, in order to interpret an altimeter's signal in terms of tides and ocean currents it is important to measure the vertical position of the satellite above the sea surface to the 0.1 m level or better, if possible. Such a stringent requirement requires a network of very precise tracking stations distributed across the globe. During Seasat the Precise Orbit Determination (POD) activity utilized ground-based radio-frequency and laser tracking as well as the onboard altimeter data itself. The satellite carried an S-band transponder, Doppler beacon and laser-retroreflector array. The tracking precision of the NASA lasers was about 10 cm while the European lasers varied from 10-100 cm. For Seasat the Doppler data produced range difference measurements with a precision of 10 cm at 30 second averaging intervals. Because of the density of stations a data set of the order of 200 passes per day was obtained which allowed a sequence of independent two-revolution orbit solutions. While the inherent accuracy of both the laser and S-band data is higher than Doppler, the sparsity of coverage requires longer arc lengths to define the satellite ephemeris.

The present level of accuracy of laser ranging is ± 5 cm but in European latitudes it is estimated that two out of three passes could not be tracked because of cloud cover.

The factors that influence the accuracy of the orbit computation of a near-Earth satellite are:

1. Accuracy of tracking
2. Distribution of tracking stations, and the amount and timing of the data they collect
3. Errors in tracking station co-ordinates
4. Ability to model spacecraft reflectivity and area-to-mass variations



3.1.3 Seasat altimeter significant wave heights for 7 July - 10 October 1978. During the Austral winter, regions of the Antarctic Circumpolar Current had averaged significant wave heights in excess of 5 m. (Chelton et al., 1981)



3.1.4 Seasat altimeter scalar wind speeds for 7 July - 10 October 1978. Wind speeds and wave heights are fairly closely correlated. (Chelton et al., 1981)

Table 3.1.1

Altimeter Missions

| Satellite and Date | Accuracies | | | Repeat Cycle | Lifetime | Objectives | Comments |
|--------------------|------------|------------------------------|------------------------------|--------------|----------|--|---|
| | Altimeter | Geoid | Orbit | | | | |
| SKYLAB 1974 | 100 cm | 5 m | 5 m | - | 20 days | test of principle | large geoid anomalies detected |
| GEO5-3 1975-1978 | 20 cm | 2 m | 2 m | 23 days | 3 years | first test mission | large volume of data gave good wind, wave, geoid, ice cap results, surface currents limited to large features |
| SEASAT 1978 | 7 cm | 1 m | 1.5 m | 17 days | 73 days | improved test mission "baseline" orbit. | good geoid and gravity results limited lifetime |
| | | | | 3 days | 27 days | improved test mission - "3-day repeat" orbit | current features including eddies derived. First demonstration of ocean tide results |
| GEOSAT 1984 | 3 cm | 0.5 m | | 150 days | 3 years | geoid mapping, waves, wind and major currents | Geodesy is primary goal, but geoid data are classified |
| ERS-1 1988/9 | 10 cm | 1 m | 1 m | 3 days | | operational for wind, waves and major currents | |
| MOS-2 1988/9 | | | | | | | Planned Japanese mission |
| TOPEX 1989/90 | 2 cm | 1 m (0.02 m with Gravsat) | 1 m (0.05 m with Gravsat) | 10 days | 5 years | operational for ocean circulation | Needed for World Ocean Circulation Experiment |
| NROSS 1988/9 | cm | 1 m | 1 m | 3 days | 1 year | waves, wind and major currents | Could be coordinated with TOPEX and ERS-1 with great increase in benefits |
| POSEIDON | 5 cm | | | | | technology development, ocean circulation | may try prototype on TOPEX followed by instrument on SPOT series satellite |

5. Errors introduced by the software and hardware used to compute the orbit
6. Errors in the models used to describe the forces acting on the satellite (Earth's geopotential, atmospheric drag and solar radiation)

At present NASA plans to provide the best ephemeris for a possible TOPEX mission relying on an upgraded Doppler system, TRANET II, of the type that proved its worth with Seasat. The proposed upgrading of the TRANET system refers to the replacement of the present oscillators in both the satellite and ground units with oscillators stable to a few parts in 10^{13} over a period of 1000 seconds. TRANET II is the recommended primary tracking system but in TOPEX this will be supported by a network of laser ranging stations.

It was hoped that the US Global Positioning System (GPS) which will employ 18 satellites and which should be fully operational by the time of the proposed ERS-1 and TOPEX missions, could be used to provide a precise tracking system of uniform accuracy around the globe. This may still be possible but at present NASA is considering using GPS in an experimental rather than operational mode on TOPEX. The proposed system called SERIES-X (Satellite Emission Range Infrared Earth Surveying Experiment) should provide very high precision range and Doppler measurements between GPS satellites and TOPEX, and between GPS satellites and SERIES ground stations. In theory the range measurements can be doubly differenced to eliminate all clock errors allowing short arc positioning of the spacecraft to a few centimeters accuracy.

An important element in future precise orbit determination could be the use of selected calibration zones, especially in ocean areas over which tracking data are not available. Areas which are oceanographically inactive (that is, with currents of small amplitude), and which preferably do not suffer unduly from strong winds, could be monitored by placing deep-ocean pressure gauges on the sea-floor and using the altimeter height itself as a measure of the radial component of the satellite's ephemeris. This is a concept which needs to be studied in greater detail.

It should be noted that the accurate tracking systems discussed above will only provide periodic determinations of range or range rate from which the continuous orbits (particularly its radial component) must be calculated. If the satellite were only affected by a uniform gravity field from the earth (and the sun and moon) these calculations would be straightforward, and only occasional tracking information would be required. The additional sources of error, however, as calculated for the TOPEX mission are due to:

1. The non-uniform gravity field of the earth. The variations are fixed and if measured with sufficient accuracy, e.g. with Geopotential Research Mission (GRM) the estimated error of about 50 cm could be removed.

2. Radiation pressure on the satellite. If the orientation of the satellite is known at all times this can be calculated, but the varying gravity field leads to errors. Again GRM would allow the error, of about 20 cm, to be reduced to about 5 cm.

3. Atmospheric drag on the satellite. For the high orbit chosen this has a very small effect of only a few centimeters.

TOPEX is planned especially to have a shape that minimizes drag and radiation pressure, and to be positioned well above levels where atmospheric drag is significant, since this varies in an unpredictable manner with solar emission levels. Other satellites such as ERS-1 and NROSS have bulkier and less regular shapes, and also need to occupy lower orbits to satisfy the requirements of other sensors.

The TOPEX mission offers another possibility for solving the orbit determination problem, in the form of SERIES-X, mentioned above. This system would allow continuous tracking of the satellite so that little or no interpolation would be needed.

3.2 Scatterometry

The earliest research into the performance of radar over the sea surface showed that backscatter depended on surface winds. Subsequent investigations into the quantitative relationship led to the design of an airborne combined microwave radiometer and scatterometer known as RADSCAT (Jones et al 1977) and later to the first satellite-borne scatterometer flown on Skylab. For incidence angles greater than 25° the data suggest that the dominant mechanism is Bragg or resonant scattering. At the Ku-band frequency used in Seasat the Bragg condition is satisfied for ocean waves of wavelength about 2 cm. These ripples which appear in light winds, grow in amplitude with increasing wind speed. The fact that backscatter for off-nadir observations has been shown to depend on radar azimuth angle, with maxima in the upwind and downwind directions and minima close to crosswind, allows an estimate to be made of wind direction with some ambiguities. In the Seasat-A Scatterometer System (SASS) the ocean was viewed at two azimuths using four dual-polarised fan-beam antennae aligned so that they pointed $\pm 45^\circ$ or $\pm 135^\circ$ relative to the satellite's track. The SASS resolution was approximately 15 km across beam and 70 km along beam and the incidence angles ranged from 25° to 55° for the regions illuminated by both forward and aft beams.

The performance of SASS and the correctness of different geophysical algorithms could be assessed by comparing them against calibrated surface data obtained in the Joint Air Sea Interaction Experiment (JASIN) which fortuitously coincided with the short-lived Seasat mission and with the specially-designed Gulf of Alaska Seasat experiment (GOASEX). Detailed assessments of SASS's performance have been given by Jones et al. (1982) and Pierson (1983).

Results show that SASS measured wind speed to an accuracy well within WMO specifications and that, provided the ambiguity between different solutions for the wind vector can be solved, wind direction can also be measured to useful accuracies. The JASIN comparison showed wind speed to agree with surface observations to ± 1.7 m/s and wind direction to $\pm 17^\circ$. Some uncertainty about SASS performance at high wind speeds (> 16 m/s) remains. Successful automatic removal of directional ambiguities from Seasat data remains an unresolved problem, but it is expected that scatterometers which measure backscatter from 3 different azimuths will be much less

Table 3.2.1

Scatterometers

| Satellite | Launch year | Waveband | Swath | Number of Antennae | Number of Polarizations | Spatial Resolution |
|-----------|-------------|----------|--|--------------------|-------------------------|--------------------|
| SEASAT | 1978 | ku | 2 x 475 km ⁽¹⁾ 140 km ⁽²⁾ | 4 | 2 | 50 km |
| NOSS | Cancelled | ku | 2 x 500 km ⁽¹⁾ 320 km ⁽²⁾ | 6 | 2 | 25 |
| ERS-1 (E) | 1988/9 | C | 400 km ⁽¹⁾ | 3 | 1 | 50 |
| NROSS | 1988/9 | ku | 2 x 500 km ⁽¹⁾ | 6 | 2 | 25 - 50 |
| MOS-2 | 1988/9 | ku | 500 km ⁽¹⁾ | 3 | 1 | 25 - 50 |

All above aim for accuracies of wind speed: ± 2 m/sec or 10%, whichever is larger, and direction: $\pm 20^\circ$, for the speed range 4 to 25 m/sec.

(1) Swath of wind vector measurements.

(2) Additional swath in which wind speed only will be deduced.

affected by this problem (O'Brien 1982). Alternate methods of data processing incorporating meteorological modelling are also being tried on Seasat data (Wurtele et al 1982). Questions also remain in relating the scatterometer outputs to surface stress, or to wind speed at buoy, ship or cloud-base heights for comparing with other data.

Achievable accuracies for future scatterometers appear compatible with requirements for surface stress measurements for determining the driving force on ocean circulation and for mapping surface wind speed for weather and wave forecasting. Sampling with a single satellite - especially with a swath width of 400 km which is the design objective of ERS-1 - falls short of that defined for a global experiment which is that 90% of the points at the equator and at latitude 35° should be observed to within 50 km at least every two days (O'Brien, 1982). Properties of different scatterometers, past and future, are compared in table 3.2.1. The NOSS instrument is included for comparison. All except the ERS-1 instrument operate at Ku band (see Table A2 in the Appendix for band names) and can therefore benefit directly from experience with the Seasat data. Spatial resolutions are 50 km or better, satisfying the requirements for global surface stress measurements. The accuracy of position location is not stringent; 50 km, absolute, is satisfactory with 10 km relative accuracy. Coastal and inland sea applications would require both greater positional accuracy and higher spatial resolution.

Determination of atmospheric liquid water content is required for accurate scatterometry, although at the C-band proposed for the ERS-1 system these effects should be less than at the Ku-band of SASS. For optimum results a scanning microwave radiometer is required, preferably not just a nadir viewing instrument as required by the altimeter.

The evolution of satellite scatterometry has produced a sensor capable of producing global estimates of wind velocity on a daily basis to an accuracy superior to ship's observations. Following the demise of Seasat in 1978 no other scatterometer system has flown from a satellite and the first systems are likely to be carried by the U.S. Navy's NROSS and by ERS-1 in about 1989.

For the future, dual-frequency instruments are being discussed to measure the wave field over the ocean surface. Further research is still required to investigate the sensitivity of different radar frequencies to the high frequency portion of the wave spectrum sensitive to changes in wind speed.

3.3 Synthetic Aperture Radar (SAR)

Synthetic aperture radars use the varying Doppler shift of the reflected signal introduced by motion of the satellite to separate the return signals from different points on the ground, when these points are closely spaced in the along-track direction. Separating targets in the across-track, or range direction, is by means of their range difference in the swath being mapped. This must therefore be off to one side of the satellite. Range measurements can be very precise, to a few meters, using techniques similar to those in altimetry, though the number of measurements to be made is here much greater. Use of the Doppler shift in the along track direction gives much greater resolution than is implied by the usual, diffraction, limit due to

the physical size of the radar antenna or "aperture." The full Doppler shift analysis applied to two seconds of coherent satellite data gives a resolution equivalent to a synthetic aperture about 15 km long for Seasat.

The synthetic aperture method brings the along track resolution down to a few meters, comparable to the achievable range resolution. Both these resolutions are now independent of range (sensitivity permitting) and allow extremely precise radar mapping of the earth's surface from orbit. Radar images suffer from the speckle effects peculiar to coherent imaging systems, which cause strong variations in the signal observed at any pixel. In practice, resolution can be degraded to suppress this, though this will cause the loss of some small scale features. In Seasat the along track resolution limit was increased from 6 to 25 meters to allow smoothing to "4 look" imagery. This simplifies the processing, and gives a match to the 7 meter range resolution which implies 20 meter ground resolution when projected from an incidence angle of 20° .

Satellite SAR's can now, in principle, provide images of the sea surface along continuous swaths of the order of 100 km width at a resolution of about 20 m. Currently, a limitation is imposed by the high power requirement of the instrument, which in the case of Seasat, for example, restricted the operating time to 10 minutes per orbit. The high bit rate (about 100Mbits/s) of the instrument precludes storage of the data on board a satellite, so that images can be obtained only within line of sight of a receiving station. This limited the coverage of the Seasat SAR and will similarly affect future free-flying satellites. On the short, Shuttle Imaging Radar (SIR), missions (Ford et al. 1983) the data is recorded and can thus be collected from over a much wider area. This will be limited in latitude by the inclination of the orbit (38° for SIR A, 57° for SIR B), and by the scheduling of the (usually crowded) missions.

The intensity of the SAR return signal at any pixel is a measure of the radar reflectivity or cross section, σ_0 , which on the large scale over the ocean is determined by the wind speed, as discussed for scatterometry (section 3.2). SAR images show small scale wind patterns round topography and near squall lines for example, but on a larger scale the scatterometer output is more complete and useful.

The Seasat SAR and Shuttle (SIR) radars have imaged ocean surface features superimposed on the mean background due to wind. These include surface waves, internal waves, water mass and current boundaries, ship wakes and surface signatures closely correlated with the detailed bathymetry, see Figs. 2.4.1 and 2.5.1 and Table 3.3.1. These become visible in microwave images through the modulation of the (largely Bragg) backscattering small scale structure of the sea surface, by the larger scale features appearing in the image. While the basic theory of backscattering and SAR imaging is believed to be fairly well understood, the dynamical details of the modulating processes are often only poorly known (Hasselmann et al., 1985). Nevertheless, even if the image transfer function cannot be specified a priori, the pattern information of a SAR image (e.g. the relative distribution of wave energy in the two dimensional surface wave spectrum, the position of fronts and current shear zones or the general features of the bottom topography) can be very valuable when the SAR data is imbedded within a general data set including the missing complementary information. This is

Table 3.3.1

Ocean features observed on SAR

| Feature | Visibility | Possible Applications |
|-----------------|---|---|
| Surface waves | Swell components and long wind wave only. Large directional effects. | Useful for wave monitoring applications. Directional information is especially useful. |
| Internal waves | Surface expressions often visible. | Useful for some indications of stratification and mixing. |
| Ship wakes | Visibility very variable | May be useful for monitoring of fisheries or arctic traffic |
| Fronts | Visibility variable Abrupt Gulf Stream fronts usually visible | Cloud penetration advantage may make this a useful complement to VIS/IR |
| Currents | Gulf Stream eddies and tidal current directions are often indicated by linear features due to shear or convergence | Feature location when clouds block visible/IR images |
| Bottom features | Surface expressions visible in shallow water (< 50 m) with high currents (> .5 m/s) | Imaging mechanism not well understood. Potentially interesting method of rapid qualitative hydrographic surveying |
| Ice cover | Ice extent and movements visible to high precision. Contrast varies with sea state for small incidence angles. Gives some information on ice types and thickness. | Very useful for general all weather ice monitoring. |

Table 3.3.2

Synthetic aperture radars

| Name | Launch | Carried On | Band | Wavelength | Swath | Incidence | Resolution | Designed for |
|-------|--------|----------------------|------|------------|--------------------|---------------------|---------------|-----------------------------|
| SAR | 1978 | SEASAT | L | 23.5 cm | 100 km | 23° | 25 m | Wave spectra |
| SIR-A | 1981 | Shuttle | L | 23.5 cm | 50 km | 50° | 40 m | Land features |
| SIR-B | 1984 | Shuttle | L | 23.5 cm | 50 km ⁺ | 15-60° ⁺ | 25 m | Experimental land and ocean |
| MRSE | 1984 | Shuttle/ SPACELAB | X | 3 cm | 10 km | | | Experimental land and ocean |
| SAR | 1988/9 | (E) ERS-1 | C | 5.7 cm | 80 km | 23° | 30 m 100 m | Experimental land and ocean |
| SAR | 1988/9 | (J) ERS-1 | L | 23.5 cm | 110 km | 23° | 25 m | Experimental land and ocean |
| SAR | 1990 | Radarsat | C | 5.7 cm | 200 km* | 20-45° | 25 m | Ice Survey |

⁺ Variable incidence angle capability or selectable offset with 200 km accessibility swath.

* Selectable offset within 500 km accessibility swath.

normally available from conventional instruments or other satellite sensors (e.g. the altimeter, which provides the significant wave height and the magnitude of the surface geostrophic current--although not at the same time or position as the SAR image).

A SAR image of surface waves shows their direction (with 180° ambiguity) and wavelength directly, since the waves appear as a series of short but nearly parallel "crest" lines (fig. 2.4.1). In fact the lines of increased radar reflectivity will correspond to positions defined by the combination of surface roughness, tilt and motion of the surface, and of image layover, rather than the actual crests, but the apparent effect on the image is similar. Visibility of waves with different heights, wavelengths and directions will be expected to vary depending on viewing azimuth and surface conditions, especially wind speed.

More precise information on wave length and direction can be derived automatically by forming two dimensional Fourier transforms of the image data. This allows separation of multiple wave components and in general gives useful wave spectrum information. However caution is required in simply relating the surface wave spectrum to this SAR image spectrum through a linear transfer function, since the imaging mechanism is linear only for dispersed swell. Wind waves are transformed in a very non-linear manner. For wind speeds less than 10 m/s it is questionable whether the wind wave spectrum can be recovered from the SAR image except perhaps for waves travelling in the radar range.

For large (ocean) scale wave data mapping, it is clearly unnecessary to compute spectra for all points on an image, since small areas (say 10 km x 10 km) separated by 50 to 100 km can give all the information that is useful. For this reason, a "wave-scatterometer" mode with burst data collection is planned for ERS-1.

The principal characteristic of SAR's which have already flown on satellite missions, or are planned for future satellites are summarized in Table 3.3.2.

The number of different areas covered by satellite SAR data is restricted by the limited lifetimes of the Seasat and SIR missions. Enough data exists to show how useful the data can be. Future missions should provide much greater coverage.

3.4 Microwave Radiometry

Passive microwave radiometry measures the radiation naturally emitted by, or reflected from the sea surface. Since the sea water has a finite temperature (near 300°K) black body radiation is emitted as microwaves as well as in the infrared, and can be measured from space to a precision approaching 0.1°C and a spatial resolution down to 30 km. Practical limitations degrade these figures.

Microwave radiation is measured using a tuned receiver to amplify the power received by a directional antenna. Because of the spectral properties of long wave black body radiation (Rayleigh-Jeans law) the microwave power emitted by a non-reflecting target is proportional to its physical

temperature. Since absorption of microwave radiation by clouds is quite small, an attractive possibility exists for measuring accurate, all weather sea surface temperatures from space. However the following important problems arise.

1. The sea surface is highly reflective (up to 70%) at microwave frequencies. The reflectivity value needs to be determined to correct the measured temperature. It will depend on surface roughness due to wind waves and foam and is strongly affected by presence of ice. Reflected microwave solar radiation can also lead to large and variable errors.
2. At the longer wavelength range in which sea surface temperature can be measured with small atmospheric influences, man made interference is a problem, and the spatial resolution of present satellite systems is coarser than 100 km. No "synthetic aperture" technique is available to easily reduce this figure (in one dimension) since the black body radiation is incoherent. Systems making use of arrays of receiving antennas could be used as in radio astronomy to achieve higher resolution.
3. Accurate sea surface temperature measurements require corrections for both surface and atmospheric effects using measurements at several microwave wavelengths which will not usually give the same field of view.

Early microwave mapping instruments operated at high microwave frequencies (short wavelengths) to achieve better resolution (about 30 km) for mapping gross signal variations due to sea ice cover and precipitating cloud water. Seasonal ice cover maps even at these coarse scales have provided valuable data on ice edge position, and on the existence of polynyas in both the Arctic and Antarctic (Carsey, 1985).

The Scanning Multichannel Microwave Radiometer (SMMR) flown on Seasat and Nimbus 7 (Gloersen and Barath, 1977) is a much more sophisticated ten channel instrument (see Table 3.4.1) designed to separate and measure the various bulk (sea surface temperature) surface (roughness due to windspeed, ice cover) and atmospheric (water vapour, liquid water) effects that influence the received signal.

A series of microwave radiometers have been flown on Russian spacecraft in the Cosmos, Meteor and Intercosmos series since 1968. These have been mostly profiling single or dual band instruments in the wavelength range 0.8 to 8.5 cm. A 0.8 cm wavelength scanner was flown on a Meteor satellite launched in 1976. These instruments have demonstrated the potential application of this type of data for oceanic and atmospheric observations, and have evaluated the optimum wavelengths for measuring temperature, salinity, roughness (wind speed), water vapour and liquid water content of the clouds (Basharinov and Shutko, 1980, Shutko and Grankov, 1982). Russian satellites have not so far produced large scale repeated coverage of these data.

Table 3.4.1

Passive Microwave Instruments

| Sensors | Satellite | Wavelength (frequency) | Swath Width | Spatial Resolution (IFOV) | Observed Items |
|---------|------------------------------|---|-----------------|---------------------------------------|--|
| ESMR | NIMBUS-5 NIMBUS-6 | 1.55 cm(19.4 GHz) | 700 km | 35 km | Sea ice cover atmospheric liquid water |
| SMMR | SEASAT-1 NIMBUS-7 | 0.81 cm(37.0 GHz) 1.43 cm(21.0 GHz) 1.67 cm(18.0 GHz) 2.80 cm(10.7 GHz) 4.55 cm(6.6 GHz) | 700 km | 28 km 136 km | Atmospheric liquid water Atmospheric vapour Surface wind Sea Surface Temp. |
| LAMMR | NOSS (now can- celled) | as for SMMR | as for SMMR | 4 x smaller than SMMR | improved spatial resolution, data as for SMMR |
| MSR | MOS-1 | 0.96 cm(31.4 GHz) 1.26 cm(23.8 GHz) | 320 km | 21 km 30 km | Atmospheric water vapour and Liquid Water |
| ATSR* | ERS-1 | .82 cm(36.5 GHz) 1.26 cm(23.8 GHz) | sounder only | 22 km | Atmospheric water vapour and liquid water for altimeter correction |
| SSMI | DMSP | 0.35 cm(85.5 GHz) 0.81 cm(37.0 GHz) 1.35 cm(22.2 GHz) 1.55 cm(19.3 GHz) | as for SMMR | as for SMMR (10 km at 85.5 GHz) | Similar to SMMR Improved spatial resolution at 85.5 GHz |

* Similar sounder measurements are needed for precise correction of any altimeter mission data, e.g. NROSS or TOPEX. GEOSAT will rely on seasonal average water vapour values.

3.4.1 Sea Surface Temperatures

Sea surface temperature (SST) retrievals from the SMMR have a spatial resolution of 150 km and can now be made with practically zero bias and a standard deviation of 1.0°C over the range 10 to 30°C when compared to high quality surface truth in the north Pacific and west Atlantic (Njoku, 1985). In data sparse regions such as the south Pacific, comparisons with climatology and fields interpolated from ship measurements indicate similar rms accuracy, although a warm SMMR bias of 0.5 to 1.0°C appears evident in the cold (4°C) Antarctic ocean region. The bias could be removed by simply changing the estimation algorithm, but it may perhaps be caused by Antarctic ice in the antenna sidelobes. The global retrieval accuracies degrade in the presence of rain, sunglint, man made interference and within 600 km of large land or ice masses. Faraday effect modelling errors sometimes cause SST in the outer SMMR swath cells to be biased by as much as 1°C in the daytime.

3.4.2 Surface Winds

Surface wind speeds from the SMMR have not been evaluated on as large a scale as the SST's. In comparison with ship and buoy spot reports, and with locally analyzed wind fields in the northern Atlantic and Pacific oceans, (Cardone et al. 1983) the SMMR winds show an rms accuracy of about 2.5 m/s over a measured range of winds from 2 to 25 m/s. (This is close to the accuracy of the surface observations themselves.) The biases appear to vary however, at different regions and times, generally within 0.7 m/s, but in one anomalous case as high as 2.9 m/s (JASIN area). Globally, the SMMR and SASS winds show very good agreement, i.e., within 2 m/s rms in most regions. Anomalies have not been investigated in detail. The SMMR wind accuracies degrade under the same conditions as mentioned above for SST. This data has been discussed recently by Chelton and McCabe (1985).

3.4.3 Atmospheric Water Vapour and Liquid Water

The SMMR vertically integrated water vapor measurements compare favorably with coincidental radiosondes in the tropics and mid latitudes, with practically zero bias and standard deviation of less than 0.4 g/cm² over the observed range of 1.0 to 6.5 g/m², with most of the scatter occurring at the high end of the range.

The accuracies discussed above have been achieved without regard to cloud cover, except for the filtering out of precipitating clouds as determined by the SMMR rain algorithm.

The remaining SMMR parameter accuracies have so far not been sufficiently demonstrated, either from lack of resources or lack of comparison data. However, theoretical accuracies are as follows: cloud liquid water (vertically integrated), 0.01 g/cm² over the range 0 to 0.2 g/cm²; rain rate, within factor of 2; sea ice concentration, ± 5%.

3.5 Infrared Imagery

Satellite infrared images of the oceans have been used for the past ten years to study ocean features which cause observable variations in surface

temperature, such as currents, fronts, upwelling and coastal mixing patterns. Imagery is provided by a variety of sensors, see Table 3.5.1. Such images are still the most widely used satellite remote sensing product for oceanography, though use of ocean colour images is now rapidly increasing.

Initially the satellite infrared data were only available in photographic form as a by-product of meteorological, cloud imaging. Recently digital image data have become more available. These allow quantitative estimates of sea surface temperatures, either using calibrated single wavelength band measurements, or to higher accuracy by combining measurements from different optical or infrared wavelengths in a variety of ways (see below). Digital data can also be radiometrically enhanced to give images showing small temperature differences, and geometrically rectified to allow data to be compared for different days (other view positions) and from different data sources (other sensors on satellites, ships, etc).

3.5.1 Imagery of Surface Features

Algorithms for calculating accurate absolute temperatures from infrared data amplify the noise and often require spatial averaging. For imaging features using temperature differences, however, the full spatial and radiometric resolutions of the sensors can be used. With present systems changes as small as 0.1°C can be mapped over distance scales down to 1 km for polar orbiting, and to 8 km for geostationary satellites. On smaller scales, 200 m resolution is sporadically available from thermal bands of scanners on later Landsats.

Western boundary currents such as the Gulf Stream, Kuroshio, Agulhas and Brazil currents give temperature contrasts as high as 5 to 10°C over distances of 10 km, and can be mapped from thermal imagery in great detail. Many other important features have smaller thermal expressions requiring higher sensitivity. Legeckis (1978) presented a survey of fronts, mostly at ocean current boundaries, detected by satellites. The images show the areal extent of such currents, variation in their frontal boundary positions, wavelike motions along these boundaries and eddies shed from them. Other studies discuss particular examples in more detail (Chamberlin 1982, Legeckis and Gordon 1982, Crepon et al, 1982, Brooks and Legeckis 1982, Van Woert 1982) or consider fronts caused by mixing on shallow continental shelves (Simpson et al 1978, Pingree and Griffiths, 1982). These reports show how satellite observations can contribute to physical and biological oceanographic studies.

Polar orbiting satellites can give images up to twice daily, but with large variations in the view geometry. Geostationary satellites can show half-hourly changes of particular dynamic features from fixed viewing points over the equator. This more frequent viewing also allows observation in brief cloud-free intervals. Cloud cover is a strong limitation for this type of data in most parts of the world. Clouds must be recognized on the images so that affected areas can be rejected. Simultaneous visible images are often needed for this. Alternatively, high clouds can be identified by their low temperature, and low clouds and fog can be distinguished from water where they cross coastlines, or by noting the characteristic eddy scales of water features. Clouds can also be distinguished by their relative transience, if

Table 3.5.1

Thermal infrared imaging sensors

| Sensors | Precision* | | Resolution | Bands | | Used for |
|--------------------|------------|------|------------|-------|-----|--|
| | °C | bits | | VIS | TIR | |
| SR | 0.5 | 8 | 8 km | 1 | 1 | Boundary current structure |
| VHRR | 0.3 | 8 | 1.1 km | 1 | 1 | APT in real time. Ice. Boundary current and other fine structure |
| AVHRR | 0.1 | 10 | 1.1 km | 2 | 3 | " |
| VISSR ¹ | 0.5 | 8 | 8 km | 1 | 1 | Movements of dynamic features |
| HSS ⁺ | 0.5 | 6 | 238 m | 4 | 1 | Coastal features |
| TM ⁺ | 0.5 | 6 | 120 m | 6 | 1 | Coastal features |
| MVISSR | 0.5 | 8 | 5 km | 1 | 2 | As for VISSR but with different spatial coverage |
| CZCS ⁺ | 0.5 | 8 | 0.8 km | 5 | 1 | Boundary current and other fine structure, with coincident colour data |
| VTIR ² | 0.5 | 8 | 0.9 km | 1 | 3 | Similar to AVHRR, with IR water vapour channel |

* Varies with noise level for different instruments of each type. See later discussion for resulting temperature accuracy.

+ Thermal channel operated for limited periods only.

1 VISSR Atmospheric Sounder on current GOES satellite also has 12 infrared bands

2 Proposed for the Japanese MOS-1

Table 3.5.2

Sea surface temperature determinations

| Sensor | Bands used | | Method | Accuracy achieved or expected (RMS) |
|--------|------------|---------|---|-------------------------------------|
| | optical | thermal | | |
| SR | 1 | 1 | Cloud screening Seasonal model | 1.5 to 2° |
| VTIR | 1 | 1 | Multiband TIR | 1.5° |
| VHRR | 1 | 1 | Cloud screening with statistical tests | 1.5° |
| VISSR | 1 | 1 | Variable path length | --- |
| AVHRR | 1 | 3 | Cloud screening with statistical tests Multiband TIR | 0.6° |
| ATSR | 1 | 3 | Variable path length Multiband TIR | 0.5 to 0.3° (expected) |

more than one thermal image is available over a fairly short time period (one day to one week).

Care must also be taken in interpreting thermal imagery to allow for effects of atmospheric absorption, and for the existence of thin surface layers of warmer water caused by solar heating, that often mask features in the tropics and at higher latitudes during the summer, especially during calm periods. Ice-melt water can similarly mask features near ice edges in the polar summers. Differential heating under patchy clouds can also lead to transient surface structure with up to 0.5° contrast. Atmospheric absorption will lead to an offset in the apparent temperature of the ocean by several degrees, and variable conditions can therefore lead to spurious temperature patterns. These variations are generally on a large spatial scale, and do not usually interfere with the identification of smaller scale features.

3.5.2 Infrared Sea Surface Temperature Measurements

Digital data from the same infrared imagers considered above have been used for a number of years to estimate the temperature of the ocean surface, although most of them were designed primarily to fulfill a meteorological objective such as cloud imaging. In addition non-scanning profiling instruments have given useful coverage for large scale studies. The accuracies achieved for sea surface temperature measurements are listed in Table 3.5.2.

Maul and Sidran (1973) made estimates, based on atmospheric radiation calculations, that the SR instrument would be capable of measuring sea surface temperature to about 2°C accuracy, the two dominant error sources arising from absorption of infrared radiation by atmospheric water vapor and spatially unresolved clouds in the radiometer's field of view.

Attempts to derive quantitative, absolute estimates of sea surface temperature routinely from the SR were initiated by NOAA in 1973, but met with limited success. Barnett et al (1979) compared the resulting satellite-derived temperatures, called GOSSTCOMP (global ocean sea surface temperature computation), with research quality in-situ measurements. They found errors of about $1-4^\circ\text{C}$ rms.

In 1978 a new generation of NOAA polar-orbiting meteorological satellites began, carrying the AVHRR-sensor. The channel centered at 3.7 m was originally intended to operate primarily as a nighttime cloud discriminator. However, it was found to have more value when combined with the 11 m and 12 m channels to correct for the variable amount of water vapor in the atmosphere, and thereby derive more accurate sea surface temperatures.

Bernstein (1982) and McClain et al. (1983) have demonstrated derivation of sea surface temperatures from AVHRR data to an accuracy of about 0.6°C rms when compared with high quality ship and buoy data. Both found that eliminating all cloud contaminated pixels is the critical step for obtaining accurate results.

It is hard to verify the accuracy of these temperature determinations because

- (a) good quality surface measurements are scarce

(b) the satellite data is averaged spatially over at least 1 km^2

(c) the satellite senses only a very thin surface layer

The accuracy of 0.6°C has been checked against large collections of ship and buoy data (Njoku, 1985). The value is near the best accuracy expected from the AVHRR sensor, and is only slightly larger than the differences expected due to (b) and (c) above. More checking of these techniques is still needed to confirm their accuracy in a wider range of conditions.

The level of computation required for the algorithms proposed may be beyond many users for some years to come, but demonstrated capabilities for atmospherically correcting satellite data will make it increasingly attractive, and lead to wider use of improved processing hardware.

Satellite infrared sea surface temperature measurements were affected over large areas for several months by the volcanic eruption of El Chichon in April 1982, which sent enough aerosol into the stratosphere to cause errors of several degrees. Changes in the algorithms were needed to correct for this. In the meantime maps of the resulting errors when compared to surface measurements showed the movement and intensity of the near global aerosol cloud.

Other approaches for improved accuracy in infrared sea surface temperature determinations are also being investigated. Observing the ocean from a satellite from two different directions, having different path lengths through the atmosphere, should also allow atmospheric effects to be determined. Experiments have been tried with geostationary satellites but present sensors lack the high accuracy required and coverage is limited by the geometry and the areas of overlap between satellite fields of view.

A sensor is now being designed to use this technique on the polar orbiting European satellite ERS-1. This is the Along-Track Scanning Radiometer (Llewellyn-Jones, 1982), designed to view the ocean at 3.7, 11 and 12 microns wavelength at two incidence angles using an offset conical scan with a half angle of 30° . It is hoped to achieve 0.5°C accuracy for the average temperature of 50 by 50 km areas within the 500 km wide field of view of the sensor. In addition it is planned to add two microwave bands for correction of the ERS-1 altimeter. Modelling experiments show that these should also allow an increase in accuracy from 0.5°C to 0.3°C in the temperature determinations. A visible channel is also being discussed. Technical details and the results of background studies are given in the above referenced report.

3.6 Visible Imagery

3.6.1 Imagery of Surface Features

Following the continued development of improved satellite optical sensors, qualitative and quantitative descriptions of various oceanic features from visible images have been extensively investigated. Compared to recent quantitative measurements of water spectral radiance (colour) with the Coastal Zone Color Scanner (CZCS) (Hovis et al. 1980) for deducing concentrations of suspended and dissolved materials in the water, many uses

Table 3.6.1

Ocean features studied with optical imaging sensors.

| Satellite-sensor | Observed Features; | Deduced Phenomena | Sample References |
|--------------------------------------|---|--|---------------------------------|
| NOAA-SR NIMBUS-4 ESSA 8 APT | cloud patterns water temperature | thermal currents ice fields | La Violette, 1974 |
| NOAA-VHRR DMSP | sunlight patterns combination with infrared imagery | ocean currents frontal processes | La Violette et al 1980 |
| GOES LANDSAT-MSS NIMBUS-7-CZCS | sediment and phytoplankton, colour patterns | phytoplankton growth particle load sediment transport | Szekiela 1982 |
| LANDSAT-MSS | surface reflectivity | internal and surface waves | Apel et al 1975 |
| LANDSAT-MSS | sediment patterns | concentration of suspended matter | Thomas 1978 |
| LANDSAT-MSS | sea ice patterns | sea ice cover and conditions | Weeks 1981 |
| LANDSAT-MSS | target classification by multiband optical imagery | coastal zone surface classifi- cation and identification | Behie and Cornillon 1981 |
| NIMBUS -7-CZCS | simultaneous colour and temperature visualizations | signatures and mor- phology of ocean fronts | Mueller and La Violette 1981 |
| NIMBUS-7-CZCS | water colour patterns associated with Gulf Stream rings | Gulf Stream ring dynamics and phyto- plankton growth patterns | Gordon et al 1982, 1983 |
| NIMBUS-7-CZCS | comparison of colour and thermal imagery | patterns of vertical mixing | Yentsch and Garfield 1981 |

of visible imagery put less stringent requirements on the capabilities of the sensor. Higher repetition rates such as can be provided by meteorological satellites are, however, often desirable for observations of the water mass dynamics, particularly in the coastal zone. Visual inspection of appropriately processed visible imagery, combined with oceanographic knowledge of the regions concerned, can reveal important oceanic structures and processes.

Photographic and TV cameras (Gemini, Apollo), visible-band radiometers (NOAA, Meteosat, GOES), broadband radiometers (Landsat) and spectral scanners (Nimbus 7) have been used (Table A1 in the Appendix). Reviews of applications are given by Sathyendranath and Morel (1983), La Violette (1974), La Violette et al (1980) and by Szekiela (1982) for coastal regions. Table 3.6.1 summarizes some representative published results of analysis of visible images. Qualitative analysis of the visible images proved to be helpful in identification and classification of various oceanic features in time and space. Applications in the open ocean, coastal waters, tidal regions and in inland waters (where water quality is often very similar to that of estuaries) were reported. Particularly of interest is the combination of visible imagery with thermal-infrared imagery, preferably co-registered.

For quantitative determination of the concentrations of suspended organic and inorganic particles and of the coloured component ('yellow substance') of dissolved organic matter, a specialized sensing instrument such as the CZCS is essential. The interpretation of broad band visible images (e.g. from the Landsat MSS) in terms of the distributions of the suspended materials is region-bounded, and often ambiguous and indirect (Sathyendranath and Morel 1983). On the other hand, CZCS scanner data can also be used for visual interpretation (Mueller and La Violette, 1981). The Thematic Mapper of Landsat 4 launched in 1982 and Landsat 5 launched in 1984, provides higher resolution data with enough spectral bands to also attempt quantitative processing. However, technical problems have restricted distribution of the data and the possibilities for frequent repeat coverage with this instrument are poor.

Processing of visible imagery is generally easier than the processing of spectral data, since the latter requires diverse algorithms and corrections in addition to geometrical correction and "navigation" (resampling of the image to a standard map projection). In spite of this, visible imagery appears to be under-utilized in many geological, biological and oceanography studies.

3.6.2 Water Colour

A major research effort has recently been directed to using visible band radiances in order to retrieve pigment concentration (" C " = $Chl\ a + Phaeo\ a$ in $mg.m^{-3}$), total seston concentration (" S " in $g.m^{-3}$) and the attenuation coefficient for upwelling radiance, (" K " in m^{-1}), at some particular wavelength, say 490 or 520 nm. Applications of the results exist in primary productivity mapping, and related biological studies as well as in atmospheric and climate research.

A distinction useful in discussing remote sensing capabilities, as well as describing the 'bio-optical' state of the sea, is to classify water into

Case 1 and Case 2 as summarized in Table 3.6.2, adapted from Gordon & Morel, (1983).

Case 1 waters are those for which phytoplankton and their by-products play the exclusive or dominant role in determining the optical properties of the water body. The by-products (2 and 3 in Table 3.6.2) include both detrital and bacterial particles (more or less coloured) and "autochthonous" yellow substances. These waters range from oligotrophic (very low pigment concentration) to eutrophic waters (with very high concentrations). Most oceanic waters are of this type. Coastal waters can also be Case 1 in the absence of terrigenous influence.

Case 2 waters. Waters depart from Case 1 and belong to Case 2 as soon as one or more of the additional substances numbered 4, 5, 6 or 7 in table 3.6.2 is present. Components 1, 2 and 3 may (or may not) be present. A high sediment load may result from the land drainage or from resuspension of sediments from the sea bottom by wave action ("sediment dominated Case 2 waters"). A high content of terrigenous yellow substances occurs in some semi-enclosed areas, e.g. the Baltic, some fjords and inlets. In the absence of high turbidity these waters form the "yellow-substance dominated Case 2 waters." Case 2 waters are frequent in coastal zones, and possibly offshore above banks and extended shallow shelves. They probably form less than 5% of the world ocean, but are of great interest from an economic and human point of view.

The required type of measurements are summarized in Table 3.6.3. They have so far been addressed by the sensors and missions listed in Table 3.6.4 with most data being provided by the CZCS on Nimbus 7 (Table 3.6.5).

3.6.2.1 Present Achievements for Case 1 Waters

C, S and K algorithms have been developed and have proved to be useful (Sathyendranath and Morel, 1983; Gordon et al., 1982, 1983; Guan et al, 1985; Viollier and Sturm, 1984; Austin and Petzold, 1981). All make use of the ratio of the blue and green signals emerging from the sea, and are inevitably redundant expressions, all deriving from a unique relationship. In other words, only one parameter, in the present state of knowledge and technology based on the CZCS, on Nimbus 7, is derived from colour imagery. Since agents 1, 2 and 3 in Table 3.6.2 are highly correlated, this is not a major drawback.

It is now estimated that C can be retrieved from colour within an accuracy of + 35% (and in fact better if restricted ranges in C and restricted geographical zones are considered). This accuracy applies to marine signals assumed to be perfectly retrieved from the total signals sensed by the satellite, and consequently it may be degraded if the atmospheric correction is not properly effected. This is the main problem with CZCS imagery where only one channel, at 670 nm, allows an estimate of the aerosol content but is insufficient to provide information on the spectral dependence of the aerosol scattering, also needed for the corrections. This could be circumvented with additional near IR channels in future sensors.

Table 3.6.2

Classification of water into case 1 and case 2
(Gordon and Morel, 1983)

| | |
|--|--|
| 1 LIVING ALGAL CELLS variable concentration | ALL CASE 1 COMPONENTS PLUS:- |
| | RESUSPENDED SEDIMENTS 4 from bottom along the coastal line and in shallow areas |
| 2 ASSOCIATED PARTICULATE DEBRIS originating from grazing by zooplankton and natural decay | TERRIGENOUS PARTICLES 5 river and glacial runoff |
| | TERRIGENOUS DISSOLVED ORGANIC MATTER 6 yellow substance from land drainage |
| 3 ASSOCIATED DISSOLVED ORGANIC MATTER liberated by algae and their debris (yellow substance, gelb stoff) | ANTHROPOGENIC INFLUX 7 particulate and dissolved materials |
| COMPONENTS OF CASE 1 WATERS | POTENTIAL COMPONENTS OF CASE 2 WATERS |

Table 3.6.3 Sensor capabilities needed for water colour observations.

| Required observation | Sensor property required | Examples |
|---|---|---|
| Suspended material patterns | Broad band radiance measurements (visible and near IR) | Landsat, NOAA, GOES, Meteosat |
| Chlorophyll determination (within a factor of 2) in the open sea | Higher sensitivity within the sea-radiance range Several bands in the visible and near IR (blue band, ~ 440 nm, is particularly important) | CZCS |
| Sediment visualization | Better spectral resolution (20 nm) Sun glint avoidance procedure | |
| Yellow substance-pigment discrimination | Additional channel (near 400 nm) | Under investigation Proposed for OCM (ERS 2) |
| Chlorophyll fluorescence measurement | Additional channels (~ 3) for peak at 685 nm and baseline | Partial test on OCE Under investigation |
| More precise chlorophyll determination | CZCS bands + additional bands in the near IR (improvement of the atmosphere correction) Calibration with diffused sunlight | Partially effected in proposed CZCS2 |
| Separate assessment of yellow substance/sediment/chlorophyll in all cases of waters | Calibration with diffused sunlight 12 bits radiometric resolution | In OCM (ERS-2) |
| Better aerosol content assessment | Improved sun glint avoidance 2 different looks of the same scene | Could be investigated with future scanners |

Table 3.6.4

Water colour scanners launched or planned

| | |
|---|---|
| CZCS on Nimbus-7 (launched) | See Table 3.6.5. Launched in 1978, still in operation. |
| OCE (Ocean Colour Experiment) on NASA shuttle | Flown on the OSTA 1 mission (OCS instrument) in Fall '81 Possible reflight in 1986 or later |
| .CZCS-2/NOSS | Deleted at the beginning of 1981. |
| .Advanced CZCS | Ocean colour imager (OCI), to be launched on U.S. NOAA satellite program, possible after 1990. |
| .OCM (Ocean colour monitor) | In spite of demand, OCM was removed from the payload of ERS 1. |
| .Advanced OCM | A solid state push broom instead of an optomechanical scanner is being investigated for possible incorporation into future European missions (ERS 1B, ERS 2). |

Table 3.6.5 Properties of the Coastal Zone Colour Scanner (CZCS)

Satellite: NIMBUS 7

| | |
|-------------|---|
| Launch date | October 24, 1978 |
| Orbit | Circular, sun synchronous Altitude: 955 km Inclination: 99.3° |

Sensor CZCS

| Band Number | Wavelength (nm) | Properties |
|--------------------|------------------|--|
| 1 | 433 to 453 | High sensitivity. Blue radiances show effects of chlorophyll absorption. |
| 2 | 510 to 530 | High sensitivity. Blue/green radiances are increased by scattering particles in water, with some chlorophyll absorption. |
| 3 | 540 to 560 | High sensitivity Green radiances are increased by scattering particles in the water. |
| 4 | 660 to 680 | High sensitivity. Red radiances are due almost entirely to scattering in the atmosphere for Case 1 water (table 3.6.2). |
| 5 | 700 to 800 | Low sensitivity. Designed to match Landsat MSS band 5 for coast and cloud identification. |
| 6 | 10,500 to 12,500 | Thermal band to give coincident sea surface temperature maps. This band operated intermittently. |
| Coverage | | Global Repetition: 3-4 times every 6 days, more at high latitudes Still in operation with some deprecation, coverage of a given area can be arranged by request. |
| Spatial Resolution | | 0.825 milliradians, 800 meters at nadir |
| Digitization | | 8 bits per sample |
| Glint Avoidance | | Tilt of scan mirror $\pm 10^\circ$ along track for $\pm 20^\circ$ pointing |
| Swath Width | | 1636 km (depending on tilt setting) |
| Data products | | Photos or tape of 2 minutes (about 800 km) of data: |
| Level 1 | | Images of the 6 above bands. Tape (CRTT) contains latitude and longitude information. |
| Level 2 | | Images of 4 computed quantities, (figs. 2.7.1, 2.7.2). Tape (CRCST) contains corrected radiance bands 1-3. Aerosol radiance at band 4, temperature, pigment concentration, diffuse attenuation coefficient and a cloud/land mask. Latitude/longitude information as before on CRTT. |

3.6.2.2 Present Achievements for Case 2 Waters

Here, unpredictable influences of a variety of independent substances (1 to 7 in Table 3.6.2) coexist and render the solution much more difficult. The assumption which allows the estimate of the aerosol content is to consider sea water as a black body in the red and near infrared part of the spectrum. This assumption progressively fails for sediment dominated Case 2 waters, with increasing sediment load. Iterative procedures, relaxing the black body conditions, similar to those developed for Case 1 waters (Smith and Wilson, 1981), could, in principle, be used for Case 2 waters, but they have to be based on optical data acquired at sea, in the area of interest.

Provided that a sufficient radiometric resolution is achievable in appropriate channels, pigment (Chl a concentration) could be detected in these waters by taking advantage of the fluorescence peak. (Gower and Borstad, 1981).

Analytical and statistical studies (using eigenvector analysis, for instance) tend to demonstrate (e.g. Sathyendranath et al (1982) that 2 independent (pigment and turbidity) or maybe 3 (including yellow substance) could ideally be separately assessed from reflectance spectra, under the proviso of a high accuracy in the reflectance determination ($<5.10^{-4}$). Such an accuracy lies uncomfortably close to the uncertainty resulting from atmospheric corrections. The same studies show that a channel centered around 400 nm is essential if discrimination between pigment and yellow substance signatures is considered necessary.

3.6.2.3 Recommended Technical Developments for Future Satellite Water Colour Sensors

a. channels: in order to improve the quality of the atmospheric correction, an increased number of near-IR channels is planned for future sensors; this should satisfy a crucial need.

Apparently no sensor is planned with a fluorescence (685 nm) channel, and only one (advanced OCM) incorporates a violet (400 nm) channel; this position should be revised.

b. radiometric resolution: with respect to CZCS, a significant progress is expected where 12 bit (advanced OCM) or 10 bit (OCI) encoding are planned.

c. geometric resolution: for the study of mesoscale processes, a sensor must be able to resolve about 1 km, as with CZCS. Such a requirement implies a high data rate. This rate becomes incompatible with current storage and processing capabilities, if studies of global scale processes with world coverage, are envisaged. For such studies, however, a degraded spatial resolution, achieved by averaging over groups of 3 x 3 or 4 x 4 pixels, is acceptable, and leads to a greatly reduced data flow. Such a two-mode operating sensor giving local coverage at full resolution and global coverage at lower resolution, already exists for an IR system (AVHRR) and could advantageously be extended to visible imagery.

d. sun-glint avoidance and changeable scan plane: the possibility of recording simultaneously two scenes viewed under different angles (two scan

planes) does not seem to have been explored, but should be examined. Such a requirement can be partially fulfilled with successive views. For the OCI the tilt mechanism will be speeded up to change from -20° to $+20^\circ$ within less than one minute.

e. simultaneous thermal imagery: since thermal and colour imagery are not redundant, but complementary, it is recommended that both should be acquired simultaneously and from the same satellite, though not necessarily from the same sensor.

3.6.2.4 Recommended studies

a. Chlorophyll a content and fluorescence response. Quantitative accuracy, peak shift and determination of an optimum baseline for making fluorescence measurements in passive optical surveys.

b. Analytical/statistical studies of the relations between the content and the optical properties of Case 2 waters.

c. Improvement of methods for atmospheric correction, including studies of the phase function and the Angstrom exponent for aerosol scattering over marine areas. (For progress in assessing several independent parameters in Case-2 waters, high accuracy in atmospheric correction is imperative. The problem is therefore primarily one of atmospheric, rather than of ocean, optics.

d. Study of the directional dependence of the upwelling radiance emerging from the sea.

3.7 Lidar

Light detection and ranging (Lidar) instruments can make measurements analogous to those that use the radio techniques of radar. In addition, however, lidar can penetrate the water surface and give information on optical properties of sea water and scatterers within it to depths of several tens of meters.

In principle, a wide variety of ocean measurements can be made by lidar (Table 3.7.1), but to date none has been demonstrated from a satellite, and temperature and sound velocity measurements have been demonstrated with only moderate success, even from a ship. Lidar cannot penetrate clouds, and hence cannot offer the all weather capabilities of microwave instruments. Only those lidar applications that use the specific advantages of optical techniques are therefore likely to be developed.

The various light scattering mechanisms give some sensitivity to temperature and sound velocity as well as to suspended solid backscattering, chlorophyll fluorescence and bottom detection. Because the light source has a narrow beam and can be rapidly modulated, a lidar can in principle scan side to side and give a vertical profile into the water (see Table 3.7.1). Altimetry, bathymetry and fluorescence measurements have been made from aircraft, but no laser has yet been operated in space for remote sensing purposes. Several techniques listed do not appear applicable to satellite applications, but new laser, detector and electronics capabilities will bring progress in the field. However, fundamental sensitivity limitations are

Table 3.7.1 Potential Ocean Lidar Capabilities.

| <u>Measurement</u> | <u>Requirement</u> |
|---|---|
| Range (altimetry) | Short transmitted pulse (1 nsec). Accurate return pulse detection and timing. |
| Sea state | Short Transmitted pulse (1 nsec). Return pulse shape analysis. |
| Suspended material (seston) | Mean return power (backscatter) measurement, with range gating to avoid surface reflection. |
| Seston depth profiles | Range gating (3 nsec) and high dynamic range for detecting subsurface returns. |
| Water depth | As for seston profiles with optimization for maximum depth penetration. Side to side scanning and rapid pulse repetition are required for charting. |
| Water colour | Return power measurements at specifically chosen wavelengths, e.g. 440 and 550 nm. |
| Fluorescence of oil, chlorophyll or dyes. | Return power measurements with appropriate short transmission, and longer detection wavelengths. |
| Temperature | Narrow band measurements (0.5 nm) for analysis of precise Raman backscatter signal spectrum and polarization. |
| Sound velocity | Very narrow band measurements (0.01 nm) for analysis of Brillouin scattering. |
| Salinity | Combination of sound velocity and temperature results. |
| Surface currents | Doppler shift of return signal. Requires optical measurements to 0.5 MHz. |

severe, even with high power lasers.

Satellite lidar applications are currently planned for atmospheric probing to give aerosol concentrations and wind measurements (to about 1 m/sec and 10° in direction) with a range resolution of about 1000 m. Recent reports on lidar use in ocean remote sensing (Gordon 1980, Carder 1981, Collins 1982), although sponsored in some cases by NASA, concentrate on ship and airborne instruments that can complement satellite observations.

3.8 Buoys

The availability of satellite systems for locating low power transmitters and storing data from them has made it possible to track relatively small and inexpensive drifting buoys to about 1 km accuracy anywhere on the earth, and use them to gather data from large areas of the ocean. The most commonly measured parameters have been atmospheric pressure (to 1 mb) for geostrophic wind calculations, and sea surface temperature (to 0.1°C), though the buoy tracks themselves have yielded the most valuable data, on near surface currents.

In the First GARP Global Experiment (FGGE), 300 drifting buoys provided coverage of the Southern Ocean (south of 20°S) in such a way that 60% of the area was within 500 km of a buoy location for an eleven-month period. Fifty per cent of the buoys continued to transmit for more than one year.

Such buoy measurements are now accepted as a standard and reliable oceanographic technique of which tracking and data relay by satellites are essential components. The large scale coverage of the surface data gathered, makes it extremely useful for combination with remotely sensed data derived from the same or other satellites. Future developments depend on developing reliable buoy sensors for such measurements as air temperature, humidity, wind speed and direction, subsurface temperatures, etc.

At present the global tracking and data relay system is operated by Service Argos, Centre Spatial de Toulouse, 18 Ave. Edouard Belin, 31055, Toulouse Cedex, France, using hardware on the NOAA series satellites. More details can be found in the report of SCOR Working Group 66.

4. USE OF SATELLITE REMOTE SENSING DATA

4.1 Matching Satellite Capabilities to Oceanographic Requirements

From the summary given in section 3, it can be seen that satellite oceanography is almost totally defined by the capabilities of electromagnetic sensors to penetrate the earth's atmosphere and gather useful ocean data from orbital altitudes. Lack of penetration into the sea limits observations to the surface or near surface. However a number of important, deeper phenomena have surface signatures. Also, this is where most human interests are concentrated. The time and space coverage of satellite sensors are essential for studying global processes of importance in climate research and are also particularly suitable for observing mesoscale phenomena with space scales of 50 to 200 km and time scales of weeks to months.

Satellite sensors can only measure the few ocean properties that give a detectable signal at a distance. These are:

- colour or spectral reflectance of incident sunlight indicating presence of phytoplankton and other suspended material, bathymetry and coastal vegetation, foam and atmospheric properties.
- thermal emission in the infrared and microwave, giving temperature, ice cover and (in the microwave) wind speed, foam, and water vapour and liquid water in the atmosphere.
- surface roughness, measuring with various microwave sensors, wind speed and direction, wave height, length and direction, ice cover and various oceanic phenomena such as internal waves.
- surface elevation, which shows the shape of the geoid and the smaller variations due to ocean circulation patterns and eddies.

Satellites also track and relay environmental and position data from drifting buoys that can add a great variety of other measurements both on the surface and to moderate depths.

The above rather short list of accessible properties suggests that one should not expect satellites to meet the major requirements of so diverse a field as oceanography, but in fact the satellites contribute in wide variety of ways.

For example the major traditional physical oceanographic measurements consist of depth profiles of water salinity and temperature down to depths of typically 1000 to 2000 m and less frequently to the deep ocean bottom. These measurements then allow calculation of circulation patterns with depth by assuming that geostrophic flows result from any apparent density imbalance between adjacent profiles. No satellite sensor has been launched to measure salinity, though low frequency microwave radiometry can in principle be used to give results of limited accuracy. No appreciable penetration below the surface would be possible for this, nor is any penetration beyond a few skin depths possible for microwave and infrared temperature measurements.

Table 4.1.1

Brief guide to satellite remote sensing of oceans

| What is measured | Why | With what type of instrument | example/satellite | With what results |
|---|--|------------------------------|---|---|
| Water colour | map movements of different coloured water; deduce plankton concentrations | optical scanner | Coastal Zone Colour Scanner/Nimbus 7 MSS/LANDSAT AVHRR/NOAA | pigment and seston images, blocked by clouds and darkness); useful for fishery management and fishermen; global coverage would show global ocean food resource ecology. |
| Water temperature | map movements of water of different temperatures; deduce accurate temperature values | thermal infra-red scanner | AVHRR/NOAA | detailed temperature images (blocked by cloud) also useful for fisheries; temperature accuracy improving, now good enough for some weather and climate purposes |
| | | microwave scanner | SMMR/NIMBUS 7 SMMR/SEASAT, SSMI* | less accurate results but penetrating cloud |
| average small-scale sea surface roughness | deduce wind speed and direction and resulting driving force for ocean currents | radar scatterometer | SASS/SEASAT AMI/ERS-1* | large scale surface wind patterns, but only brief examples so far. |
| | deduce wave height | radar altimeter | ALT/GEOS-3 ALT/SEASAT ALT/ERS-1* | data more accurate and widespread than conventional. global wave data for the first time |
| pictures of sea surface roughness | deduce wavelength and direction, look at roughness patterns | imaging radar | SAR/SEASAT SIR/Shuttle SAR/ERS-1* | detailed images in all weather, day and night, showing longer surface and internal waves and ice; also wind patterns, current boundaries and bottom features. |
| sea surface height | measure shape of earth, tides and height changes due to currents | radar altimeter | ALT/GEOS-3 ALT/SEASAT ALT/ERS-1* ALT/TOPEX* | increasingly precise results (to 3 cm) now good enough to map global water movements with launch of TOPEX/GM. |

*Planned

Satellite altimetry can however measure the surface deformations which give surface geostrophic currents, and which, together with relative subsurface profiles, can indicate the depth integrated geostrophic current. Altimetry thus provides one important end point of the above oceanographic measurements, though without producing the intermediate depth profiles which are needed for studying the three dimensional flow. For the World Ocean Circulation Experiment it is planned to supplement the altimetry with a coarse mapping of ocean density structure to calculate this flow.

In addition satellite images show thermal and colour patterns associated with circulation, scatterometry measures the large scale surface wind stress and its derivatives that drive much of the flow, and tracking of buoys shows the near surface water movements.

Ocean satellite sensor capabilities demonstrated up to the present are listed in table 4.1.1.

In the future we may expect developments in both precision and accuracy of measurements and in data processing and distribution capability. These should greatly increase the use of satellite data of the oceans.

Surprisingly, few new types of sensors are at present proposed for satellite launch. Exceptions are in the two-frequency scatterometer which may one day make wave directional measurements using resonance with the low, difference frequency, and in development of a SAR with sufficient sensitivity to measure the Doppler shift due to surface currents. Lidar systems may be developed but adequate sensitivity requires difficult and dangerous power levels and the cloud limitation will remain. Surface salinity may one day be measured with a large passive microwave antenna but present results indicate that the signal will be hard to separate from interference and natural confusing effects.

To some degree, the scarcity of new sensors may reflect the incomplete assimilation of the results from existing instruments on the part of the ocean science community; however, a clear lack of vigour in the sensor development programmes of nations has contributed to this shortage.

Before discussing satellite capabilities in more detail a brief summary of the relevant orbital and sensor properties is presented in the next two sections.

4.2 Possible Types of Orbits

Satellites are launched into circular orbit by the thrust of rocket engines which propel them above the atmosphere (altitude greater than about 300 km) and give them a sufficient horizontal velocity that their centripetal acceleration in orbit matches the acceleration due to gravity at that height. Satellites can then be transferred into orbits at greater height by further bursts of power, sending them initially into an elliptical transfer orbit and then to the higher circular orbit half a revolution later.

Properties of orbits are determined by classical mechanics in the earth's gravitational field (Table 4.2.1). The plane of an orbit remains nearly fixed in space, with ground track patterns being largely determined by

the earth's rotation. At a typical altitude a satellite will make about 14 circuits round the earth in a day. This defines the interval with which its path crosses the equator, i.e., as about one fourteenth of the earth's circumference. In many cases a sensor cannot cover such a wide swath, leaving gaps in its daily coverage, and it would be advantageous if the satellite could orbit faster. Table 4.2.1 shows that even at the lowest orbit the increase is only to 16 per day. In practice the field of view is increased at higher altitudes, but this increases cost and power, especially for active microwave systems, and decreases resolution.

The non-spherical shape of the earth will in general cause satellite orbits to precess slowly. A precession rate of 0.99° per day matches the orbital period of the earth about the sun and gives a "sun synchronism" in which the satellite's orbital plane is at a constant angle to the sun. This leads to more constant solar illumination of the satellite (simplifying solar power generation) and of the ground (bringing the satellite over each point at the same local time each day).

Altitudes greater than about 500 km are needed to give the several years of stable life-time required for most earth observing missions. Higher altitudes have the advantages of allowing a wider area of view for scanning sensors, the possibility of data communication over larger distances, and the more precise tracking (also over longer distances) and freedom from small atmospheric perturbations that are required for altimetric missions.

The orbit inclination (the angle between the equator eastwards and the ascending orbit track) is usually determined in the initial launch process. Small changes in inclination and altitude are commonly made during a satellite's lifetime to stabilize the orbit against the effects of solar radiation pressure, residual atmospheric drag and tidal perturbations.

The orbital path of a satellite takes it up to over a north latitude equal to its inclination and down to an equal south latitude. For mapping most of the earth's surface a high inclination must be chosen, with inclinations approaching 90° giving improved coverage of areas near each pole. For altimeter missions the angle between ascending and descending tracks at the equator should not be smaller than about 40° , limiting the inclination to lower values, typically 65° - 75° . A sun-synchronous orbit requires a specific inclination which varies between 70° and 83° or (110° to 97° since these orbits are retrograde) as the altitude varies between 500 and 2500 km.

At any given instant a satellite can view an area whose size depends on the properties of its sensors (see next section), and on its altitude. The range over which data can be transmitted in real time to a ground station is similarly determined by the altitude, though satellite relay systems, such as the U.S. TDRSS, can remove this restriction. Onboard data recording has, up to the present, required equipment whose moving parts seriously limit its useful life.

Typical polar orbiting, earth observing satellites move at a velocity of about 7.5 km/sec, so that the field of view of the sensor moves forward on the earth's surface at 6 to 7 km/sec (Table 4.2.1). Most satellite imaging sensors make use of this motion to provide scanning in one image coordinate,

Table 4.2.1 Expressions for orbital properties of satellites in terms of the earth's radius R (6378 km), the acceleration due to gravity at the earth's surface g (9.80 m/sec²) and the satellite's altitude H and inclination i.

| Property | Expression | Value for H: | | |
|---|--|--------------|-------|---------------------|
| | | 150km | 800km | 1500km |
| Satellite speed | $V = \sqrt{\frac{gR^2}{R+H}}$ | 7.81 | 7.45 | 7.11 km/sec |
| Satellite ground speed [†] | $V_g = \frac{R}{R+H} V$ | 7.63 | 6.62 | 5.76 km/sec |
| Satellite period | $T = \frac{2\pi(R+H)^{3/2}}{R\sqrt{g}}$ | 1.28 | 1.41 | 1.56 |
| Number of orbits/day | $N = \frac{24}{T}$ | 16.5 | 14.3 | 12.4 |
| Separation of ascending tracks on equator | $D = \frac{2\pi R}{N}$ | 2434 | 2807 | 3227 km |
| Track separation if evenly distributed for M months | $\frac{D}{30.44 \times M}$ | 13.3 | 15.4 | 17.7 km in 6 months |
| Satellite precession rate [*] | $\Omega = \frac{-A \cos i}{(R+H)^{7/2}}$ | 3.14 | 2.26 | 1.63 °/day |

* $A = 2.07 \times 10^{14}$ for R+H in km and Ω in degrees/day.
Example values of Ω are for $i = 110^\circ$. Orbit is sun synchronous at a precession rate of 0.99° per day.

† Velocity due to earth's rotation must be added to this.

while the sensor scans in the other (cross track) coordinate.

The above velocities are with reference to the centre of mass of the earth. Earth rotation causes the earth's surface to move beneath the satellite, in general resulting in a geometrical distortion of the image formed by a scanning sensor.

If a satellite orbit has zero inclination with motion in the same direction as earth rotation, then if its altitude is 35,786 km the earth's surface will appear stationary, and can be studied repeatedly from the same, fixed, viewpoint. Such an orbit is called geosynchronous or geostationary. The high altitude limits the resolution achievable, and the lack of relative velocity means that imaging sensors have to scan both image coordinates. Also, no Doppler shift is present to allow synthetic aperture radar observations or precise data buoy location. However, the meteorological satellites in this orbit provide thermal and visible imagery of the earth at resolutions down to 8 km and 1 km respectively and can repeat the observation at intervals down to half an hour, or less for limited areas. Such satellites have the great advantage of requiring only a relatively simple fixed (non steerable) transmitting/receiving antenna.

From the nature of the physical situation, a geostationary orbit is only possible over the equator. With sufficient propulsive power a satellite could in principle be arranged to appear stationary over other points on the earth, and indeed a hovering rocket at high altitude (about 150,000 km) over the north pole was proposed for a 6 month ice mapping mission. Such proposals are not usually serious possibilities for earth observations.

A powered low orbit double satellite is proposed for the GRM, in this case to allow compensation for atmospheric drag at an altitude of 150 km. The thrust will be controlled to keep the outer shell of each satellite centred around an unsupported, freely falling reference mass, which will be screened from the atmosphere and can thus follow a drag free low earth orbit.

A summary of these orbit types is given in Table 4.2.2.

4.3 General Properties of Satellite Sensors

4.3.1 Field of View

The satellite's primary advantage for oceanography is its wide field of view. From a typical height of 800 km the horizon is 3000 km from the sub-satellite or nadir point. For visible and infrared measurements, even a clear, cloud free atmosphere limits the useful view to lines of sight that pass more steeply than about 30° through the atmosphere, i.e. out to distances of about 1000 km, giving a 2000 km usable swath.

4.3.2 Usable Wavelengths

To pass through the earth's atmosphere, radiation must have wavelengths in the clear "windows": 0.4 to 0.7 μm in the visible, 0.7 to 1.4 , 1.5 to 1.8 and 2.1 to 2.1 μm in the near infrared (NIR), 3.5 to 4.1 μm and 8.2 to

13.5 μm in the thermal infrared (TIR) and in the microwave at wavelengths longer than about 2 mm, except for regions of strong oxygen absorption near wavelengths of 2.5 and 5 mm.

4.3.3 Spatial Resolution

From the distance of 800 km the spatial resolution of a sensor is fundamentally limited by diffraction to $(800/N)$ km where N is the dimension of the receiving aperture expressed as the number of wavelengths (λ) of the radiation used. Thus a nadir viewing microwave radiometer using a 1-meter dish antenna at $\lambda = 10$ cm would give a spatial resolution of 80 km, whereas an optical sensor with a 2 cm diffraction limited aperture would have a 20 m resolution.

A synthetic aperture radar overcomes the diffraction limitations of its "real" aperture or antenna size, by radiating a coherent signal and processing the return over a much longer "synthetic" aperture represented by the satellite's path during a few seconds of orbital motion. The Seasat SAR achieved 25 m resolution in this way even though its real 10.5 m antenna would have limited it to approximately 20 km.

4.3.4 Data Bandwidth

The microwave radiometer mentioned in the previous section might scan a 60° field of view beneath the satellite, but the coarse resolution would only give 10 to 15 samples of information or pixels in this range and could only give new information after the satellite had moved forward (at about 6 km/sec) for 10 to 15 seconds. With a data output of 1 number per second, this would be considered a very low bandwidth sensor. The above optical sensor on the other hand could record 50,000 pixels across a 1000 km swath and would need to repeat this when the satellite had moved forward only 20 metres or every 3 milliseconds. It would therefore produce 15,000,000 measurements per second requiring an extremely wide bandwidth, especially if data is recorded to many bits accuracy per measurement, in each of several spectral bands. Maximum data bandwidth is about 100 megabits per second for present transmission systems, so that high resolution sensors are limited as to the swath width they can cover.

4.3.5 Swath Width Covered

Typically both radar and visible scanners with 20 m resolution are limited to about 100-200 km coverage for data bandwidth reasons. Landsat covers 185 km at 30 and 100 m resolution, whereas the AVHRR sensors scan about 3000 km with 1 km resolution with a much lower bandwidth. Geometrical distortions are severe over such wide scans since the earth is imaged at 70° incidence angle at the edges of the scene, giving a 3 to 1 foreshortening. Also a 3 times greater thickness of atmosphere must be penetrated at this angle.

The CZCS images over a swath typically 2000 km wide, varying with the tilt of the field of view used to avoid sun glint.

Table 4.2.2

Types of orbit useful in remote sensing missions
(not all have been used up to the present).

| Orbit type | Altitudes possible or typical (km) | Inclinations possible or typical | Uses |
|------------------------------|------------------------------------|---|---|
| Low energy for simple launch | 250 - 400 | approximately equal to latitude of launch site | tests of space systems |
| Near polar | 500 - 2000 | 60° to 120° | general earth mapping. Repeat cycle depends on exact orbit chosen. |
| Near Polar sun-synchronous | 500 - 2000 | 97.5° to 105.1° specific value required for given altitude (see Table 4.2.1) | earth mapping with more constant illumination of the ground or the target. |
| Geostationary | 36000 | 0° | repeated observations from the same viewpoint over the equator at a given longitude. Field of view about 60° radius of great circle distance. |
| Equatorial | 500 - 2000 | 0° | repeated observations of the tropics |
| Low altitude | about 150km | 60° to 120° | geopotential research, with thrust to counteract atmospheric drag |

From a geosynchronous orbit, over the equator at an altitude of nearly 36,000 km, a satellite can view 85% of one hemisphere, but large areas are again very foreshortened. The horizon is 81.3 degrees of latitude away from the subsatellite point, but beyond 62° this foreshortening, and the increase in atmospheric slant thickness, again exceed 3 to 1. Data collection is therefore possible over 85% of a hemisphere, but useful imaging is limited to 50% or less, and cannot cover any Arctic or Antarctic areas.

Other sensors have coverage defined by more specialized constraints. The scatterometer scans the sea surface at incidence angles between about 20° and 50° so as to observe the difference in radar cross-section, σ_0 , due to wind, which can best be measured in this range. Since it views azimuths 45° forward and aft of the satellite rather than directly to the side, its coverage is limited to two strips about 500 km wide on each side of the satellite's track separated by about 400 km.

The altimeter measures only directly downwards, but relies for precise range measuring on averaging over the area of sea surface that is first illuminated by the short pulse of microwave radiation emitted. This area varies from 2 to 5 km across, as the sea state increases from calm to 5 m waveheight. Apart from this small averaging diameter, the measurements are along the satellite's sub-track only.

Imaging radars can rely on synthetic aperture techniques to increase their resolution only in the along-track direction. For cross-track resolution the radar must look off to one side of nadir and rely on ranging of the reflected signal. This can be very precise, to 7 m in the case of Seasat to match the 25 m along-track resolution with the 20° incidence angle used.

This incidence angle cannot be made too large without increasing the range and greatly increasing the radar power required (as the fourth power of the range). Also ocean surface image contrast is lost at larger angles. 20° was needed for Seasat to study ocean wave patterns, and also kept the range increase small. Higher values, to 45°, are needed for iceberg and ship location. A typical SAR covering a 100 km swath from 800 km altitude with 30° incidence angle would survey a strip between 420 and 520 km off to one side of the satellite track. Which side to choose is generally not of major importance, but can improve the latitude coverage at the north or south extremes of the satellite's orbital path.

4.3.6 Environmental Limits to Coverage

Cloud cover is the most severe limitation for both visible and infrared sensing. The longer infrared wavelengths are less scattered by haze, but clouds block both visible and infrared radiation. Clouds, therefore, greatly restrict imaging of surface temperatures and phytoplankton pigments in many temperate regions, and in areas of oceanographic significance such as where upwelling and boundary currents tend to cause cloud formation. Microwave techniques provide cloud penetration, but the radiometry is limited by diffraction to coarse spatial resolutions, and to areas well removed from land masses and the sun's reflection on the sea.

Sun glint is an important limitation for optical and microwave radiometry, but is insignificant in the thermal infrared at wavelengths longer than about 6 μm . The CZCS visible scanner can be tilted 20° along track to avoid this.

SAR imagery is a particularly interesting microwave technique in that it penetrates cloud and is independent of solar illumination, but retains the high resolution that makes visible and infrared mapping so useful. These properties make it especially valuable in operational applications such as wave and ice mapping. In the future, as power and processing problems become less severe, use of such imagery may be expected to become much more routine.

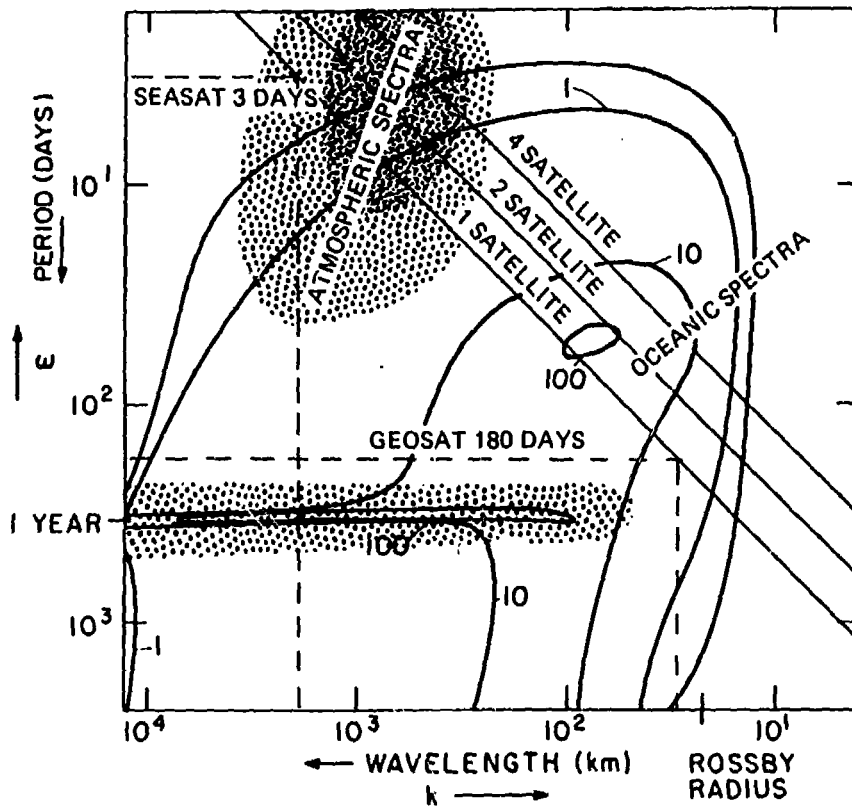
4.4 Strategies for the Use of Satellite Data

The greatest single advantage of satellite remote sensing over conventional observations is clearly its wide area, potentially global coverage. For the understanding of several marine physical and biological processes the classical methods of obtaining occasional data from research ships and moored arrays of sensors are now seen to be hopelessly inadequate.

If all sensors on a polar orbiting satellite could penetrate clouds and provide data over a wide swath, then for larger scale features there would be little conflict between the extent of spatial coverage and sampling frequency. Most sensors, on the other hand, obtain data over narrow swaths -- 400 km for the proposed ERS-1 scatterometer, 80 km for the synthetic aperture radar and a few kilometres for the radar altimeter. In these circumstances decisions must be made on the best sampling strategy based on the characteristic time and space scales of the oceanographic variables under study, and the different, often conflicting requirements of the suite of sensors carried on the satellite. For example, some features studied by SAR, particularly those in coastal areas, are relatively time-invariant. High resolution coverage rather than frequent sampling may then be called for. In a typical near polar orbit, complete coverage at the equator might be achieved in 27 days, but this may be an unacceptably long interval for sampling dynamic ocean phenomena. It is now agreed that it was only during Seasat's three-day repeat pattern that sea surface height changes due to currents and mesoscale features could be distinguished from the shape of the geoid. However, a three-day repeat orbit produces a 900 km spacing between tracks at the equator and very coarse spatial sampling.

If only one satellite were available for altimetric studies of ocean circulation the general consensus at present is for an 8 - 20 day repeat pattern as the best compromise between monitoring mesoscale variability and obtaining the necessary geoidal information. This sampling, in turn, is of limited operational value for forecasting fast changing phenomena such as surface winds and waves. To measure tides, the repeat period must avoid aliasing important tidal frequencies to unacceptably low values (c.f. Fig. 2.1.1).

For water colour and thermal mapping, the sensors image over a wide swath but cloud cover is often a severely limiting factor in the possible sampling frequency. Near-daily coverage of a given area can be achieved with 1 km resolution from polar orbiting satellites, allowing observation in a reasonable fraction of the available cloud free periods. For smaller scale



4.4.1 Wavenumber-frequency diagram similar to Fig. 2.1.1 showing how satellite orbit characteristics and number can be chosen to sample regions of ω - k space. Oceanic mesoscale dynamics have energy peaks near 10^2 km and 50 days; atmospheric mesoscales peak near 1000 km and 10 days. One satellite near 800 km altitude can operate at a point on the straight line so marked, and determine dynamics to the lower left of the dotted lines (modified from Munk & Wunsch, 1982)

studies (implying small pixels and thus relatively narrow swath widths), some planned sensors provide a lateral swath offset to reduce the disadvantages of the resulting low revisiting rate. This is a major problem, since small scale features correspond to small temporal scales, and tidal influences, requiring hourly rather than daily coverage, become important.

For global scale phenomena, a geostationary orbit appears useful for long term observation of tropical and mid-latitude oceanic areas. The geometric and radiometric resolution may be degraded with regard to lower orbiting sensors, but such a disadvantage can be accepted, given in compensation the continuous, very large area coverage. It is recommended that the possibilities should be investigated for developing sensors to measure, for example, water colour from future satellites in the Meteosat, GOES, GMS, GOMS and INSAT series (c.f. Fig. 4.4.3 ahead).

Because of the difficulties in directly matching satellite coverage capabilities to the scientific requirements, there is a clear need either for additional sources of data from more, coordinated satellites or from in situ observations, or for more sophisticated methods of analysis involving modelling of the relevant ocean and atmospheric processes. Let us consider these three options.

1. Coordinated satellite missions

Figure 4.4.1 illustrates three items: (a) the regions of frequency-wavenumber space having the highest energy in the ocean (solid lines); (b) the highest energy in the lower atmosphere (stippled regions); and (c) the regions of that space that can be sampled by 1, 2 or 4 satellites in a low-earth orbit (about 800 km). Seasat was in a 3-day repeat orbit with tracks separated by approximately 800 km, implying it could see ocean feature variations with wavelengths longer than 1600 km and time scales longer than three days. Thus it could observe the region of ω - k space to the lower-left of the dotted lines marked "Seasat." Geosat, with a planned repeat originally of 180 days, could have sampled down to wavelengths of order 35 km; however, it was placed in a non-repeat orbit.

From the diagram, it can be seen that two spacecraft could comfortably sample the maxima in both the oceanic mesoscale and annual signals, if placed in a repeat orbit of about 30 days and 60 km spacing. (Other considerations may move this choice some direction away from that operating point, however.) They could not optimally sample atmospheric phenomena unless placed in a repeat orbit near three days and 1000 km spacing, which is near to where the current NOAA polar orbiters operate. As seen in Fig. 4.4.1, a single satellite cannot sample the required frequencies of both wind/wave and sea level topography measurements, no matter which repeat period is chosen.

This diagram assumes that a satellite sensor covers only a narrow swath. A satellite, or set of satellites, could be used to study almost the full ω, k range plotted, if their sensors covered a wide enough swath to give full, global coverage in one, or a small number of days. It is this possibility that makes coordination of satellite programmes so important. Two, simultaneous scatterometer missions, for example, could approach this situation. Multi-satellite observing systems would be possible if existing plans in Europe, USA and Japan were suitably coordinated.

There is some degree of coordination existing among the five geosynchronous satellites, as seen on Fig. 4.4.2. If the INSAT Indian national satellite is included, the entire globe equatorward of about 50° will be under hourly weather surveillance (ESA, 1984). The data would be even more useful if similar scanning sequences, data characteristics and data formats were to be attempted. The future may see much coordination. Similarly, Fig. 4.4.3 shows the status of receiving stations for Landsats, as of October 1984 (ESA, 1984). It may be seen that much of the coastal oceans of the world may be viewed and the data directly received, even in developing countries. Landsat imagery, properly processed, is of value in semi-quantitative studies of certain coastal ocean processes such as sediment transport, internal waves and shallow bathymetry. Coordination between nations has made these data potentially available to a large number of scientists.

2. Surface observations

Since satellites can measure only sea surface or near sea surface properties, additional in situ measurements of the interior density distributions and current fields are clearly needed for addressing most problems of physical oceanography. Remote sensing measurements normally also rely on conventional in situ measurements for calibration or at least verification.

The optimal strategy for the deployment of conventional oceanographic instrumentation in conjunction with satellites depends on the phenomenon being studied. Because of their continuous global sampling capability, satellites may be expected to be most valuable for the study of global ocean circulation and productivity, and the role of the oceans for climate (in addition to real time global wave forecasting applications). In these cases, clearly, it will never be possible to match the space-time sampling capacity of satellites with conventional measurements made from ships, or individual in situ instruments. The only feasible strategy in the design of large scale, long period experiments such as the World Ocean Circulation Experiment (WOCE) or the Tropical Ocean-Global Atmosphere (TOGA) programme is to identify a critical set of these conventional measurements which can be carried out with the limited resources available to test optimally the physics of models. The model output would then provide the subsurface data with the time and space sampling needed to match the satellite data. At present it appears that the difficulties in the design of such ambitious international projects lies as much in the determination of the required conventional measurement system as in the definition of the satellite requirements.

3. Modelling

Various concepts of an optimal sampling strategy for WOCE or TOGA using conventional research ship surveys, ship-of-opportunity data, drifting surface buoys and deep floats, moored instrument stations and other measurement techniques such as acoustic tomography, in conjunction with ocean satellites are under discussion. The concepts differ considerably. Perhaps the greatest difficulty in establishing a consensus in the oceanographic community on this question is the lack of detailed sensitivity studies with numerical ocean circulation and coupled ocean/atmosphere models.



4.4.2 Coverage provided by five geosynchronous satellites operating cooperatively over the equator. Images are possible every 30-60 minutes (ESA, 1984)



4.4.3 Receiving stations and areas where line-of-sight telemetry reception is possible for the Landsat series, as of October 1984. Coverage consists of circles round each station of a radius typical for all polar orbiting, earth observing satellites. The map projection causes variations in shape and size. (ESA, 1984)

In view of the considerable resources which need to be committed to these projects by the international oceanographic community a programme of extensive numerical experimentation is required from oceanographic modellers to clarify these questions. This programme will need to be of comparable magnitude to the efforts mounted by the meteorological modelling community in preparation of the First GARP Global Experiment (FGGE). It should be pointed out in this context that the large data fluxes and global modelling requirements of satellite oceanography will generate a strong modelling demand from oceanographers, with the need for powerful computing facilities.

Such facilities are clearly needed to handle the flow of data. It must be noted that for a continuously operating satellite system the data must be used (or discarded), at approximately the same rate as it is produced, regardless of whether or not the application is real time.

4.5 Availability of Satellite Data

4.5.1 Data Processing and Distribution

As can be seen from the preceding sections, many of the satellite data types available to date are experimental and as such have covered relatively small areas, short time periods, (or both) of the world's oceans and coastal areas. At present large volumes of image data are being collected routinely by the few operational or longer-lived sensors (table 4.5.1), but with the exception of the (mostly classified) Geosat altimeter no active microwave systems are operating. Also many sensors were primarily designed for use in other fields, with resulting disadvantages for oceanographic studies. The sole exceptions beyond Seasat are the CZCS and SMMR on Nimbus 7, which is still producing useful data many years beyond its expected lifetime, and the Geosat altimeter recently launched, from which only wave and wind data are being made available.

The volume of the available image data is however extremely large when compared to the oceanographic community's present capabilities to process and analyse it, or even to archive it in permanent but accessible form.

Up to the present the funds allocated to promoting and assisting in use of the ocean satellite data have remained inadequate. They are certainly minuscule in comparison to the cost of the satellite hardware. Some moderate programmes illustrate what can be done with adequate funding in this regard. Examples are:

1. The GOSSTCOMP compilation of sea surface temperatures to form global monthly mean maps. These have slowly improved in quality over the years.
2. The compositing of Nimbus ESMR passive microwave maps to produce time series of Arctic and Antarctic ice cover. (Casey, 1985; Zwally 1983).
3. The processing of Seasat scatterometer data to produce global composites of wind stress. This has taken several years even for the short Seasat data set.
4. Production of global maps based on altimeter data showing waves, wind and ocean circulation variability. It has similarly taken many years to

process GEOS-3 and Seasat data. (Chelton et al. 1981, Cheney and Marsh, 1981).

5. Production of time series of CZCS ocean chlorophyll maps for both the east and west coast of North America. Such analysis is running five years behind the data collection.

Such products demonstrate the satellite's capability to collect global data sets of relevance to climate and biological studies, but also demonstrate our present inabilities for timely analysis.

Programmes need to be undertaken by the space agencies both to supply satellite data to individual users for limited geographical areas, and to compile time series of processed data sets that can be used in studying global scale problems.

The individual researcher needs to be able to find out what satellite data exists for particular dates of a particular area. At present, this is not easy. The best method varies with the type and source of the satellite data.

For Landsat, the EROS Data Centre at Sioux Falls, (address in section 4.5.2, below) can produce a computer listing of images with corner coordinates, dates and an estimate of cloud cover. Image location is greatly speeded by use of standard image centres made possible by stabilizing the orbit and by suitably organizing data processing. Cloud cover estimates are subjective and often inaccurate in the presence of snow and ice and also give no information on its location.

Only a fraction of AVHRR data is archived digitally. Many tapes are recycled after a few weeks. Oceanographic users are making a variety of arrangements to collect data from the various receiving stations (see section 4.5.2). Most of these stations are predominantly concerned with meteorological applications.

CZCS data is archived digitally. NASA Goddard distributes maps of data acquired, though currently with a four year delay. NOAA's NESDIS has recently started to distribute microfilms of quicklook CZCS data that efficiently show cloud-free areas covered, as well as giving orbit and time information.

Various other archives exist for other data sets. The situation for a new user to acquire satellite data is certainly improving, but could improve further.

Users who could afford the expense have installed their own satellite receiving stations (Evans et al, 1980). These are becoming cheaper and more automated, but still require constant supervision and a continuing effort to archive the data. Duplicate receivers and dishes are often needed to receive data from different satellites. Arrangements must be made to receive data at satellite overpass times through the 24 hours, seven days a week, but the more automated stations handle this satisfactorily.

Table 4.5.1

Satellite Sensor Ocean Data Now Being Collected

| Data | Satellite | Primary purpose | Disadvantages for ocean programmes |
|--|--|--------------------------|---|
| Thermal and visible images 1 km resolution | NOAA, DMSP, Meteor polar orbit | Meteorology | Lack of reliable digital archive, lack of bands, sensitivity in visible |
| Thermal and visible images 1 km/4 km resolution | GOES, GMS Meteosat INSAT geosynchronous | Meteorology | Lack of reliable digital archive, lack of bands, sensitivity in visible |
| Visible images 100 m and 30 m resolution | Landsat polar | Land studies | Infrequent repeat cycle High data volume and cost for small scenes |
| Visible (ocean colour) images 1 km resolution | Nimbus 7 (CZCS) polar | Oceanography | Sensor improvements needed, data not adapted for global studies |
| Microwave images 30 - 150 km resolution | Nimbus 7 (SMMR) polar | Atmosphere ocean, ice | Processing still being refined, low spatial resolution |
| Altimetry | Geosat polar | Geoid determinations | Range measurements not being released |

In the U.S. the use of synchronous satellite links are now being discussed as part of a shared data processing system. Three government agencies will contribute processed image and other data, to be sent to the satellite in a daily sequence. This can then be received by users anywhere in the range of the RCA DOMSAT system. Costs to the user will consist of the terminal rental and the manpower and hardware needed to create the appropriate archive from the data received. The system presents users with data from various satellites in a more ordered sequence, but the scheduling and archiving tasks remain.

Solutions to the present data distribution problem will come slowly with improving technology. Other countries are discussing wide band data distribution systems, and ocean users need to be represented in the planning stages to ensure that their needs are included.

4.5.2 Sources of Data

Data from the NOAA operational satellites, from experimental meteorological satellites, from the CZCS and SMMR on Nimbus 7 and from Seasat are available from the National Environmental Satellite Data and Information Service (NESDIS) at:

NOAA/NESDIS
Satellite Data Services Division
Room 100, World Weather Building
Washington, D.C. 20233, U.S.A.
Telephone: (301) 763-8111

Summaries of the NOAA Meteorological satellite data are printed in Environmental Satellite Imagery and in the Oceanographic Monthly Summary, both published monthly by NESDIS. More general information is contained in the Satellite Data Users Bulletin, published at irregular intervals by the same group.

Data from the space shuttle, including data from the Shuttle Imaging Radar (SIR-A and B), the Ocean Color Experiment (OCE), and the Shuttle Multispectral Infrared Radiometer (SMIRR), as well as data from the Heat Capacity Mapping Mission (HCMM), are available from:

National Space Data Center
World Data Center A for Rockets and Satellites
NASA/Goddard Space Flight Center Code 601
Greenbelt, Maryland 20771
U.S.A.

Photographs from the manned space flights (Gemini, Apollo, Skylab and Shuttle) and the Landsat data sets are available from:

NOAA Landsat Customer Services
EROS Data Center
Sioux Falls, South Dakota 57198 U.S.A.
Telephone: (605) 594-6515

Data from the Defense Meteorological Satellite Program is stored at NOAA/NESDIS, and at the Cooperative Institute for Research in Environmental Sciences (CIRES) through:

World Data Center A for Glaciology
CIRES
Campus Box 449
University of Colorado
Boulder, Colorado 80309
U.S.A.

Data from the GOES geosynchronous satellites visible and infrared scanners and the DMSP are available from:

The Space Science and Engineering Center
University of Wisconsin
Madison, Wisconsin 53706
U.S.A.

To help reduce the problems of finding and using satellite data, NASA has experimented with several pilot data systems to collect, store, and distribute data from a variety of sources. The one for oceanographic data is the

Pilot Ocean Data System
NASA/Jet Propulsion Laboratory
4800 Oak Grove Dr.
Pasadena, California 91109
U.S.A.

It contains, in machine readable form, the Seasat and Geos-3 data, the extensive sets of surface observations used to calibrate the instruments on these satellites, and a bibliography of descriptions of the satellites, their instruments, the calibration of the instruments, and the application of the satellite data to oceanography.

Within Europe, data from the NASA Landsat, Nimbus-7, HCMM, and Seasat satellites are distributed through the Earthnet Program Office of the European Space Research Institute (ESRIN) at:

ESRIN/Earthnet Program Office
Via Galileo Galilei
00044 Frascati, Italy
Telephone: (06)9422401

The satellite station operated by the University of Dundee has made a specialty of ocean data collection and is a useful source of CZCS and AVHRR data:

Department of Electrical Engineering and Electronics
The University of Dundee
Dundee, DD1 4HN, U.K.

Meteosat data are distributed by the European Space Operation Center (ESOC) at:

Meteosat Data Services
Meteosat Data Management Department
ESOC
Robert-Bosch-Strasse 5
D-6100 Darmstadt, West Germany

ESA also publishes a newsletter, the Earth Observation Quarterly, available from:

ESA Scientific and Publications Branch
ESTEC - PB299
2200 AG Noordwijk
The Netherlands

Other sources of satellite data are as follows:

Comision Nacional De Investigaciones
Espaciales (CNIE)
Central De Teleobservacion
Av. Del Libertador 1513
Vincente Lopez 1638
Buenos, Aires
ARGENTINA

CSIRO Division of Land Management
P.O. Box 28
Belconnen
A.C.T. 2616
AUSTRALIA

Instituto De Pasquisas Espaciais
C.P. 01
12630 Cachoeira Paulista, S.P.
BRAZIL

Chief, Aerospace Meteorology Division
Atmospheric Environment Service
4905 Dufferin Street
Downsview, Ontario
CANADA M3H 5T4

National Remote Sensing Agency
Plot No. 4, Sadar Patel Road
OPP: Secunderabad Cantonment
Board Office, Secunderabad
INDIA

Indonesian National Institute of
Aeronautics & Space (Lapan)
JLN, Pemuda Persil 1
P.O. Box 3048, Jakarta
INDONESIA

Director, Earth Observation System Dept.
Remote Sensing Technology Centre of Japan
UNI-ROPPONGI Building
7-15-17 ROPPONGI, MINATOKU, TOKYO
JAPAN 106

National Institute for telecommuni-
cations Research
P.O. Box 3718
Johannesburg 2000
REPUBLIC OF SOUTH AFRICA

Kanya Jirapayoongchai
Remote Sensing Division
National Research Council
THAILAND

5. APPLICATIONS IN DEVELOPING COUNTRIES

Coastal management and survey are among the applications possibilities of remote sensing recognized by the UN Committee on the Peaceful Uses of Outer Space (COPUOS). Remote sensing offers an effective tool to developing countries for the exploration of the marine environment and for producing a marine resources survey and management system, as stressed during the second United Nations Conference on the Exploration and Peaceful Uses of Outer Space (UNISPACE, Vienna, Austria, 9-21 August 1982, see e.g. document A/CONF. 101/NP/11 concerning the Indonesian participation).

Satellite sensors have now demonstrated their capability to provide observations of wind and waves, coastal dynamics and productivity patterns, and, on a small scale, sediment and pollution transport and river run off. The data can clearly play a useful role in surveying the economically and ecologically important coastal zones, especially of countries where an efficient coastal protection and management system is difficult to establish and maintain.

Up to the present, use of oceanic satellite remote sensing has been practiced almost exclusively by scientists from industrially developed countries which can afford to develop and launch satellites, or at least to receive and process the data from them. Since the cost of even a modest satellite mission is on the order of \$100 million U.S., and most receiving stations have cost \$1 million or more, it is not surprising that developing countries have found the price of involvement more than they are prepared to spend. Even the cost of purchasing a single image, on the order of \$10, becomes appreciable when many must be ordered, or when data tapes, at \$100 per scene, are required so that low contrast features, which are often important in ocean scenes, can be digitally enhanced.

The relative cost of electronic hardware is decreasing, making sophisticated yet simple-to-operate satellite receiving stations more widely available. Location of receiving stations in developing countries would solve the problem of sending the data to those countries, as well as providing an interesting and educational focal point for local scientific and technical developments. The satellite station at the Scripps Institution of Oceanography in the U.S.A. has demonstrated the capabilities of a small station for receiving the relatively narrow band signals characteristic of sensors having about 1 km resolution. The University of Dundee in the U.K. has demonstrated a lower cost approach for the same type of data, by using the in house capabilities of a university electrical engineering department. Departments capable of similar work exist in developing countries.

Because such countries often lack the extensive ship and/or aircraft facilities which can provide higher resolution surveillance of near coastal areas, there is also a need for high resolution satellite data, which generally requires more expensive equipment for data reception directly from the satellite. While direct reception is still desirable and may not be beyond some local resources, there will remain, in many cases, a need for transfer of image data as photographs or tape, especially if user fees for receiving stations are levied by the launching countries.

The present situation therefore presents several alternatives for acquiring the data for study of local areas. In addition it is important

that scientists from all countries should be given access to the large scale experiments, directed for example at climate studies, whose relevance may only become apparent on a longer term.

At the present time all satellite ocean remote sensing missions have been experimental. This will also be true for the next few years. A major program that encourages developments of too broad and specific a nature in developing countries may therefore be premature. However it is important that the technical problems and capabilities of the field should be widely appreciated, and encouraging and supporting development of local facilities for receiving and processing the data seems a worthwhile step in this direction.

In this respect, education and training in remote sensing application, processing and interpretation are of crucial importance. Courses at different levels on subjects specifically related to the problem of developing countries are given at the International Institute for Aerial Survey and Earth Science (ITC, Enschede, The Netherlands) and at Imperial College (London, U.K.). The European Association of Remote Sensing Laboratories has sponsored a number of summer schools both in land and marine uses of remote sensing, supported by the Council of Europe, the European Space Agency and the European Economic Community.

Joint research programmes should be supported and encouraged to include adequate knowledge transfer. Recently, such activities have been reported: e.g. the Netherlands oceanographic expedition Snellius II to Indonesian waters planned for 1984-85, which includes international participation in the remote sensing experiments, data collection and processing; the German Marine Remote Sensing Experiment in Indonesia conducted in 1982 by DFVLR; and the JRC-ORSTOM program in the waters of Senegal.

Studies on the satellite remote sensing applications and mission objectives in developing countries are being performed by Netherlands institutions with respect to the existing plans for launching of a satellite dedicated to the remote sensing of the tropical regions (TERS, Tropical Earth Resources Satellite) (Voute 1982). The Snellius II expedition will include measurements appropriate to the TERS case studies.

6. CONCLUSIONS AND RECOMMENDATIONS

6.1 Conclusions

Satellite sensors have demonstrated their advantages for studying the oceans by providing repeated global coverage, and precise images of local areas, with a data quality that in some cases exceeds that available by other means. Absolute accuracies are sometimes less satisfactory, but progress is being made in improving atmospheric, sensor and other corrections.

Satellite oceanography has benefited from the large investment by the U.S. in the space technology that has produced the weather and land satellites, and the specialized ocean satellites such as Geos-3, Seasat, Nimbus 7 and, most recently, Geosat. Other countries are now contributing with the geosynchronous satellites Meteosat, GMS and Insat to complete the coverage round the equator that was begun by the U.S. GOES satellites. This international cooperation gives sufficiently global coverage to allow world climate studies of solar heating of the oceans and atmosphere, and of winds derived from cloud motion.

Major recent disappointments have been in the lack of new systems launched, and in the slowness with which data distribution and processing have improved in throughput and quality. Several ocean satellites are however now planned for launch by various countries in the next 5 to 10 years. It is now clearly urgent to prepare to handle the greatly increased flow of data to users round the world.

All this data is similar to that provided from previous satellites, but we may expect that the major short-fall of these sources, i.e., lack of continuity and long term coverage, can now be overcome.

In summary, planned programmes by nations, as listed in the various tables in the text, can with suitable coordination, meet the existing requirements for type and quality of ocean data from satellites. The potentially missing elements are: full international cooperation, assured data continuity, greatly improved archiving, and better means of processing by users around the globe. National sponsors must pay particular attention to these items if the very large investments in space hardware are to pay the returns that justified the programmes originally.

6.2 Recommendations

6.2.1 General

1. The properties of satellite orbits and sensors should be coordinated internationally to maximize benefits from national programmes.

2. Improved systems of data and image distribution and processing should be prepared to handle the very large volume of data from ocean satellites due to be launched in the near future. There is a need both for large-scale central processing systems, and for smaller systems for individual users.

3. Such systems should take into account the needs of users in developing countries, for ocean and coastal data covering their areas.

4. Development of cheap, permanent digital data recording systems such as optical disks must be encouraged. Much potentially useful satellite data of the oceans is discarded because of the cost of archiving it. This is particularly true of data in digital form. Even where data has been archived, the storage and duplication costs passed on to users deters many studies. Improved archives would make an enormous difference to the value that can be extracted from satellite missions, especially those designed for long term operation.

5. There is a widely felt need for advanced training of scientists in techniques of satellite oceanography. This need must be addressed by special educational programmes and should not be left to automatic fulfillment by the laws of supply and demand. The situation will surely become critical with the increased launch rate of new satellites.

6.2.2 Ocean Circulation, Tides and Geoid

To prepare for the large scale or global data sets that must be acquired for experiments such as WOCE or TOGA, oceanographers need to develop improved ocean models having the capability of accepting satellite data with time and space sampling determined by the satellite orbit. Much work on assimilating the non-traditional variables measured from space into numerical models needs to be done. Coordination between oceanographers and organizations responsible for building and operating satellites must be improved.

6.2.3 Ice

1. Since polar observations are only possible from satellite orbits that also pass over temperate and tropical zones, compromise designs of ice sensors will often be favoured in spite of the economic and environmental importance of ice mapping. This trend should be resisted. It is also recommended that attention be given to sensor designs on polar orbiting satellites, especially radar altimeters and SARs, to improve ice observations even when this is not the primary mission target.

2. Since a polar orbit implies coverage of both Arctic and Antarctic regions, attention should be given to data gathering and international projects in both areas even if only one is the primary target (as in the Canadian Radarsat).

6.2.4 Biology and Coastal Processes

The Coastal Zone Color Scanner has demonstrated the potential of water colour observations both for quantitative pigment mapping and for flow visualization.

1. In view of the importance of this type of data to a large number of countries for management of their coastal zones, it is recommended that both the quantity and quality of the available data should be increased as soon as possible.

2. It should be noted that the CZCS does not have adequate spatial resolution for truly coastal studies, which require both higher resolution and more frequent repeat cycles. This is a difficult combination to achieve but possibilities, e.g. steerable sensors in geostationary orbit, should be investigated.

3. Improved capabilities over this "first generation" sensor are clearly possible and are recommended:

- . Longer wavelength channels and improved calibration for better atmospheric correction.
- . New channels for fluorescence and yellow substance estimation.
- . Higher radiometric precision in all bands.
- . High quality co-registered images should also be provided.

4. Because of the complexity and variety of processes affecting optical properties of the water and the atmosphere, appropriate studies, for example on atmospheric corrections, Case 2 water properties, and fluorescence, should be encouraged.

5. For global productivity monitoring the possibility of adding one or two additional "colour" channels to the VISSR type sensors on geostationary satellites should be evaluated. Resolution is already comparable to that of the CZCS (about 1 km) and the much more rapid repeat cycle, as short as one-half hour, would allow for improved cloud avoidance.

6.2.5 Air Sea Interaction

1. To satisfy the research and forecasting needs of the oceanographic community, the surface vector wind field or stress measurements over the ocean must be measured from space with accuracies obtainable with a radar scatterometer. It is recommended that a scatterometer be placed on each of two satellites flown in coordinated orbits, in order to achieve the coverage and timeliness required.

2. A strong need exists for mapping the air-sea temperature difference and the fluxes of energy and momentum across the interface. New sensor ideas are required if these data are to be provided by satellites.

6.2.6 Internal Waves and Other Surface Phenomena

Basic studies should be conducted in order to understand the causes of surface signatures appearing in high-resolution optical, IR and radar imagery. Some candidate sources are surface wave beats, internal, shelf and inertial waves, bathymetry, temperature/stability variations, water mass differences, rainfall, wind, and surface oils.

6.2.7 Bottom Topography

Satellite optical sensors are now approaching the resolution needed for charting requirements in shallow water. Attention should be given to using

water penetrating bands for depth estimation as well as for pigment and seston measurement.

7. ANNOTATED BIBLIOGRAPHY - GENERAL REPORTS

(Note: some of these reports are referenced in the text.)

Allan, T. (Ed.) 1983. Satellite Microwave Remote Sensing. Ellis Horwood, Ltd., Chichester, UK. Proceedings from meeting of Seasat Users Working Group of Europe held at Royal Society, April 1982, with emphasis on scientific results from several sensors.

AGU. 1982. Seasat Special Issue I: Geophysical Evaluation. Bernstein, R.L. (Ed.), J. Geophys. Res., 87, pp. 3173-4338. Research level papers on data algorithms and evaluation for Seasat up to publication date.

AGU. 1983. Seasat Special Issue II: Scientific Results. J. Geophys. Res., 88, pp. 1529-1952. Research papers on selected scientific results from Seasat.

Apel, J.R. 1980. Satellite Sensing of Ocean Surface Dynamics. Ann. Rev. Earth Planet. Sci. 1980, 4, 303-342. Examples of dynamical studies carried out with satellite data.

Bretherton, F.P. 1981. Technical Studies Related to the Development of a System for Ocean Climate Monitoring. Vols. I-III. National Oceanic & Atmospheric Administration, Data Buoy Office, NSTL Station, MS. A planning and evaluation document relating to ocean observational needs for a global climate programme, including ship, buoy and satellite data.

Brown, O.B., and R. E. Cheney. 1983. Advances in satellite oceanography. Rev. Geophys. and Space Phys., 21, 1216-1230. Review of major advances in satellite-oriented remote sensing of oceanic processes.

Charnock, H., and R.T. Pollard (Eds.). 1983. Results of the Royal Society Joint Air-Sea Interaction Project (JASIN). Royal Society, London. Scientific papers from the 1978 Joint Air-Sea Interaction Experiment in the North Atlantic, with some discussions of Seasat contributions.

COSPAR. 1980. Space-Based Observations in the 1980s and 1990s for Climate Research: A Planning Strategy. Committee on Space Research Commission A, National Center for Atmospheric Research, Boulder, CO. A report to the Joint Scientific Committee for WMO/ICSU World Climate Research Program that outlines needs and strategies for climate-oriented observations from space, for both atmosphere and ocean.

Dornier. 1985. ERS-1: ESA Remote Sensing Satellite. Dornier System GmbH, Friedrichshafen, FRG. A brochure describing the missions and technical capabilities of the European Remote Sensing Satellite.

ESA. 1984. Earth Observation Quarterly, No. 8. December 1984. ESA Scientific and Technical Publications Branch. ESTEC, Noordwijk, The Netherlands. (See also other issues.) Article on international coordination for earth observing satellite programs.

ESA. 1983. Looking down-looking forward. B. Battrick (Ed.), ESA Scientific and Technical Publications Branch. ESTEC, Noordwijk, The Netherlands. A nicely illustrated general description of earth observations from satellites, and ESA's present work and future plans.

Gower, J.F.R. (Ed.). 1981. Oceanography From Space. Plenum Press, New York. N.Y. Proceedings of a conference covering ocean remote sensing techniques and results including coastal (Landsat) work, thermal and water colour results, and results of the Seasat mission.

Hibbs, A.R., and W.S. Wilson. 1983. Satellites map the oceans. IEEE Spectrum, 46-53. Semi-popular article on satellite oceanography and programs.

IEEE. 1980. Special Issue on Seasat-1 Sensors. Weissman, D.E. (Ed.). IEEE J. of Oceanic Engr. OE-5, 71-180. Research level papers on Seasat instruments and performance as of publication date.

IOS/NSERC. 1985. Remote Sensing of the Oceans. Natural Environment Research Council, Institute of Oceanographic Sciences, Wormley, Godalming, U.K. Brochure on satellite oceanography at IOS.

ISRO. 1982. Remote Sensing of Oceans. Indian Space Research Organisation, Technical Report ISRO-TR-21-82, Bangalore, India. Five papers summarizing a range of ocean remote measurement prospects with some applications to Indian coastal regions.

JOI. 1984. Oceanography from Space: A Research Strategy for the Decade 1985-1995. Part 1: Executive Summary; Part 2. Proposed Measurements and Missions. Joint Oceanographic Institutions, Inc., Washington, DC, 20037. Succinct summaries of requirements for ocean-oriented satellites and a proposed sequence of U.S. programmes to meet them.

JOI. 1985. OCI: Ocean Color Imager. Joint Oceanographic Institutions, Inc. Washington, DC 20037. A brochure on the Ocean Color Imager proposed for U.S. spacecraft.

JSC/CCCO. 1981. Report of the meeting on the coordination of plans for future satellite observing systems and ocean experiments to be organized within the WCRP, Chilton, U.K., 26-31 January 1981. WCRP Report Series WCP-8. A report on this important and highly relevant topic. Now slightly dated and currently out of print.

Legler, D.M., and J.J. O'Brien. Atlas of Tropical Pacific Wind-Stress Climatology 1971-1980. The Florida State University, Tallahassee, FL, 32306. Valuable summary of surface stress fields on monthly and annual bases.

Levitus, S. 1983. Climatological Atlas of the World Ocean. NOAA Professional Paper 13. NOAA, Rockville, MD. Exceedingly useful data on oceanic fields reduced to standard formats.

Maul, G.A. 1985. Introduction to Satellite Oceanography. Dordrecht, Boston, MA. Textbook on ocean remote sensing, concentrating on the visible and infrared.

Munk, W. and C. Wunsch. 1982. Observing the Oceans in the 1990s. Phil. Trans. R. Soc. London A307, 439-464. Discussion of hypothetical observational systems for basin-wide measurements.

NAS. 1979. Applications of a Dedicated Gravitational Satellite Mission. Committee on Geodesy, National Academy of Sciences, Washington, DC. Discussion of missions for a gravity-determining spacecraft, including solid earth, oceanographic and geodetic applications.

NAS. 1982a. A Strategy for Earth Science from Space in the 1980s: Part I: Solid Earth and Oceans. Committee on Earth Sciences, Space Science Board, National Academy Press, Washington, DC. A strategy report that sets scientific goals and priorities for the U.S. program in earth science in general, and ocean dynamics in particular; needs for observations of surface heights, wind stress, circulation, and temperatures are developed.

NAS. 1982b. Two Special Issues in Satellite Oceanography: Ocean Dynamics and Biological Oceanography. Ocean Sciences Board, National Academy Press, Washington, DC. Opportunities and priorities for satellite usage in the areas cited, with recommendations for U.S. national programs utilizing satellites and aircraft in conjunction with in situ measurements.

NASA. 1979. ICEX: Ice and Climate Experiment. Report of Science and Applications Working Group, NASA/Goddard Space Flight Center. Scientific background and applications of ice research; ICEX program objectives and data requirements, with emphasis on satellite sensors and system.

NASA. 1982a. Scientific Opportunities Using Satellite Wind Stress Measurements Over the Ocean. NASA Satellite Surface Stress Working Group, Nova University, Ft. Lauderdale, FL. A review of oceanic wind stress measurement needs, with applications to satellite, modeling, and forecasting.

NASA. 1982b. The Marine Resources Experiment Program (MAREX). Report of the Ocean Color Science Working Group, NASA Goddard Space Flight Center, Greenbelt, MD. A review of remote ocean color measurements and their application to chlorophyll production and carbon and nitrogen fluxes in coastal waters; includes summaries of spacecraft, sensors and algorithms of relevance to MAREX.

NASA. 1982c. TOPEX: Observing the Oceans from Space. NASA/JPL, Pasadena, CA. Brochure giving mission and characteristics of TOPEX spacecraft.

NASA. 1983a. Global Geodynamics. National Aeronautics and Space Administration, Geodynamics Program Office, Washington, DC, 20546. Brochure on U.S. programs in solid earth dynamics.

NASA. 1983b. Satellite Data Relay and Platform Locating in Oceanography. Report of the In Situ Ocean Science Working Group. Nova University/N.Y.I.T. Press. Fort Lauderdale, FL. Report summarizing needs and capabilities of data relay and platform location via satellite.

NASA. 1983c. GRM: Geopotential Research Mission. Gravity/Magnetic Fields: Solid Earth Geophysics. NASA, Geodynamics Program Office, Washington, DC 20546. Brochure on GRM requirements and missions.

NASA. 1983d. Satellite-Derived Sea Surface Temperature: Workshop-1. NASA/JPL Publication 83-84, Pasadena, CA. Report on evaluation of sea surface temperature measurements using current satellite sensors.

NASA. 1984a. Passive Microwave Remote Sensing for Sea Ice Research. National Aeronautics and Space Administration, Oceanic Processes Branch, Washington DC, 20546. Report on the Special Sensor Microwave Imager for use in sea ice problems.

NASA. 1984b. Frontiers of Remote Sensing of the Oceans and Troposphere from Air and Space Platforms. J. Goldkirsh (Ed.), NASA Publication 2303. Proceedings of a conference on scientific progress and advanced instrumentation for oceans and atmosphere.

Oort, A.H. 1983. Global Atmospheric Circulation Statistics, 1958-1973. NOAA Professional Paper 14, National Oceanic and Atmospheric Administration, Rockville, MD. Exceedingly useful data on atmospheric fields reduced to standard formats.

Peixoto, J.P., and A.H. Oort. 1984. Physics of Climate. Rev. Mod. Phys. 56, 365-430. A comprehensive review of the physics and theoretical formulation of climate dynamics.

Pounder, E. (Ed.). 1980. Seasat Final Report, Vol. I: Program Summary. NASA/JPL Publication 80-38, Pasadena, CA. A summary of Seasat mission execution, functions, and operations.

Rasmusson, E.M., P.A. Arkin, T.H. Carpenter, J. Koopman, A.F. Krueger, and R.W. Reynolds. 1983. A warm episode in the eastern equatorial Pacific Ocean. Tropical Ocean-Atmosphere Newsletter 16, 1-3. Up-to-date paper on the 1982-1983 El Nino.

Ruttenberg, S. (Ed.). 1981. Needs, Opportunities and Strategies for a Long-Term Oceanic Sciences Satellite Program. National Center for Atmospheric Research, Boulder, CO. A report to NASA by the NOSS Science Working Group that summarizes applications and opportunities for a broad range of satellite derived information, including altimetry, scatterometry, and colorimetry.

Smith, D., Langel, R. and Keating, T. 1982. Geopotential Research Mission (GRM). NASA Goddard Space Flight Center, Greenbelt, MD. An outline of mission requirements and satellite configurations for the GRM, the re-named Gravsat/Magsat mission.

Stewart, R.H., (Ed.). 1981. Satellite Altimetric Measurements of the Ocean: Report of the TOPEX Science Working Group. NASA/JPL, Pasadena, CA. A highly useful summary of large scale ocean circulation from the standpoint of its determination via satellite altimetry, plus requirements for the Ocean Topography Experiment.

Stewart, R.H. 1984. Oceanography from Space. Ann. Rev. Earth. Planet. Sci., 12, 61-82. A short review of instruments and measurement capabilities.

Stewart, R.H. 1985. Methods of Satellite Oceanography. Univ. of California Press. Textbook on oceanography from space with a quantitative emphasis.

Sverdrup, H.U., M.W. Johnson and R.H. Fleming. 1962. The Oceans: Their Physics, Chemistry and General Biology. Prentice Hall, Englewood Cliffs, NJ. Excellent but old oceanography text.

Takeda, A. 1981. Remote Sensing of the Ocean with Applications to the Prevention of Marine and Coastal Disasters. National Research Center for Disaster Prevention; Japanese International Cooperation Agency; Hiratsuka, Japan. A short primer on various ocean remote sensing methods and results, with coastal emphasis.

WHOI. 1981. Oceanography from Space. Oceanus Vo. 24, No. 3. Eight brief review articles covering the field with emphasis on large scale experiments.

8. REFERENCES

- Apel, J.R., H.M. Byrne, J.J. Proni, and R.L. Charnell. 1975. Observations of oceanic internal and surface waves from the Earth Resources Technology Satellite. *J. Geophys. Res.* 80, 865-871.
- Austin, R.W. and T.J. Petzold. 1981. The determination of the diffuse attenuation coefficient of sea water using the Coastal Zone Color Scanner, in *Oceanography from Space*. J.F.R. Gower (Ed.), Plenum Press, New York, 239-256.
- Barnett, T.P., S.C. Patzert, W.C. Webb, and B.R. Bean. 1979. Climatological usefulness of satellite determined sea-surface temperature in the tropical Pacific. *Pull. Am. Met. Soc.* 60, 197-205.
- Basharinov, A.E. and A.M. Shutko. 1980. Research into the measurement of sea state, sea temperature and salinity by means of microwave radiometry. *Boundary-Layer Meteorology*, 18, 55-64.
- Behie, G. and P. Cornillon. 1981. Remote Sensing: a Tool for Managing the Marine Environment: Eight Case Studies. Univ. of Rhode Island, Mar. Tech. Rep. No. 77, 42-44.
- Bernstein, R.L. 1982. Sea surface temperature estimation using the NOAA-6 satellite Advanced Very High Resolution Radiometer. *J. Geophys. Res.*, 87, 9455-9465.
- Born, G.H. 1984. Satellite altimetry, *Marine Geodesy*. 8, Nos. 1-4, special issue. G.H. Born (Ed).
- Brooks, D.A. and R. Legeckis. 1982. A ship and satellite view of hydrographic features in the western Gulf of Mexico. *J. Geophys. Res.* 87, 4195-4206.
- Carder, K.L. 1982. Oceanic Lidar. NASA Conference Publication.
- Cardone, V., T. Chester and R. Lipes. 1983. Evaluation of Seasat SMMR wind speed measurements, *J. Geophys. Res.*, 88, 1709-1726.
- Carsey, F.D. 1985. Summer Arctic sea ice character from satellite microwave data, *J. Geophys. Res.*, 90, 5015-5034.
- Cartwright, D.E. and G.A. Alcock. 1981. On the precision of sea surface elevations and slopes from Seasat altimetry of the north-east Atlantic Ocean, in *Oceanography From Space*. J.F.R. Gower (Ed), Plenum Press, New York. 883-896.
- Chamberlin, J. Lockwood. 1982. Application of satellite infrared data to analysis of ocean frontal movements and water mass interactions off Northeastern United States. Northwest Atlantic Fisheries Organization, Scientific Council Studies, No. 4, Special report on remote sensing, R.W. Trites (Session convener).
- Chelton, D.B., K.J. Hussey, and M.E. Parke. 1981. Global satellite measurement of water vapor, wind speed and wave height. *Nature* 294, 529-532.

- Chelton, D.B., and P.J. McCabe. 1965. A review of satellite altimeter measurement of wind speed: with a proposed new algorithm. *J. Geophys. Res.*, 90, 4707-4720.
- Cheney, R.E., and J.G. Marsh. 1981. Global mesoscale variability from Seasat colinear altimeter data. *EOS, Trans. Am. Geophys. Union* 62, 298 (abstr.).
- Collins, D.J. 1982. Lidar and acoustics applications to ocean productivity. NASA. JPL Publication 82-86.
- Crepon, M., L. Wald and T.M. Monget. 1982. Low frequency waves in the Ligurian Sea during December 1977. *J.G.R.*, 87, 595-600.
- Evans, R.H., S.S. Kent and J.B. Seidman. 1980. Satellite Remote Sensing Facility for Oceanographic Applications. NASA JPL publication 80-40.
- Ford, J.P., J.B. Cimino, and C. Elachi. 1983. Space Shuttle Columbia views the world with imaging radar: the SIR-A experiment, NASA, JPL Publication 82-95.
- Gloersen, P., and F. Barath. 1977. A scanning multichannel microwave radiometer for Nimbus G and Seasat. *IEEE J. Ocean Eng.*, OE-2, 172-178.
- Gordon, H.R. 1980. Ocean remote sensing using lasers. NOAA Technical Memorandum ERL PMEL-18.
- Gordon, H.R., D.K. Clark, J.W. Brown, O.B. Brown, and R.H. Evans. 1982. Satellite measurements of the phytoplankton pigment concentration in the surface waters of a warm core Gulf Stream ring. *J. Mar. Res.*, 40, 491-502.
- Gordon, H.R., D.K. Clark, J.W. Brown, O.B. Brown, R.H. Evans, and W.W. Broenkow. 1983. Phytoplankton pigment concentrations in the Middle Atlantic Bight: comparison of ship determinations and CZCS estimates. *Applied Optics*, 22, 20-36.
- Gordon, H.R. and A. Morel. 1983. Remote Assessment of Ocean Color for Interpretation of Satellite Visible Imagery, A Review. *Lecture Notes on Coastal and Estuarine Studies*, 4, 114 pp., Springer-Verlag, New York.
- Gower, J.F.R., and G.A. Borstad. 1981. Use of the in vivo fluorescence line at 685nm for remote sensing surveys of surface chlorophyll a, in *Oceanography from Space*. J.F.R. Gower (Ed.). Plenum Press, New York, 329-338.
- Gower, J.F.R. 1984. Water colour imaging from space, in *Remote Sensing of Shelf Sea Hydrodynamics*. C.J.C. Nihoul (Ed.). Elsevier Science Publishers, 1-24.
- Guan, F., J. Pelaez, and R.H. Stewart. 1985. The atmospheric correction and measurement of chlorophyll concentration using the Coastal Zone Color Scanner. *Limnology and Oceanography*, 30, 273-285.
- Hasselmann, K., R.K. Raney, W.J. Plant, R.A. Shuchman, D.R. Lyzenga, C.L. Rufenach and M.J. Turner. 1985. Theory of synthetic aperture radar ocean imaging: a MARSEN view, *J. Geophys. Res.*, 90, 4659-4686.

Haxby, W.F. 1984. Geotectonic Imagery from Seasat, 1982-83 Lamont-Doherty Geological Observatory Yearbook, p. 12.

Hendershott, M.C. 1973. Ocean tides, EOS, Trans. A.G.U., 54(2).

Hovis, W.A., D.K. Clark, F. Anderson, R.W. Austin, W.H. Wilson, E.T. Baker, D. Ball, H.R. Gordon, J.L. Mueller, S.Y. El Sayed, B. Sturm, R.C. Wrigley and C.S. Yentsch. 1980. Nimbus 7 Coastal Zone Color Scanner: system description and initial imagery. Science, 210, 60-63.

Jones, W.L., L.C. Schroeder, D.H. Bloggs, E.M. Bracalente, R.A. Brown, G.J. Dome, W.J. Pierson, and F.J. Wentz. 1982. The Seasat-A satellite scatterometer: the geophysical evaluation of remotely sensed wind vectors over the ocean. J. Geophys. Res., 87, 3297-3317.

Jones, W.L., L.C. Schroeder, and J.L. Mitchell. 1977. Aircraft measurements of the microwave scattering signature of the ocean. IEEE Trans. Ant. Prop., AP-25, 52-61.

LaViolette, P.E. 1974. in Optical Aspects of Oceanography, N.G. Jerlov and E. Steeman Nielsen (Eds.), Academic Press, London, 289-316.

LaViolette, P.E., S. Peteherych, and J.F.R. Gower. 1980. Oceanographic implications of features in NOAA satellite visible imagery. Boundary Layer Meteorology, 18, 159-175.

Llewellyn-Jones, D.T. 1982. The Along Track Scanning Radiometer with Microwave Sounder (ATSR/M) Llewellyn-Jones, D.T. (Principal Investigator). Rutherford Appleton Laboratory, proposal to ESA.

Legeckis, R. 1978. A survey of worldwide sea surface temperature fronts detected by environmental satellites. J. Geophys. Res., 83, 4501-4522.

Legeckis, R. and A.L. Gordon. 1982. Satellite observations of the Brazil and Falkland currents 1973 to 1976 and 1978. Deep Sea Res. 29, 375-401.

Marsh, J.G. and T.V. Martin. 1982. The Seasat altimeter mean sea surface model. J. Geophys. Res., 87, 3269-3280.

Maul, G.A. and M. Sidran. 1973. Atmospheric effects of ocean surface temperature sensing from the NOAA satellite scanning radiometer. J. Geophys. Res., 78, 1909-1916.

McClain, E.P., W.G. Pichel, C.C. Walton, Z. Ahmad, and J. Sutton. 1983. Multichannel improvements to satellite derived global sea surface temperature. Adv. Space Res., 2, 43-47.

Ministere de l'Environnement, France. 1979. Airborne remote sensing of oil spills in coastal waters. Ministere de l'Environnement et du Cadre de Vie.

Mueller, J.L. and P.E. LaViolette. 1981. Color and temperature Signatures of ocean fronts observed with the Nimbus 7 CZCS, in Oceanography from Space. J.F.R. Gower (Ed.), Plenum Press, New York, 295-302.

- NASA. 1981a. Seasat Data Utilization Project. Final Report, No. JPL-622-233.
- NASA. 1981b. Satellite altimetric measurements of the ocean. Report of the TOPEX Science Working Group. R.H. Stewart (Project Scientist) JPL.
- NOAA. 1977. Pacific Marine Environmental Laboratory, Annual Report. FY 1976 and 1976T. Seattle, WA 98105.
- Njoku, E. 1985. Satellite derived sea surface temperature: workshop comparisons, Bull. Am. Met. Soc., 66, 274-281.
- O'Brien, J.J. 1982. Scientific opportunities using satellite wind stress measurements over the ocean. Report of the Satellite Surface Stress Working Group. J.J. O'Brien (Chairman). Nova University Press.
- Pierson, W.J. 1983. The measurement of the synoptic scale wind over the ocean. J. Geophys. Res., 88, 1683-1708.
- Pingree, R.D. and D.K. Griffiths. 1978. Tidal fronts on the shelf areas around the British Isles. J. Geophys. Res., 83, 4615-4622.
- Sathyendranath, S., and A. Morel. 1983. Light emerging from the sea - interpretation and uses in remote sensing, in Remote Sensing Applications in Marine Sciences and Technology, A.P. Cracknell (Ed.) Reidel Publishing, 323-357.
- Sathyendranath, S., L. Prieur, and A. Morel. 1982. Interpretation of ocean colour data with special reference to OCM, Contract Report ESA 4726-81, 61 pp.
- Schwiderski, E.W. 1980. Global ocean tides, Part 1: A detailed hydrodynamical interpolation model. Marine Geodesy, 3, 161-217.
- Shutko, A.M. and A.G. Grankov. 1982. Remote sensing of the ocean and atmosphere with passive microwave measurements, in Oceanography from Space. J.F.R. Gower (Ed.), Plenum Press, New York, 735-740.
- Simpson, J.M., C.M. Allen, and N.C.G. Morris. 1978. Fronts on the continental shelf. J. Geophys. Res., 83, 4607-4614.
- Smith, R.C., and W.H. Wilson. 1981. Ship and satellite bio-optical research in the California Bight, in Oceanography from Space. J.F.R. Gower (Ed.), Plenum Press, New York, 281-294.
- Szekielda, K.H. 1982. Mitt. Geol.-Palaont. Inst. Univ. Hamburg, 52, 13.
- Thomas, Y.F. 1978. Publ. Sci. Techn. CNEXO, Actes Colloq., No. 5, 199-121.
- Van Woert, M. 1982. The subtropical front: satellite observations during FRONTS 80. J. Geophys. Res., 87, 9523-9536.
- Viollier, M., and B. Sturm. 1984. CZCS data analysis in turbid coastal water. J. Geophys. Res., 89, 4977-4985.

Voute, C. 1982. TERS (Tropical Earth Resources Satellite). ITC Journal, 1, 37.

Weeks, W.F. 1981. Sea ice: the potential of remote sensing. Oceanus, 24, 39-47.

Woiceshyn, P.M., M.G. Wurtele, D.H. Boggs, L.F. McGoldrich, and S. Peteherych. 1984. A new parameterization of an empirical model for wind/ocean scatterometry, in *Frontiers of Remote Sensing of the Oceans and Troposphere from Air and Space Platforms*. J. Goldhirsch (Ed.), NASA Publication 2303.

Wurtele, M.G., P.M. Woiceshyn, S. Peteherych, M. Borowski, and W.S. Appleby. 1982. Wind direction alias removal studies of Seasat scatterometer derived winds. J. Geophys. Res., 87, 3365-3377.

Yentsch, C.S. and N. Garfield. 1981. Principal areas of vertical mixing in the waters of the Gulf of Maine, with reference to the total productivity of the area, in *Oceanography from Space*, J.F.R. Gower (Ed.), Plenum Press, New York, 303-312.

Zwally, H.J., J.C. Comiso, C.L. Parkinson, W.J. Campbell, F.D. Carsey and P. Gloersen. 1983. Antarctic Sea Ice 1973-1976 Satellite Passive Microwave Observations, NASA Scientific and Technical Information Branch. NASA SP-459.

APPENDIX A General Reference Tables: Satellites and Microwave Band Names

TABLE A1 Satellites of importance to oceanography

| | | | | |
|--|-----------------------------|-------|--------------------------|---|
| Weather satellites civilian U.S. (polar orbiting) | TIROS | 1-6 | 1960-65 | TV visible and IR sensors |
| | ESSA | 1-9 | 1966-69 | TV visible and IR sensors |
| | NOAA | 1-5 | 1970-76 | VHRR visible and IR scanners |
| | TIROS | N | 1978 | AVHRR visible and IR scanners |
| | NOAA | 6-9 | 1978- 1989 | OGI ocean colour scanner |
| Weather satellites military U.S. (polar orbiting) | DMSF | F1-F6 | 1976- 1986 | OLS visible and IR scanners SSM/I |
| Weather satellites Russian (polar orbiting) | Meteor | | 1968- | Visible, IR scanners plus experimental sensors |
| Weather satellites U.S. (synchronous) U.S. Japan Europe India | SMS | 1-2 | 1974-5 | VISSR, visible and IR scanner |
| | GOES | 1-6 | 1975- | VISSR, visible and IR scanner |
| | GMS | 1-2 | 1977- | VISSR, visible and IR scanner |
| | Meteosat | 1-2 | 1977 1981- | IR, visible and IR scanner |
| | INSAT | | 1984- | Visible and IR scanners |
| Experimental satellites (polar orbiting) | Nimbus | 1-7 | 1964- | ESMR, SMR, CZCS |
| Ocean satellites (polar orbiting) | GEOS 3 Seasat Geosat | | 1975-81 1978 1984- | radar altimeter SAR, ALT, SCAT, SMR radar altimeter |
| Land satellites (polar orbiting) | Landsat | 1-5 | 1972- | MSS, RBV, TM, visible and IR scanners |
| | SPOT | | 1985- | HRV visible scanner |
| Various manned missions (polar orbiting) | Skylab Salyut Shuttle | | 1973 1976- 1981- | visual, photographic and experimental |

Table A2 Microwave band names

| Name | Wavelength (cm) | Frequency GHz |
|------------|-----------------|---------------|
| P or UHF | 30 - 100 | .300 - 1.0 |
| L | 15 - 30 | 1.0 - 2.0 |
| S | 7.5 - 15 | 2.0 - 4.0 |
| C | 3.75 - 7.5 | 4.0 - 8.0 |
| X | 2.4 - 3.75 | 8.0 - 12.5 |
| Ku | 1.67 - 2.4 | 12.5 - 18.0 |
| K | 1.13 - 1.67 | 18.0 - 26.5 |
| Ka | 0.75 - 1.13 | 26.5 - 40 |
| Millimeter | <0.75 | >40 |

APPENDIX B**SCOR WG 70 Addresses of Members**

| | |
|-------------------------------|---|
| Tom D. Allan | Institute of Oceanographic Sciences Brook Road, Wormley Godalming, Surrey GU8 5UB England |
| John R. Apel Vice-Chairman | Applied Physics Laboratory The Johns Hopkins University Laurel, MD 20707 U.S.A. |
| Jim F.R. Gower Chairman | Institute of Ocean Sciences P.O. Box 6000 Sidney, B.C. Canada V8L 4B2 |
| Preben Gudmansen | Electromagnetics Institute Building 348 Technical University of Denmark DK2800, Lyngby Denmark |
| Klaus Hasselmann | Max-Planck-Institut für Meteorologie Bundesstr. 55 2000 Hamburg 13 F.R.G. |
| Andre Morel | Laboratoire d'Océanographie Physique BP 8 Villefranche-sur-mer 06230 France |
| Boris A. Nelepo | Marine Hydrophysical Institute Ukr SSR Academy of Sciences 28 Lenin St. Sevastopol 335000 USSR |
| Anatoli M. Shutko | Institute of Radio Engineering and Electronics Academy of Sciences Marx Avenue 18 Moscow GSP-3, 103907 USSR |
| Daniel Spitzer | Netherlands Institute for Sea Research Postbox 59 Den Burg - Texel The Netherlands |
| Atsushi Takeda | Science and Technology Agency National Research Center for Disaster Prevention, Hiratsuka Branch 9-2 Nijigahama Hiratsuka, 254, Japan |

UNESCO TECHNICAL PAPERS IN MARINE SCIENCE

Titles of numbers which are out of stock

| No. | Year | SCOR WG | No. | Year | SCOR WG |
|---|------|------------|--|------|------------|
| 1 Incorporated with Nos. 4, 8 and 14 in No. 27 | 1965 | WG 10 | 13 Technical report of sea trials conducted by the working group on photosynthetic radiant energy, Gulf of California, May 1968; sponsored by SCOR, IAPSO, Unesco | 1969 | WG 15 |
| 2 Report of the first meeting of the joint group of experts on photosynthetic radiant energy held at Moscow, 5-9 October 1964. Sponsored by Unesco, SCOR and IAPSO | 1965 | WG 15 | 14 Incorporated with Nos. 1, 4 and 8 in No. 27 | 1970 | WG 10 |
| 3 Report on the intercalibration measurements in Copenhagen, 9-13 June 1965. Organized by ICES | 1966 | — | 15 Monitoring life in the ocean, sponsored by SCOR, ACMRR, Unesco, IBP/PM | 1973 | WG 29 |
| 4 Incorporated with Nos. 1, 8 and 14 in No. 27 | 1966 | WG 10 | 16 Sixth report of the joint panel on oceanographic tables and standards, Kiel, 24-26 January 1973; sponsored by Unesco, ICES, SCOR, IAPSO | 1974 | WG 10 |
| 5 Report of the second meeting of the joint group of experts on photosynthetic radiant energy held at Kauizawa, 15-19 August 1966. Sponsored by Unesco, SCOR, IAPSO | 1966 | WG 15 | 17 An intercomparison of some current meters, report on an experiment of Research Vessel Akademik Kurchatov, March-April 1970, by the Working Group on Current Velocity Measurements; sponsored by SCOR, IAPSO, Unesco | 1974 | WG 21 |
| 6 Report of a meeting of the joint group of experts on radiocarbon estimation of primary production held at Copenhagen, 24-26 October 1966. Sponsored by Unesco, SCOR, ICES | 1967 | WG 20 | 18 A review of methods used for quantitative phytoplankton studies; sponsored by SCOR, Unesco | 1974 | WG 33 |
| 7 Report of the second meeting of the Committee for the Check-List of the Fishes of the North Eastern Atlantic and on the Mediterranean, London, 20-22 April 1967 | 1968 | — | 20 Ichthyoplankton. Report of the CICAR Ichthyoplankton Workshop-Also published in Spanish | 1975 | — |
| 8 Incorporated with Nos. 1, 4 and 14 in No. 27 | 1968 | WG 10 | 21 An intercomparison of open sea tidal pressure sensors. Report of SCOR Working Group 27: "Tides of the open sea" | 1975 | WG 27 |
| 9 Report on intercalibration measurements, Leningrad, 24-28 May 1966 and Copenhagen, September 1966; organized by ICES | 1969 | — | 22 European sub-regional co-operation in oceanography. Report of Working Group sponsored by the Unesco Scientific Co-operation Bureau for Europe and the Division of Marine Sciences | 1975 | — |
| 10 Guide to the Indian Ocean Biological Centre (IOBC), Cochin (India), by the Unesco Curator 1967-1969 (Dr. J. Tranter) | 1969 | — | 23 An intercomparison of some currents meters, III. Report on an experiment carried out from the Research Vessel Atlantis II. August-September 1972, by the Working Group on Continuous Velocity Measurements: sponsored by SCOR, IAPSO and Unesco | 1975 | WG 21 |
| 11 An intercomparison of some current meters, report on an experiment at WHOI Mooring Site "D", 16-24 July 1967 by the Working Group on Continuous Current Velocity Measurements. Sponsored by SCOR, IAPSO and Unesco | 1969 | WG 21 | | | |
| 12 Check-List of the Fishes of the North-Eastern Atlantic and of the Mediterranean (report of the third meeting of the Committee, Hamburg, April 1969) | 1969 | — | | | |